INSIDE TRACK with **Tim Morin,** Microsemi | **34**

6 Challenges For Signal Generators | **38**

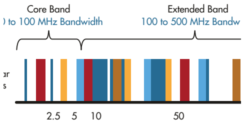

DGS Shrinks Bandpass Filters | **52**

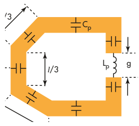

microwaves&rf

MARCH 2015 TRUSTED ENGINEERING RESOURCE FOR OVER 50 YEARS www.mwrf.com

TEST & MEASUREMENT ISSUE

Low-Noise Sources Build On Novel ASIC

p | 87

$10.00 Powered by Penton

Planar Monolithics Industries, Inc.

LEADER IN CUSTOM DESIGNS OF DC-40GHz, MINIATURE INTEGRATED MIC/MMIC MODULES & ASSEMBLIES

- Amplifiers
- Attenuators - Variable
- DLVA & ERDLVA & SDLVA's
- DTO's & Frequency Synthesizers
- Filters
- Form, Fit & Function Products
- IFM's & Frequency Discriminators
- Integrated MIC/MMIC Modules
- I/Q Vector Modulators
- Limiters & Detectors
- Log Amplifiers
- Pulse & Bi-Phase Modulators
- Phase Shifters
- Rack & Chassis Mount Products
- Receiver Front Ends & Transceivers
- Single Sideband Modulators
- SMT & QFN Products
- Solid-State Switches
- Switch Matrices
- Switch Filter Banks
- Threshold Detectors
- USB Products

INTEGRATED DOWN-CONVERTER CONTROL MODULE
MODEL No: LCM-7R7G8R2G-CD-1

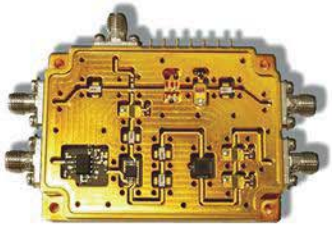

SPECIFICATIONS

- Frequency Range: 7.7 to 8.2GHz (J1, J2, J4, J5)
- Gain (J1 - J2): 16dB ±2dB Maximum at 0dB Attenuation
- Output 1dB Compression (J2): 28dBm Typical
- Conversion Gain: 0dB ±3dB Maximum (J1=10dBm, J4=-10dBm)
- Tap Output Insertion Loss (J1-J5): 16dB ±2dB Typical
- Survival Input Power: 20dBm (J1) & 14dBm (J4) Maximum
- VSWR (All Ports): 2.0:1 Maximum
- Size: 2.5" x 1.75" x 0.4"

LNA 1, 2 & 3:
- Gain: 14dB
- Psat: 16dBm
- Noise Figure: 2.5dB
- Reverse Isolation: 40dB

PHASE SHIFTER:
- Phase Shift Range: 0 to 360 Degrees Minimum
- Control Range: 0 to 10 Volts
- Non-Linear Slope Ratio: 4:1
- Switching Speed: 200ns Maximum

ATTENUATOR:
- Attenuation Range: 0 to 20dB Minimum
- Control Range: 0 to 10 Volts
- Non-Linear Slope Ratio: 8:1
- Switching Speed: 1us Maximum

FILTERS 1 - 5:
- 2dB Passband: 7.7 to 8.2GHz
- Lower Stopband: -20dB at DC to 6.8GHz
- Upper Stopband: -20dB at 10.3 to 18.0GHz

IF ACTIVE LOWPASS FILTER:
- Passband: DC to 10kHz Minimum (J3)
- Stopband: 10kHz (Roll Off of 6dB per Octave)

FUNCTIONAL BLOCK DIAGRAM

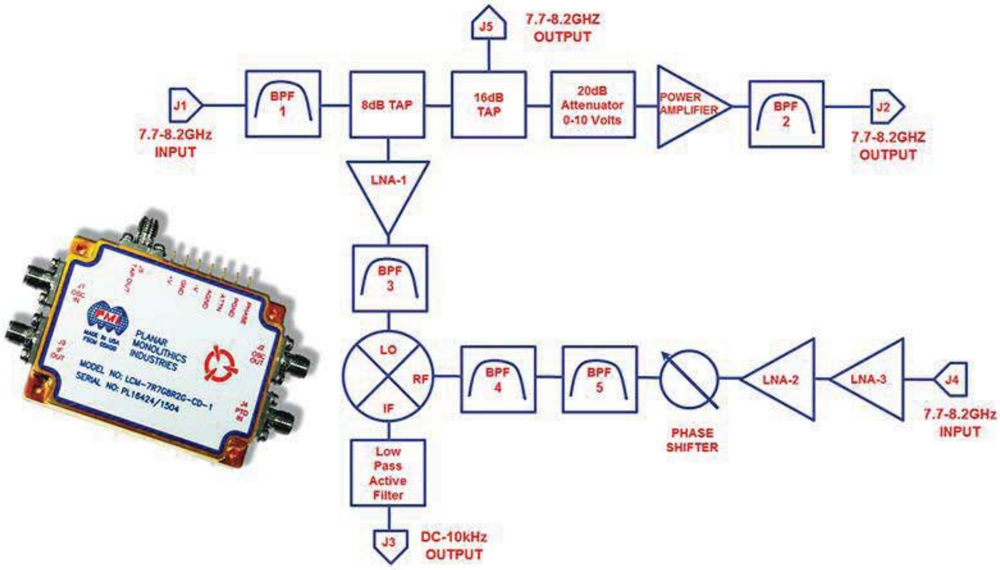

West Coast Operation:
4921 Robert J. Mathews Pkwy, Suite 1
El Dorado Hills, CA 95762 USA
Tel: 916-542-1401 Fax: 916-265-2597
ISO9001:2008 REGISTERED
Email: sales@pmi-rf.com

East Coast Operation:
7311-F Grove Road
Frederick, MD 21704 USA
Tel: 301-662-5019 Fax: 301-662-1731
ISO9001:2008 REGISTERED
Website: www.pmi-rf.com

Hermetic Sealing, High Reliability to Mil-Std-883, Small Quantity Requirements accepted & we offer Custom Designs too.

Fast and accurate power meters.

The new champions from Rohde & Schwarz.

For decades, RF professionals have trusted power measurement solutions from Rohde & Schwarz. With their unrivaled speed and fidelity, the Rohde & Schwarz USB and LAN capable power sensors are the market leaders.

More to explore:
www.rohde-schwarz.com/ad/powersensors

ROHDE&SCHWARZ

In This Issue

VOLUME 54, ISSUE 3

FEATURES

87

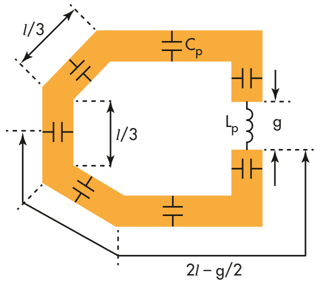

52

49

INDUSTRY TRENDS & ANALYSIS

PRODUCT TECHNOLOGY

NEWS & COLUMNS

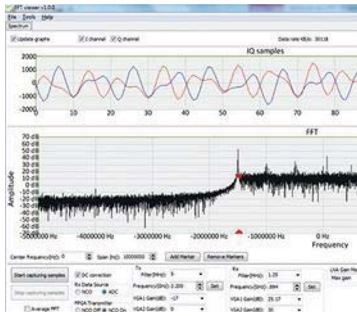

72

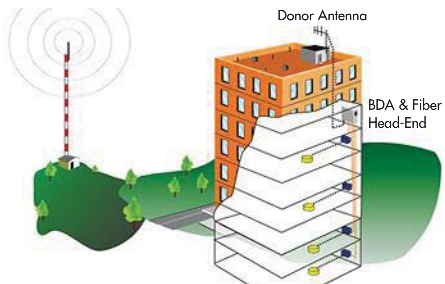

45

Keysight W1715EP SystemVue
MIMO channel builder

Keysight N9040B UXA signal analyzer
with 89600 VSA software

Keysight MIMO PXI test solution
with N7624/25B Signal Studio software for LTE-Advanced/LTE FDD/TDD and 89600 VSA software

Keysight E7515A UXM wireless test set
with E7530A/E7630A LTE-Advanced/LTE test/lab application software

Keysight Infiniium S-Series
high-definition oscilloscope
with N8807A MIPI DigRF v4 (M-PHY) protocol decode software

Keysight N5182B MXG X-Series
RF vector signal generator
with N7624/25B Signal Studio software for LTE-Advanced/LTE FDD/TDD

Keysight E6640B EXM wireless test set
with V9080/82B LTE FDD/TDD measurement applications and N7624/25B Signal Studio software for LTE-Advanced/LTE FDD/TDD

HARDWARE + SOFTWARE

The more complex your LTE-A design, the more you need help from test and measurement experts. Keysight is the only company that offers benchtop, modular and software solutions for every step of the LTE-A design process. From R&D to manufacturing, we can give you the expertise, instruments and applications you need to succeed.

- *Complete LTE-Advanced design and test lifecycle*
- *Identical software algorithms across platforms*
- *300+ software applications for the entire wireless lifecycle*

PEOPLE

We know what it takes for your designs to meet LTE-A standards. After all, Keysight engineers have played major roles in LTE-A and other wireless standards bodies, including 3GPP. Our engineers even co-authored the first book about LTE-A design and test. We also have hundreds of applications engineers. You'll find them all over the world, and their expertise is yours for the asking.

- *Representation on every key wireless standards organization globally*
- *Hundreds of applications engineers in 100 countries around the world*
- *Thousands of patents issued in Keysight's history*

KEYSIGHT
TECHNOLOGIES

Unlocking Measurement Insights

on microwaves&rf.com

WHAT WOULD TESLA DO?

http://mwrf.com/blog/what-would-tesla-do

It boggles the mind how the pioneers of electronics—and microwaves in particular—did their research and development with little or no test equipment. After all, how can you design or repair anything without being able to measure key parameters? Yet with little more than basic meters at their disposal, Hertz, Tesla, Marconi, and other greats were able to accomplish a tremendous amount.

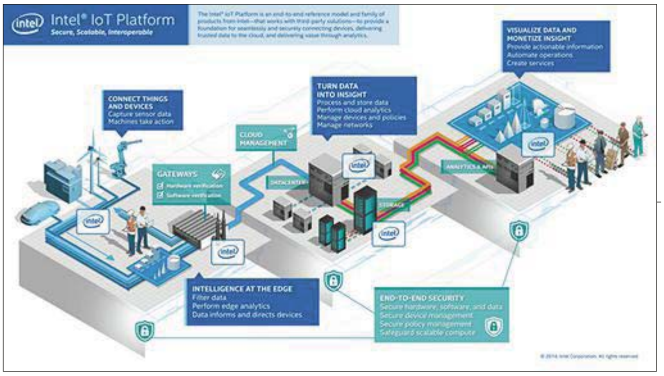

4 MAJOR M2M AND IoT CHALLENGES YOU NEED TO KNOW

http://mwrf.com/systems/4-major-m2m-and-iot-challenges-you-need-know

There are serious considerations to take into account when implementing machine-to-machine (M2M) and industrial Internet of Things (IoT) technologies. Every aspect must be carefully considered, ranging from cost and power to long-term product-lifecycle challenges and interference.

TOP USB TEST INSTRUMENTS:
POWER SENSORS

http://mwrf.com/test-measurement-analyzers/top-usb-test-instruments-power-sensors

Searching for a new power sensor? Look no more: We've rounded up some of the best options for your USB test-instrument needs. Click through this gallery to see some of the top sensors on the market over a range of frequencies.

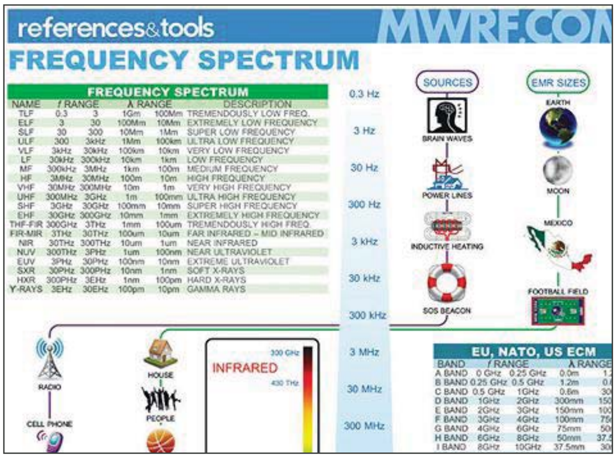

REFERENCES & TOOLS

http://mwrf.com/references-tools

Visit our online References & Tools section to quickly and easily download tables covering topics such as Connector Frequency, which include Coaxial and Waveguide; Frequency Nomenclature: Kilohertz to Terahertz; Frequency Spectrum & Allocations; and Wireless Coexistence: From 300 MHz to 6 GHz.

join us online

twitter.com/MicrowavesRF facebook.com/microwavesrf

Editorial

NANCY K. FRIEDRICH
Content Director
nancy.friedrich@penton.com

Reaching that Last Mile

This year is already proving to be a dynamic one for technology, as our homes, cars, wristwatches, and more become technology hubs. And we just saw a ruling that supported "net neutrality," which translates into an "open" Internet in the United States. Yet many fear that the Internet will suffer too much control, given the many rules imposed on it during the ruling. While I defer to the lawmakers and other experts on that front, I do have some concerns of my own. The largest one is probably that many areas across the globe still do not have access to the Internet.

Different solutions to the "last mile" problem have been posed over the years. In recent years, some particularly interesting approaches were, and are being, attempted by Google. According to *The Guardian* ("Google's Titan drones to take flight within months," March 3, 2015, www.theguardian.com), the company now intends to make Internet access more widely available via high-altitude atmospheric satellites.

At last month's Mobile World Congress, according to *The Guardian*, Google Senior VP of Products Sundar Pichai announced, "The drones will be used as atmospheric satellites, part of Google's plan to provide Internet access to areas without ground-based access and the 4 billion people currently without access." Leveraging its purchase of unmanned-aerial-vehicle (UAV) maker Titan Aerospace, Google will test-flight a set of lightweight, solar-powered, high-altitude drones. These drones will work in tandem with Google's "Project Loon" balloons, which were announced two years ago. At that time, 30 high-altitude balloons were evaluated for their ability to provide Internet connectivity to an area covering about 10,000 square kilometers. Using radio antennas, they could enable Internet access at a level similar to third-generation (3G) networks.

Meanwhile, Facebook has its internet.org initiative, which promises to "connect the next billion people to the Internet through free or subsidized mobile broadband." A sky dotted with Google drones and balloons could certainly help in disasters or in areas with no Internet, provided the solution is reliable. We'll have to wait to see if Facebook has any technology trials of its own that focus on making the Internet available across the globe. In the meantime, Google also unveiled plans to become a service provider. It looks like Silicon Valley is once again driving engineering opportunity and development. Providers of telecommunications equipment, infrastructure, and more, it may be time to meet your next partners—or clients. mw


MCL B 744
ADP-2-10
MCL A 745
MCL BP2C
MCL BP4C
SBA-2-20
071840
QBA-12
071838

MARCH | 2015 microwaves&rf

A Penton® Publication

EDITORIAL

CONTENT DIRECTOR: **NANCY K. FRIEDRICH** nancy.friedrich@penton.com
TECHNICAL CONTRIBUTOR: **JACK BROWNE** jack.browne@penton.com
TECHNICAL ENGINEERING EDITOR: **JEAN-JACQUES DELISLE** jean-jacques.delisle@penton.com
CONTENT PRODUCTION DIRECTOR: **MICHAEL BROWNE** michael.browne@penton.com
PRODUCTION EDITOR: **JEREMY COHEN** jeremy.cohen@penton.com
CONTENT PRODUCTION SPECIALIST: **ROGER ENGELKE** roger.engelke@penton.com
ASSOCIATE CONTENT PRODUCER: **ILIZA SOKOL** iliza.sokol@penton.com
ASSOCIATE CONTENT PRODUCER: **LEAH SCULLY** leah.scully@penton.com

ART DEPARTMENT

GROUP DESIGN DIRECTOR: **ANTHONY VITOLO** tony.vitolo@penton.com
SENIOR ARTIST: **JIM MILLER** jim.miller@penton.com
CONTRIBUTING ART DIRECTOR **RANDALL L. RUBENKING** randall.rubenking@penton.com

PRODUCTION

GROUP PRODUCTION MANAGER: **CAREY SWEETEN** carey.sweeten@penton.com
PRODUCTION MANAGER: **VICKI MCCARTY** vicki.mccarty@penton.com
CLASSIFIED PRODUCTION COORDINATOR: **LINDA SARGENT** linda.sargent@penton.com

AUDIENCE MARKETING

USER MARKETING DIRECTOR: **BRENDA ROODE** brenda.roode@penton.com
USER MARKETING MANAGER: **DEBBIE BRADY** debbie.brady@penton.com
FREE SUBSCRIPTION/STATUS OF SUBSCRIPTION/ADDRESS CHANGE/MISSING BACK ISSUES
T | 866.505.7173 microwaves&RF@halldata.com **F** | 847.763.9673

SALES & MARKETING

AL, AR, CT, DE, FL, GA, IA, IL, IN, KS, KY, LA,MA, MD, ME, MI, MN, MO, MS, NC, NE, NH, NJ, NY, OH, OK, RI, SC, TN, PA, VA, VT, WV, E/CANADA:
MANAGING DIRECTOR: **TRACY SMITH** **T** | 913.967.1324 **F** | 913.514.6881 tracy.smith@penton.com

REGIONAL SALES REPRESENTATIVES
AZ, NM, TX: **BILL YARBOROUGH** **T** | 713.636.3809 **F** | 913.514.7251 bill.yarborough@penton.com
AK, CA, CO, ID, MT, ND, NV, OR, SD, UT, WA, WI, WY, W/CANADA: **JAMIE ALLEN** **T** | 415.608.1959 **F** | 913.514.3667 jamie.allen@penton.com

PLEASE SEND INSERTION ORDERS TO: orders@penton.com
PENTON REPRINTS: **WRIGHT'S MEDIA** **T** | 877.652.5295 penton@wrightsmedia.com
CIRCULATION: **CUSTOMER SERVICE** **T** | 866.505.7173 **F** | 847.763.9673 microwaves&rf@halldata.com

INTERNATIONAL SALES
EUROPE: **TRACY SMITH** **T** | 913.967.1324 **F** | 913.514.6881 tracy.smith@penton.com
PAN-ASIA: **HELEN LAI** **T** | 886 2-2727 7799 helen@twoway-com.com
LIST RENTALS, CUSTOMER SERVICE--SUBSCRIPTIONS:
ONLINE MARKETING MANAGER: **SARAH NOWOWIEJSKI** **T** | (212) 204 4295 sarah.nowowiejski@penton.com

ONLINE

PRODUCT DEVELOPMENT DIRECTOR: **RYAN MALEC** ryan.malec@penton.com

DESIGN ENGINEERING & SOURCING GROUP

VICE PRESIDENT & MARKET LEADER: **BILL BAUMANN**
EXECUTIVE DIRECTOR OF CONTENT AND USER ENGAGEMENT: **NANCY K. FRIEDRICH**
GROUP DIRECTOR OF OPERATIONS: **CHRISTINA CAVANO**
GROUP DIRECTOR OF MARKETING: **JANE COOPER**

PENTON MEDIA INC.

CHIEF EXECUTIVE OFFICER: **DAVID KIESELSTEIN** david.kieselstein@penton.com
CHIEF FINANCIAL OFFICER: **NICOLA ALLAIS** nicola.allais@penton.com
SENIOR VP, DESIGN ENGINEERING GROUP: **BOB MACARTHUR** bob.macarthur@penton.com
1166 AVENUE OF THE AMERICAS, 10TH FLOOR NEW YORK, NY 10036 **T** | 212.204.4200

Penton

Electronic Design | Machine Design | Microwaves & RF | Medical Design | Source ESB | Hydraulics & Pneumatics | Global Purchasing | Distribution Resource | Power Electronics | Defense Electronics | Electronic Design Europe | Engineering TV

RF Amplifiers and Sub-Assemblies for Every Application

Delivery from Stock to 2 Weeks ARO from the catalog or built to your specifications!

- Competitive Pricing & Fast Delivery
- Military Reliability & Qualification
- Various Options: Temperature Compensation, Input Limiter Protection, Detectors/TTL & More
- Unconditionally Stable (100% tested)

ISO 9001:2000 and AS9100B CERTIFIED

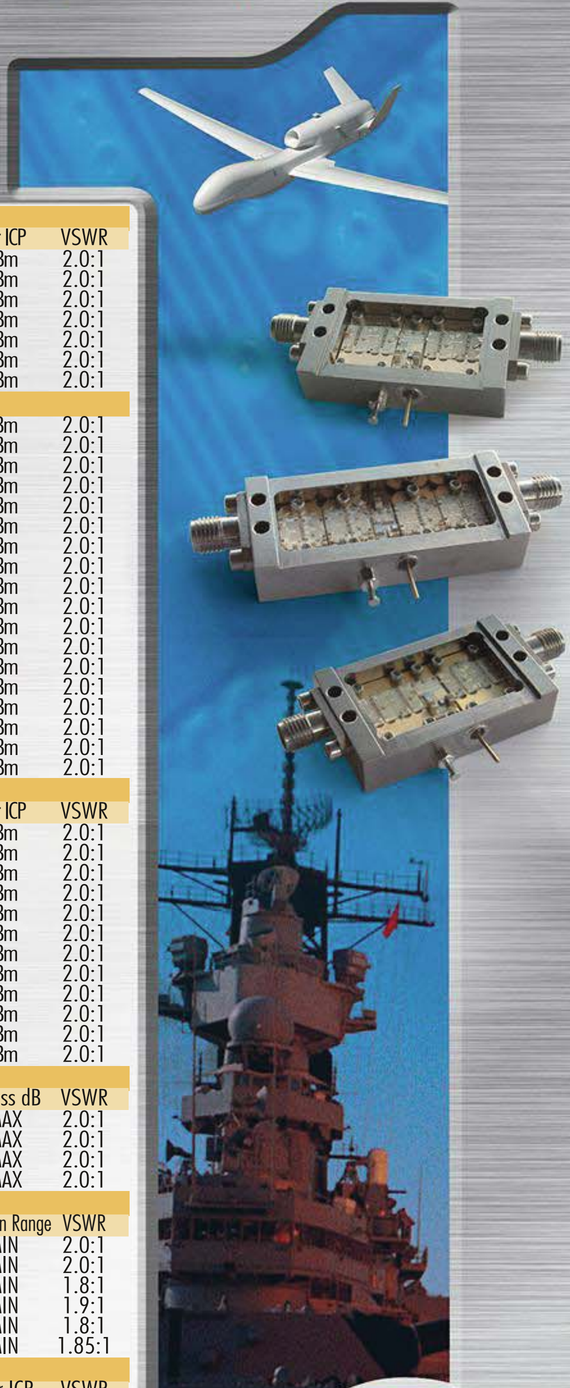

OCTAVE BAND LOW NOISE AMPLIFIERS

Model No.	Freq (GHz)	Gain (dB) MIN	Noise Figure (dB)	Power-out @ P1-dB	3rd Order ICP	VSWR
CA01-2110	0.5-1.0	28	1.0 MAX, 0.7 TYP	+10 MIN	+20 dBm	2.0:1
CA12-2110	1.0-2.0	30	1.0 MAX, 0.7 TYP	+10 MIN	+20 dBm	2.0:1
CA24-2111	2.0-4.0	29	1.1 MAX, 0.95 TYP	+10 MIN	+20 dBm	2.0:1
CA48-2111	4.0-8.0	29	1.3 MAX, 1.0 TYP	+10 MIN	+20 dBm	2.0:1
CA812-3111	8.0-12.0	27	1.6 MAX, 1.4 TYP	+10 MIN	+20 dBm	2.0:1
CA1218-4111	12.0-18.0	25	1.9 MAX, 1.7 TYP	+10 MIN	+20 dBm	2.0:1
CA1826-2110	18.0-26.5	32	3.0 MAX, 2.5 TYP	+10 MIN	+20 dBm	2.0:1

NARROW BAND LOW NOISE AND MEDIUM POWER AMPLIFIERS

Model No.	Freq (GHz)	Gain (dB) MIN	Noise Figure (dB)	Power-out @ P1-dB	3rd Order ICP	VSWR
CA01-2111	0.4 - 0.5	28	0.6 MAX, 0.4 TYP	+10 MIN	+20 dBm	2.0:1
CA01-2113	0.8 - 1.0	28	0.6 MAX, 0.4 TYP	+10 MIN	+20 dBm	2.0:1
CA12-3117	1.2 - 1.6	25	0.6 MAX, 0.4 TYP	+10 MIN	+20 dBm	2.0:1
CA23-3111	2.2 - 2.4	30	0.6 MAX, 0.45 TYP	+10 MIN	+20 dBm	2.0:1
CA23-3116	2.7 - 2.9	29	0.7 MAX, 0.5 TYP	+10 MIN	+20 dBm	2.0:1
CA34-2110	3.7 - 4.2	28	1.0 MAX, 0.5 TYP	+10 MIN	+20 dBm	2.0:1
CA56-3110	5.4 - 5.9	40	1.0 MAX, 0.5 TYP	+10 MIN	+20 dBm	2.0:1
CA78-4110	7.25 - 7.75	32	1.2 MAX, 1.0 TYP	+10 MIN	+20 dBm	2.0:1
CA910-3110	9.0 - 10.6	25	1.4 MAX, 1.2 TYP	+10 MIN	+20 dBm	2.0:1
CA1315-3110	13.75 - 15.4	25	1.6 MAX, 1.4 TYP	+10 MIN	+20 dBm	2.0:1
CA12-3114	1.35 - 1.85	30	4.0 MAX, 3.0 TYP	+33 MIN	+41 dBm	2.0:1
CA34-6116	3.1 - 3.5	40	4.5 MAX, 3.5 TYP	+35 MIN	+43 dBm	2.0:1
CA56-5114	5.9 - 6.4	30	5.0 MAX, 4.0 TYP	+30 MIN	+40 dBm	2.0:1
CA812-6115	8.0 - 12.0	30	4.5 MAX, 3.5 TYP	+30 MIN	+40 dBm	2.0:1
CA812-6116	8.0 - 12.0	30	5.0 MAX, 4.0 TYP	+33 MIN	+41 dBm	2.0:1
CA1213-7110	12.2 - 13.25	28	6.0 MAX, 5.5 TYP	+33 MIN	+42 dBm	2.0:1
CA1415-7110	14.0 - 15.0	30	5.0 MAX, 4.0 TYP	+30 MIN	+40 dBm	2.0:1
CA1722-4110	17.0 - 22.0	25	3.5 MAX, 2.8 TYP	+21 MIN	+31 dBm	2.0:1

ULTRA-BROADBAND & MULTI-OCTAVE BAND AMPLIFIERS

Model No.	Freq (GHz)	Gain (dB) MIN	Noise Figure (dB)	Power-out @ P1-dB	3rd Order ICP	VSWR
CA0102-3111	0.1-2.0	28	1.6 Max, 1.2 TYP	+10 MIN	+20 dBm	2.0:1
CA0106-3111	0.1-6.0	28	1.9 Max, 1.5 TYP	+10 MIN	+20 dBm	2.0:1
CA0108-3110	0.1-8.0	26	2.2 Max, 1.8 TYP	+10 MIN	+20 dBm	2.0:1
CA0108-4112	0.1-8.0	32	3.0 MAX, 1.8 TYP	+22 MIN	+32 dBm	2.0:1
CA02-3112	0.5-2.0	36	4.5 MAX, 2.5 TYP	+30 MIN	+40 dBm	2.0:1
CA26-3110	2.0-6.0	26	2.0 MAX, 1.5 TYP	+10 MIN	+20 dBm	2.0:1
CA26-4114	2.0-6.0	22	5.0 MAX, 3.5 TYP	+30 MIN	+40 dBm	2.0:1
CA618-4112	6.0-18.0	25	5.0 MAX, 3.5 TYP	+23 MIN	+33 dBm	2.0:1
CA618-6114	6.0-18.0	35	5.0 MAX, 3.5 TYP	+30 MIN	+40 dBm	2.0:1
CA218-4116	2.0-18.0	30	3.5 MAX, 2.8 TYP	+10 MIN	+20 dBm	2.0:1
CA218-4110	2.0-18.0	30	5.0 MAX, 3.5 TYP	+20 MIN	+30 dBm	2.0:1
CA218-4112	2.0-18.0	29	5.0 MAX, 3.5 TYP	+24 MIN	+34 dBm	2.0:1

LIMITING AMPLIFIERS

Model No.	Freq (GHz)	Input Dynamic Range	Output Power Range Psat	Power Flatness dB	VSWR
CLA24-4001	2.0 - 4.0	-28 to +10 dBm	+7 to +11 dBm	+/- 1.5 MAX	2.0:1
CLA26-8001	2.0 - 6.0	-50 to +20 dBm	+14 to +18 dBm	+/- 1.5 MAX	2.0:1
CLA712-5001	7.0 - 12.4	-21 to +10 dBm	+14 to +19 dBm	+/- 1.5 MAX	2.0:1
CLA618-1201	6.0 - 18.0	-50 to +20 dBm	+14 to +19 dBm	+/- 1.5 MAX	2.0:1

AMPLIFIERS WITH INTEGRATED GAIN ATTENUATION

Model No.	Freq (GHz)	Gain (dB) MIN	Noise Figure (dB)	Power-out @ P1-dB	Gain Attenuation Range	VSWR
CA001-2511A	0.025-0.150	21	5.0 MAX, 3.5 TYP	+12 MIN	30 dB MIN	2.0:1
CA05-3110A	0.5-5.5	23	2.5 MAX, 1.5 TYP	+18 MIN	20 dB MIN	2.0:1
CA56-3110A	5.85-6.425	28	2.5 MAX, 1.5 TYP	+16 MIN	22 dB MIN	1.8:1
CA612-4110A	6.0-12.0	24	2.5 MAX, 1.5 TYP	+12 MIN	15 dB MIN	1.9:1
CA1315-4110A	13.75-15.4	25	2.2 MAX, 1.6 TYP	+16 MIN	20 dB MIN	1.8:1
CA1518-4110A	15.0-18.0	30	3.0 MAX, 2.0 TYP	+18 MIN	20 dB MIN	1.85:1

LOW FREQUENCY AMPLIFIERS

Model No.	Freq (GHz)	Gain (dB) MIN	Noise Figure dB	Power-out @ P1-dB	3rd Order ICP	VSWR
CA001-2110	0.01-0.10	18	4.0 MAX, 2.2 TYP	+10 MIN	+20 dBm	2.0:1
CA001-2211	0.04-0.15	24	3.5 MAX, 2.2 TYP	+13 MIN	+23 dBm	2.0:1
CA001-2215	0.04-0.15	23	4.0 MAX, 2.2 TYP	+23 MIN	+33 dBm	2.0:1
CA001-3113	0.01-1.0	28	4.0 MAX, 2.8 TYP	+17 MIN	+27 dBm	2.0:1
CA002-3114	0.01-2.0	27	4.0 MAX, 2.8 TYP	+20 MIN	+30 dBm	2.0:1
CA003-3116	0.01-3.0	18	4.0 MAX, 2.8 TYP	+25 MIN	+35 dBm	2.0:1
CA004-3112	0.01-4.0	32	4.0 MAX, 2.8 TYP	+15 MIN	+25 dBm	2.0:1

CIAO Wireless can easily modify any of its standard models to meet your "exact" requirements at the Catalog Pricing.

Visit our web site at **www.ciaowireless.com** for our complete product offering.

Ciao wireless

Ciao Wireless, Inc. 4000 Via Pescador, Camarillo, CA 93012

Tel (805) 389-3224 Fax (805) 389-3629 sales@ciaowireless.com

SEARCHING FOR TESTING GUIDANCE

In reading through your magazine these many years, it is impossible not to notice the dramatic changes in technologies that take place and force engineers to adapt to these new technologies where appropriate. At one time, for example, many microwave systems were based on waveguide transmission lines for transferring signals from one location to another. As coaxial connector and cable manufacturers refined their machining capabilities and pushed coaxial transmission lines higher in frequency and with lower loss, waveguide grew more scarce in high-frequency systems. This is just one example of many different active and passive component technologies that seem to change year after year.

Often, new technologies are introduced in magazines such as yours, but with little guidance for readers on how to characterize or test the components or devices based on these new technologies. Granted, your magazine presents a fair share of new test instruments from leading manufacturers of test gear, and the occasional white paper in your "Application Notes" section, to help readers learn how to operate new test equipment. But what could truly help the engineering readers of *Microwaves & RF* would be some kind of blog or series on test equipment and measurement techniques that could be used to keep pace with new technologies. This could help make your website even more valuable than simply a listing of previous magazine issues.

SAM EWING

EDITOR'S NOTE

Your suggestion echoes the queries of quite a few readers in recent months, to provide additional feedback on available test equipment in the RF/microwave industry and guidance on performing measurements that are of current interest with the industry's engineers and its customers. Many parameters that are often used to sort through different products simply didn't exist a number of years ago; test methodologies were not developed for those parameters, such as passive intermodulation (PIM) in coaxial cables and connectors. Similarly, many test-equipment suppliers have changed over the years (Keysight, anyone?), and keeping track of available sources of test-equipment can be a chore. By devoting a regular online blog to test-and-measurement topics in the near future, *Microwaves & RF* hopes to aid its readers with expanded educational resources that will be both practical and newsworthy. Keep tuned (or posted, shall we say?).


SKYWORKS®
Powering the Media Revolution
Innovative Solutions for
Set-top Boxes • HDTVs
Gaming Consoles • Wireless Audio
▶ www.skyworksinc.com
sales@skyworksinc.com | NASDAQ: SWKS | USA: 781-376-3000 | Asia: 886-2-2735 0399 | Europe: 33 (0)1 43548540 |

SKYWORKS®

Media Solutions

Set-top Boxes | HDTVs | Gaming Consoles | Wireless Audio

High Performance Front-end Modules

| Dual-band 802.11a/g/n/ac Wireless LAN Front-end Module: SKY85806-11

- For set-top box, wireless high fidelity, USB dongle and personal computer applications
- All RF ports matched to 50 Ω
- Integrated 2.4 GHz PA, 5 GHz PA, transmit filter, diplexers and T/R switches
- Integrated logarithmic power detector for each transmit chain
- Bluetooth® ready; functional when V_{CC} = 0 or 3.3 V
- Package: QFN 28-pin 4 x 3 x 0.8 mm

| 5 GHz, 802.11ac Switch/Low-noise Amplifier Front-end Module: SKY85608-11

- For 802.11a/n/ac set-top box, TV, audio, personal computer and WLAN-enabled wireless video system applications
- Integrated SP2T switch and LNA with bypass mode
- Receive gain: 12 dB
- Noise figure: 2.1 dB
- Transmit path loss: 0.8 dB
- Package: DFN 8-pin 1.5 x 1.5 x 0.4 mm

| 2.4 GHz, 256 QAM Switch/Low-noise Amplifier Front-end Module: SKY85203-11

- For 802.11b/g/n set-top box, mobile device, gaming and tablet applications
- Integrates an SP3T switch and LNA with bypass mode
- Receive gain: 14 dB
- Noise figure: 2.1 dB
- Transmit/Bluetooth® path loss: 0.8 dB
- Package: QFN 12-pin 2 x 2 x 0.45 mm

| 2.4 GHz ZigBee® RF4CE/Smart Energy Front-end Module: SKY66109-11

- For set-top box, in-home appliance and smart meter applications
- Integrated PA with up to 24 dBm output power
- Integrated LNA with programmable bypass
- Integrated antenna switching with transmit and receive diversity function
- Package: MCM 20-pin 3 x 4 x 0.9 mm

Learn More ▶
www.skyworksinc.com

Scan to join our customer email program today!

sales@skyworksinc.com | NASDAQ: SWKS | USA: 781-376-3000 | Asia: 886-2-2735 0399 | Europe: 33 (0)1 43548540 |

News

TROPOSCATTER SYSTEM
Maintains 50-Mb/s Connection Over 100 Miles

Wireless technology advances continue to push the boundaries of long-distance data throughput. Recently completed tests of TeleCommunication Systems' Tactical Transportable Troposcatter (3T) system proved this point: The Army-supported test, led by TCS and Comtech, maintained a 50-Mb/s troposcatter communication link of over 100 miles at White Sands Missile Range in New Mexico.

The system, otherwise known as AN/TSC-198 (V3), provides high-bandwidth, low-latency, non-satellite, beyond-line-of-sight network transport for existing (and future) bandwidth intensive C5IR platforms. It combines the battle-tested SNAP Very Small Aperture Terminal (VSAT) system with Comtech's IP-capable troposcatter technology. The Modular Transportable Troposcatter System (MTTS) has a much smaller form factor than previous systems and is backward-compatible.

Specifically designed for long-haul, over-the-horizon communication or where line-of-sight is obstructed, the 3T provides secure Internet Protocol (IP) connectivity to command and control centers. The system's quad diversity combines space and frequency or space and polarization diversities. C-Band frequencies and a SNAP 2.0 M antenna help optimize communications. Its position in the troposphere makes it possible for warfighters to communicate in conditions that would otherwise be near-impossible for other systems. ■

A Tactical Transportable Troposcatter (3T) system recently completed testing, successfully delivering high-bandwidth 50-Mb/s speeds over 100 miles. *(Image courtesy of TeleCommunication Systems)*

TECHNOLOGY PROVIDES EASY Switch Between Satellite, Cellular Communications

FURTHERING THE EFFORTS to deliver secure defense and cellular communications in remote areas, Chemring Technology Solutions, Avanti Government Services, and Spectra collaborated to bring SmartLink capabilities to Avanti's Ka-band satellite system. They system, which uses Spectra's Hostile Area Deployment Environment (SHADE) solutions, proved effective in trials. SmartLink supports military units in need of a secure connection and mobile network operators (MNOs) that need to extend their services to remote locations.

> "Trials of the technology delivered a range of cellular services using multiple handsets, including file sharing, push-to-talk, and situational awareness applications."

Trials of the technology delivered a range of cellular services using multiple handsets, including file sharing, push-to-talk, situational awareness applications, video streaming, VoIP calls, and web browsing. SHADE utilizes a Very Small Aperture Terminal (VSAT), operating on C, Ka, Ku, and X-bands. The MicroSHADE solution helps create a secure "tunnel" for communications in transit, utilizing BGAN, Wi-Fi, or 3G. It is flexible and can be deployed on a global scale by small teams or even a single user.

SmartLink, as a highly-portable, cellular-network-in-a-box, has proven itself within a 5-km range. Because the SHADE solutions are bearer agnostic, the deployment of SmartLink is further enhanced by the ability to switch from cellular networks to a satellite network without the need for reconfiguring endpoints. This means that if there's a loss of terrestrial service or if there's a requirement to change location, the network can simply be switched over to satellite. ■

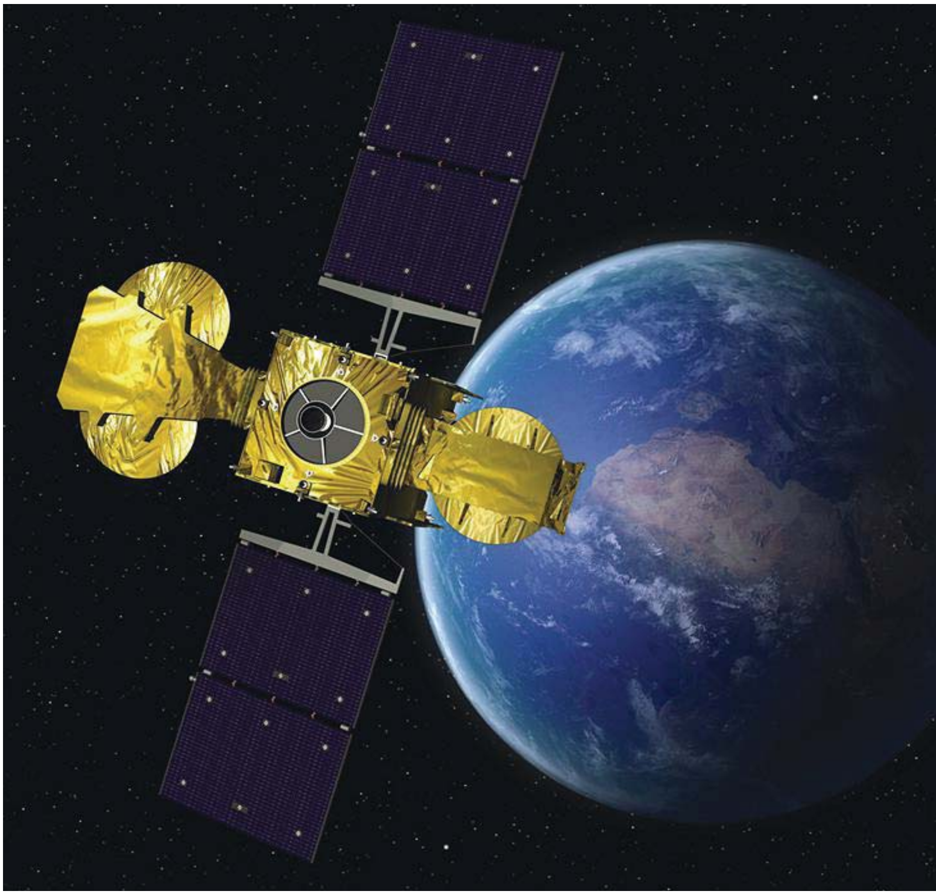

Avanti's satellite, HYLAS-1, was Europe's first Ka-band satellite.

(Image courtesy of the UK Space Agency)

FREESCALE AND NXP Announce Merger

A DEFINITIVE AGREEMENT reached between NXP Semiconductors and Freescale Semiconductor will merge the two companies—an enterprise valued at over $40 billion. The newly combined company will look to become a leader in automotive semiconductor solutions and general-purpose microcontroller (MCU) solutions, capitalizing on opportunities created by the demand for security, connectivity, and processing.

The transaction was unanimously approved by the boards of directors for both companies, and is now subject to regulatory approvals and customary closing conditions. NXP will fund the transaction with $1 billion from its balance sheet, $1 billion of new debt, and approximately 115 million NXP ordinary shares. Following the transaction, Freescale shareholders will own approximately 32% of the joint company. The deal is expected to close in the second half of 2015. ■

INTEGRATED CHIPSETS BREAK Ground for 5G Communications

AS MOBILE CARRIERS move toward 5G, major players in the embedded-system arena are following suit with more powerful chipsets. Broadcom recently introduced two new systems-on-a-chip (SoCs), said to be two of the first to deliver 5-Gb/s speeds. According to the company, the integrated chipsets can deliver four times the spectral efficiency of previous devices for microwave backhaul. The SoCs are designed to support the surge of data traffic over wireless networks.

The BCM85650 features integrated cross-polarization interference cancellation (XPIC) and line-of-sight multiple-input, multiple-output (LoS-MIMO) functionalities. This helps boost spectral efficiency to 48 bits/s/Hz by supporting flexible antenna placement and reducing external connection and hardware requirements. It includes a dual-core wideband modem and supports advanced channel aggregation functionality for efficient capacity doubling. The SoC also offers quadrature amplitude modulation (4K-QAM).

The BCM85820 boosts both capacity and spectral efficiency thanks to integration of XPIC, MIMO, 4K-QAM, and 112-MHz channels, plus channel-aggregation functionality. It also utilizes digital RF correction mechanisms like adaptive digital-pre-distortion (ADPD) to achieve high system gain. The chipset includes a full transceiver as well as synthesizer components.

Although both chipsets are currently sampling, their introduction represents a key step toward meeting increased traffic demands spawned by 5G and LTE technology. Such devices make it possible to expand capacity and coverage across a wider network to further augment the existing microwave backhaul infrastructure. ■

Raytheon began upgrading the electronic equipment units (EEUs) for the AN/TPY-2 ballistic radars to fine-tune the tracking of ballistic missiles in potential large-scale raids. *(Image courtesy of Raytheon)*

PROCESSOR UPGRADE BOOSTS X-Band Radar's Missile-Tracking Capabilities

The AN/TPY-2 radar is a critical part of the Ballistic Missile Defense System (BMDS), which helps defend against raids of multiple, simultaneously impacting ballistic missiles. Raytheon recent upgrade to the radar's computer processor enhances system performance during potential raids, and quickly and accurately discriminates between a missile's warhead and non-threats. The new electronic equipment unit (EEU) weighs less, requires less power, and occupies less space than previous versions, while supplying approximately five times the processing power.

The high-resolution, mobile, rapidly deployable X-band radar offers long-range acquisition, precision track, and discrimination of short-, medium-, and intermediate-range ballistic missiles. It can be deployed globally in terminal or forward-based modes. With the terminal mode, the radar can function as the search, detect, track, discrimination, and fire-control radar for the THAAD weapon system. In forward-based mode, the AN/TPY-2 cues the BMDS by detecting, discriminating, and tracking enemy missiles in the ascent flight phase.

Raytheon delivered the first upgraded EEU to the Missile Defense Agency in January 2015. The MDA announced plans to replace all 10 EEUs currently in U.S. inventory with the upgraded versions. The EEUs will be replaced one at a time to ensure constant radar coverage throughout the entire process. This is especially important due to the rising threat of global ballistic missiles—U.S. intelligence agencies estimate more than 6300 ballistic missiles are not controlled by the U.S., NATO, China, or Russia. By 2020, that number is expected to reach 8000. ■

LED CONTROL SYSTEM Simplifies Wireless Setup

WHILE LEDS REPRESENT the latest advances in lighting, utilizing them to their fullest potential involves further simplification while complying with increasingly rigorous standards. To enable OEMs with the basic building blocks, EnOcean has launched a complete wireless LED control system. Leveraging the company's portfolio of self-powered wireless switches and occupancy and light-level sensors, the LED control system combines the former with LED fixture controllers and commissioning tools, simplifying installation and setup.

EnOcean has launched a complete LED control system that includes a family of LED controllers to support instantaneous and simplified wireless control. *(Image courtesy of EnOcean)*

The LED controller family includes a transceiver module (TCM 330U) for integration into drivers and modules. Also featured are LED fixture/zone controllers with relay and 0- to 10-V output (LEDR) and without relay (LEDD). The controllers operate at 902 MHz; they can be used for dimming control of a single feature or a zone of multiple, daisy-chained fixtures. They also support daylight harvesting scenarios, occupancy control, and manual dimming processing data. Their compact size facilitates flexible installation inside of, or next to, electrical boxes and fixtures, enabling them to be wired out of sight using standard practices.

Users can connect the LEDR or LEDD controller to a central controller or gateway to implement lighting control into building automation systems. The transceiver module can also be implemented into existing controllers and includes the firmware for instantaneous wireless control. The controls further provide a simplified user interface for the configuration and linking of devices: With two buttons, they can link and unlink sensors and switches, dim up and down manually, and set the minimum dimming value.

To configure more advanced settings, EnOcean offers Navigan, a wireless remote commissioning software. This enables users to link devices and set parameters—such as ramp speeds, dimming levels, and integrated repeater—from a laptop computer. The controllers can then be aligned over the air with on-site requirements, define properties, and settings. Navigan also offers the ability to edit and store projects. ■

GRAPHENE, SILICON COMBO Could Replace Copper for Electronics Coatings

Graphene's virtual impermeability makes it ideal for implementation in ultra-thin coatings for electronics to combat corrosion. 2-DTech, a corporate spin-off of the University of Manchester (where graphene was first isolated), is spearheading a project to improve anti-corrosive coatings through incorporation of graphene via a scalable and commercially viable process.

Copper, with its inherent ability to conduct electricity, has been extensively used for this purpose. But in application scenarios with elevated levels of moisture, hydrogen sulfide, sulfur dioxide, and the like, copper corrosion severely infringes on system performance. Such corrosion can eventually lead to overheating or malfunction, or else be in direct defiance of current environmental directives such as RoHS. The research team's ultimate goal is to produce high-crystalline-quality, silicon-doped graphene as a replacement.

The introduction of silicon as a dopant aims to fortify the multi-layer graphene's domain boundaries. This could then result in a step change improvement in anti-corrosive silicon-graphene conductive films for application on to copper substrates via thermal chemical vapor deposition (TCVD). The combination would create an extremely thin coating while protecting against corrosion without disrupting the intra-domain crystalline structure. ■

A grant has been awarded to 2-DTech to find a process in which a graphene and silicon combination could be used to coat electronics without corrosion. *(Image courtesy of 2-DTech)*

CONTRACTS

Keysight Technologies Inc.—Announced that China Telecom Corp. Test labs (GSTA) in Guangzhou, China, has selected Keysight's T3111S NFC Conformance System for near-field communications (NFC) device acceptance test. The T3111S is a compact and flexible tool that helps engineers gain insight into NFC performance through RF and protocol measurements. Additionally, the system provides standard test suites and the widest test coverage required by NFC Forum, EMV L1, and ISO test specifications.

CHINA TELECOM
Chooses Keysight

7LAYERS
Upgrades R&S Test Platforms

DRS Technologies Inc.—Announced that its Canadian subsidiary will provide tactical integrated communications systems to the New Zealand Ministry of Defense for the Royal New Zealand Navy's ANZAC-class frigates. This subcontract was awarded to DRS Technologies Canada Ltd. in support of a communications modernization contract from Lockheed Martin Canada in September 2014. DRS Technologies Canada Ltd. is the primary subcontractor to Lockheed Martin Canada.

SGS—Selected Rohde & Schwarz to strengthen its industry conformance and carrier acceptance testing capabilities for key LTE/4G technologies. Expanding on its existing R&S TS8980FTA-2 and R&S CMW500 wireless test platforms, SGS has increased its test capabilities areas including: LTE LBS (AGNSS/OTDOA) minimum performance, VoLTE E-911 protocol; LTE eMBMS RF performance and protocol; and LTE carrier aggregation data throughput, RF performance, and protocol.

7Layers—Upgraded its Rohde & Schwarz TS8980FTA, R&S CMW-PQA wireless test platforms to increase test capabilities including LTE location-based services (LBS) performance; VoLTE E-911 protocol; eMBMS RF performance, video performance, and protocol; LTE carrier aggregation RF performance, data throughput performance, and protocol; IMS/VoLTE protocol; Rich Communications Services (RCS) protocol; ePDG/Wi-Fi calling over IMS; and Wi-Fi offloading.

FRESH STARTS

API Technologies Corp.—Was awarded a new patent for its aiming device for a bomb-disarming disrupter. The Hawk-I Video Aiming Device uses a camera and a rangefinder to automatically assess range to target, then generates crosshairs on a video monitor. Bomb technicians then use this targeting guidance to fire a precise shot, which disarms the explosive. Use of the Hawk-I speeds aiming time and decreases chances of misfire due to human error.

Anite—Will expand its device application testing capability by entering into an agreement to acquire the trade and assets of Setcom Wireless Products GmbH, a supplier of wireless-device application test solutions based in Munich, Germany. The transaction is expected to wrap up by April 1, 2015, at which time Setcom will be fully integrated into Anite's Device & Infrastructure Testing business unit. Setcom's flagship solution S-CORE will further expand Anite's device application testing portfolio into Wi-Fi offload, IMS-, and RCS-based services.

AT4 wireless—Has appointed Swift Labs, an expert company in wireless R&D, functional testing, pre-testing and consultancy services, as its Canadian agency. These companies have entered into agreement to provide added-value services to the Canadian telecommunications industry through local pretesting, functional testing, R&D support, and Carrier Lab Entry Services. Swift Labs will provide direct access to AT4 wireless' complete service offering, bringing global reach to the wireless and cellular testing market in Canada.

Amphenol RF—Launched a new corporate website, www.amphenolrf.com. The new website is home to thousands of standard products and boasts an advanced feature set that allows buyers and engineers to quickly find the ideal RF connector, coaxial adapter, or cable assembly for use in their application.

TeleCommunication Systems Inc. (TCS)—Has been awarded approval by the U.S. General Services Administration (GSA) to add O3b Networks satellite products and services to TCS's IT Schedule 70 contract. The GSA IT Schedule 70 is the largest, most widely used acquisition vehicle in the federal government, providing direct access to products, services, and solutions to federal, state, and local government agencies.

Newtec—Received the "Factory of the Future" award as part of the Belgian campaign "Made Different." The "Factory of the Future" is just one part of the campaign, which was created to recognize the market challenges faced by Belgian companies and the need for them to be innovative and future-proof.

Qorvo—Announced that its board of directors has authorized the repurchase of up to $200 million of the company's outstanding common stock. The primary objective of the share repurchase program is to reduce dilution from issuances relating to employee equity awards and the company's employee stock purchase program.

IEEE Compound Semiconductor IC Symposium (CSICS)—Announced a call for papers for its meeting being held in New Orleans, La., Oct. 11-14, 2015. First-time papers addressing the utilization and application of InP, GaAs, GaN, silicon, germanium, SiGe, and other compound semiconductors in military and commercial products are invited. For more information, visit http://csics.org/sites/csics.org/files/2015_IEEE_CSICS_First_Call.pdf. The deadline for submission is April 17, 2015.

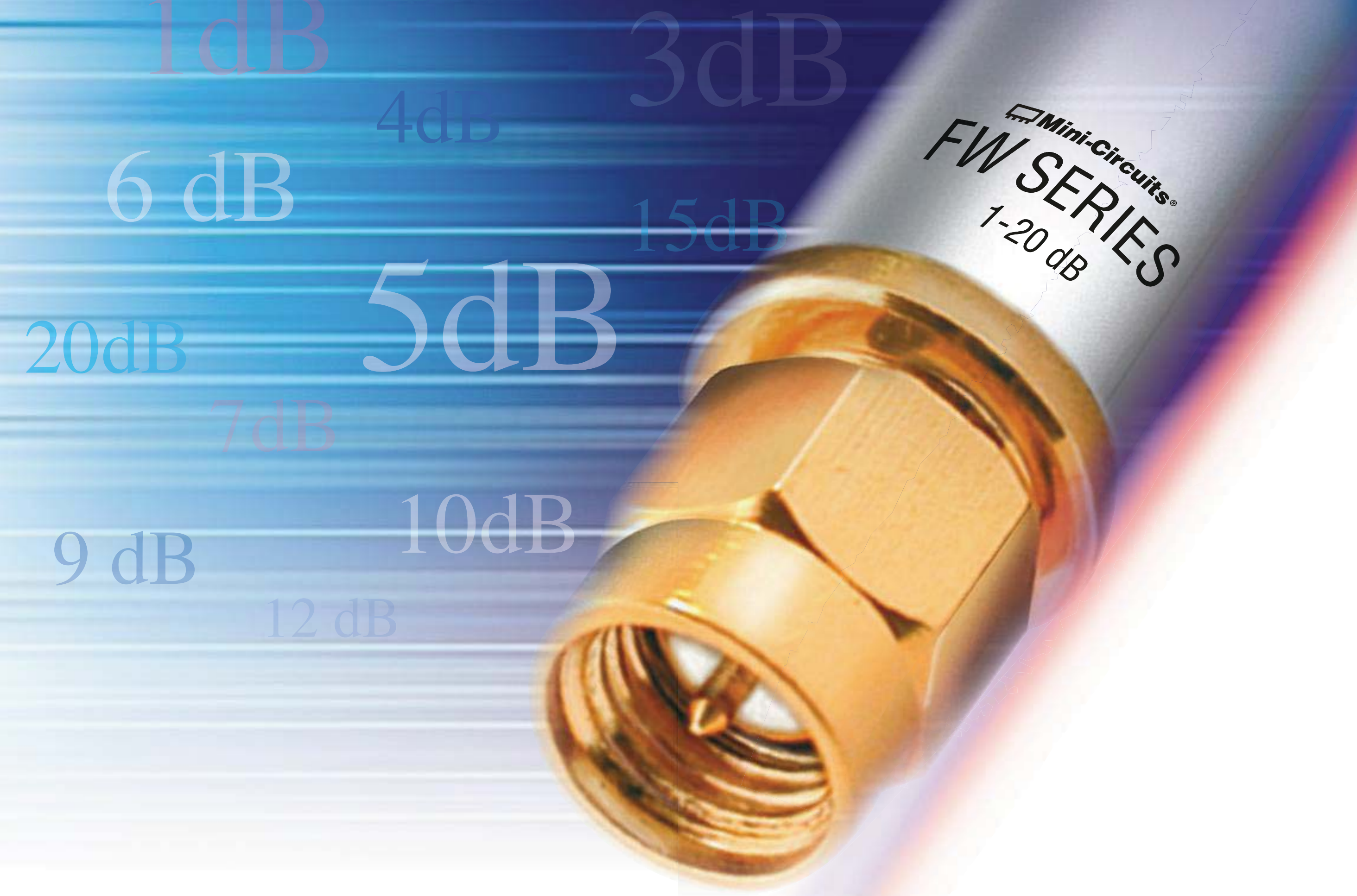

DC-12 GHz 1W Attenuators

only $18.95 ea. qty.1-9

Accurate attenuation over ultra-wide frequency range at low cost! Mini-Circuits' new FW-series fixed SMA attenuators cover your applications from DC – 12 GHz with a wide selection of attenuation values to meet your needs. All models offer excellent attenuation flatness versus frequency, low VSWR, and 1W input power handling, making them ideal, cost-saving solutions for impedance matching and signal level adjustment in a broad range of systems.

Built using Mini-Circuits rugged unibody construction with SMA(M) to SMA (F) connectors, FW-Series attenuators provide outstanding reliability in tough operating conditions. Just go to minicircuits.com for full specs and see how these attenuators can add performance and value to your design! They're available off the shelf for immediate shipment. Order today, and have them in hand as soon as tomorrow!

	ATTENUATION			
Model	Nominal (dB)	Flatness (dB)	VSWR (:1) Midband Typ.	Power (W)
FW-1+	1	±0.15	1.15	1.0
FW-2+	2	±0.15	1.15	1.0
FW-3+	3	±0.20	1.15	1.0
FW-4+	4	±0.20	1.15	1.0
FW-5+	5	±0.20	1.15	1.0
FW-6+	6	±0.25	1.15	1.0
FW-7+	7	±0.25	1.15	1.0
FW-8+	8	±0.30	1.15	1.0
FW-9+	9	±0.30	1.15	1.0
FW-10+	10	±0.30	1.15	1.0
FW-12+	12	±0.30	1.20	1.0
FW-15+	15	±0.35	1.20	1.0
FW-20+	20	±0.50	1.20	1.0

RoHS compliant.

Mini-Circuits®

www.minicircuits.com P.O. Box 350166, Brooklyn, NY 11235-0003 (718) 934-4500 sales@minicircuits.com

Inside TRACK with Tim Morin,

Director of Marketing, Microsemi

Interview by JEAN-JACQUES DeLISLE

JJD: What are the largest technology challenges in fulfilling Internet of Things (IoT) market demand and growth?

TM: it's important to note that some semiconductor manufacturers focus on edge devices for the IoT and other hyperconnected applications. In contrast, companies like Microsemi are primarily focused on the associated communications infrastructures and how they are being impacted by growing security requirements—not just in the IoT, but also in the power grid, avionics, mobile networks, medical telemetry, transportation, and space systems, among others.

From our standpoint, there are several challenges in the IoT space—the first being availability of a proper Internet connection throughout the home or enterprise environment. Available connectivity drives the need for technologies like power-line communications (PLC). The second challenge relates to content and applications that can apply to in-car communications as easily as smart TVs and others. Once the connection, content, and applications are available, there also is the issue of ease of use and flexibility. Finally, security becomes important in a hyperconnected world. Communication must be secured against malicious monitoring and modification if connected machines are to be used safely and with confidence. This is most effectively achieved with machine-to-machine (M2M) authentication using Public Key Infrastructure (PKI), where the Private Key in the Public/Private Key scheme is derived from a physically unclonable function (PUF).

Additionally, a key challenge and common requirement for IoT and other infrastructure segments is "time." There is a need to discover how to harness time in order to synchronize secure communications systems, protocols, and applications so they all work together. Technologies for timing and synchronization solutions include ICs focused on timing for package networks and open-transport-network (OTN) systems. Otherwise, solutions are already available to tackle the challenges that arise across the rest of the IoT's security, power, reliability, and performance requirements. Examples include field-programmable gate arrays (FPGAs); RF and mixed-signal technology; and integrated circuits spanning applications including Power over Ethernet (PoE) and Reverse Power Feed (RPF), for next-generation power and data networking.

JJD: As the smart vehicle—specifically the electric car—becomes an integral part of our connected world, where does vehicle-to-grid (V2G) communications come into play?

TM: According to Navigant Research, V2G applications modulate the power flowing to (and in some cases, from) electric vehicles (EVs) to enable grid operators to match power supply and demand. This capability is expected to make the grid more energy efficient. The firm has reported that by 2022, demand response programs will be able to control nearly 640 MW of load from EVs. In the V2G infrastructure, however, privacy concerns will again be an issue. Plugging the vehicles in the recharging infrastructure may expose private information such as a user's locations and traveling habits.

JJD: How are the technologies developed for V2G communications also useful for RF applications for home automation, industrial IoT, and smart-grid solutions?

TM: In today's enterprise, telecommunications, and mobile-network infrastructures, a host of requirements is pushing semiconductor solutions to help implement, secure, and synchronize everything from X-band weather/radar systems and GPS solutions to medical telemetry and mobile backhaul equipment. One of these application examples is the power grid, which is moving to a two-way system that allows homes to generate their own electricity with solar energy. Such systems require secure and precise bidirectional communications between utilities and customers for more efficient power production and use.

JJD: As everything becomes connected and that information is readily available, what are some concerns for IoT security regarding home, automotive, and personal devices in particular?

TM: Security is a major concern for the remote, increasingly compact, and power-conscious advanced systems that support the IoT. These systems offer an ideal gateway for malevolent hackers. As a result, there is a critical need for security solutions that protect embedded intellectual property, system data, and the system itself by defending against the installation of malicious code, cloning, reverse-engineering, or tampering. FPGAs play a significant role in meeting these objectives.

JJD: As a recent component in all flexible radio devices, how are FPGAs enabling cutting-edge security features for IoT solutions?

TM: FPGAs are making base-level security easy to use and adopt by system architects. As FPGAs with embedded processors become the core of new systems, system-on-a-chip (SoC) FPGAs will ideally be provided with leading-edge embedded security features. Examples include physical unclonable functions, cryptographic accelerators, random number generators, and Differential Power Analysis (DPA). With such countermeasures in place, the system architect can layer in the security needed throughout the system.

"FPGAs are making base-level security easy to use and adopt by system architects."

JJD: What are the additional costs and technology options for adding security to IoT solutions?

TM: The Internet of Things is essentially a collection of electronic networks that need end-to-end layered security that begins at the device level—and includes secure hardware, design security, and data security. Adding this security does come at a cost. These cost-related decisions begin with the choice between application-specific integrated circuits (ASICs), application-specific standard products (ASSPs) and FPGAs for IoT-system designs.

While FPGAs have traditionally been more costly than ASSPs or ASICs, they generally offer the fastest way to integrate a specific design into a single device. On top of that, they promise to support and facilitate field upgradability, design flexibility, and faster time-to-market. With the promise of significantly better overall total cost of ownership (TCO) compared to ASICs in many next-generation designs, FPGAs can play a pivotal role in improving security through the utilization of unique built-in features and differentiated capabilities.

However, it is essential that all FPGAs used in IoT and other hyper-connected system designs be protected from cloning, reverse engineering, and tampering in order to protect embedded intellectual property (IP). In addition, FPGAs need to include embedded-device security technology that makes base-level security easy to use and adopt. The best way to achieve this is to use flash memory rather than static random access memory (SRAM). The latter requires configuration from an external memory device each time it is turned on, which exposes the design to reverse engineering. Storing the configuration information in on-chip nonvolatile memory makes it impossible to capture the information. At the same time, it prevents reverse engineering and tampering.

JJD: How do FPGAs impact the power budget of low-power IoT systems?

TM: On the power front, FPGAs enable today's high-speed, DSP-intensive system designs by delivering not only the lowest possible static power, but the lowest total power as well—especially at lower frequencies and high temperatures. This requires a comprehensive approach encompassing process technology, architecture, and the design of configurable logic, as well as the inclusion of embedded features including SerDes, DDR2/3, and DSP blocks. mw

MEMS SWITCH HITS MILLIMETER-WAVE FREQUENCIES

ACTIVE COMPONENTS, SUCH as millimeter-wave switches, will be critical to the use of millimeter-wave frequencies beyond 60 GHz. With that in mind, researchers Nahid Vahabisani and Mojgan Deneshmand at the University of Edmonton, Canada, developed a monolithic wafer-level, micro-electromechanical-systems (MEMS) waveguide switch for mm-wave applications.

The pair designed the waveguide switch using staggered layers of MEMS actuators based on cantilever structures. The actuators are designed to bridge their contact from the bottom groundplane to the grounded top plane of the waveguide.

To analyze the cantilever's effectiveness, a simulation and fabrication study of 400-μm and 1-mm lengths and 50-μm and 100-μm widths was performed. The experimental results yielded a wideband switch covering 60 to 75 GHz that exhibits on-state insertion loss down to 0.2 dB and off-state isolation of 22 dB. See "Monolithic Millimeter-Wave MEMS Waveguide Switch," *IEEE Transactions on Microwave Theory and Techniques*, Feb. 2015, p. 340-351.

CARDBOARD AND INKJET-PRINTED SILVER MAKE ONE GOOD POWER HARVESTER

DUE TO THE proliferation of sensors, these devices are beginning to fully embrace disposable packaging. Concerns over the environmental impact of RFID and wireless-sensor-network technologies, however, demand the development of environmentally conscious antenna solutions that are also cost-effective. To meet this future need, an inkjet-printed wideband planar monopole antenna on thin cardboard packaging was designed and tested by researchers Hossein Saghlatoon, Toni Bjorninen, Lauri Sydanheimo, and Leena Ukkonen from Finland's Tempere University of Technology, together with Manos M. Tentzeris from the Georgia Institute of Technology in Atlanta.

The researchers first had to choose viable materials that would perform well in fabricated and efficient power-harvesting technology while maintaining high standards of environmental safety. Naturally, already environmentally degradable and safe materials were chosen—fibrous cardboard and silver nanoparticles. To keep costs low, they decided to use common and cost-efficient inkjet-printing processes.

The challenge of developing a conformal planar monopole antenna was exacerbated by the uneven and fibrous roughness of the cardboard surface. Thus, a coating for the cardboard using the same inkjet process was developed. The nanoparticles could then be deposited conformably with a significant increase in efficiency. In experimental results, the antenna harvesting energy from 800 to 1500 MHz exhibited a minimum of 72% efficiency. Although this is substantially lower than the simulated efficiencies of 92%, the desired efficiency levels were achieved—even considering a variable conformity to the cardboard structure. See "Inkjet-Printed Wideband Planar Monopole Antenna on Cardboard for RF Energy-Harvesting Applications," *IEEE Antennas and Wireless Propagation Letters*, Oct. 2014, p. 325-328.

300-GHz TRANSCEIVER BOASTS ON-CHIP LOs AND MIXERS

AS AN ALTERNATIVE to high-speed communication buses, terahertz frequencies may be an option for close point-to-point communications for Internet of Things (IoT) and machine-to-machine (M2M) communications—both between devices and within larger systems. When implementing terahertz technology, though, the extremely small wavelengths force researchers to develop complete integrated solutions on a single chip. To achieve a fully functioning terahertz transceiver on-chip, for example, a 250-nm indium-phosphide (InP) double-heterojunction-bipolar-transistor (DHBT) process with integrated local oscillators (LOs) and mixers was used by researchers from Korea and the United States—Sooyeon Kim, Jongwon Yun, Daekeun Yoon, Moonil Kim, Jae-Sung Rieh, Miguel Urteaga, and Sanggeun Jeon.

To fabricate such a device, the researchers needed to build the LOs and mixers on-chip and with the same technology. Because they operate in the fundamental mode on the same chip, the LOs and mixers reduce the chip area and direct-current (dc) consumption. They also improve the RF performance characteristics of the transceiver. For its part, the RF amplifier typology includes a five-stage differential amplifier chain with input and output matching networks. It comprises five common-base HBT pairs cascaded with 32-μm intervals.

The receiver has a noise figure of 12.0 to 16.3 dB with an intermediate frequency of 1.1 to 7.7 GHz, 3-dB bandwidth of 20 GHz, and a peak conversion gain of 26 dB at 298 GHz. With comparable performance to the receiver, the transmitter exhibits a conversion gain of 25 dB at 298 GHz, a 3-dB bandwidth of 18 GHz, and output power of –2.3 dBm. Both the transmitter and receiver operate with a combined dc power consumption of less than 1 W. See "300 GHz Integrated Heterodyne Receiver and Transmitter With On-Chip Fundamental Local Oscillator and Mixers," *IEEE Transactions on Terahertz Science and Technology*, Jan. 2015, p. 92-101.

JEAN-JACQUES DELISLE | Technical Editor

THE TOP 6 CHALLENGES for Signal Generators Handling LTE, Wi-Fi, and 5G

With the onrushing bandwidth, frequency, and configurability demands, the next generation of signal generators is pushing the boundaries to cope with the data-driven LTE, Wi-Fi, and 5G standards.

FOR SIGNAL GENERATORS, the latest wireless standards and technologies are once again demanding performance that is beyond the capability of standard instruments. For research and development (R&D), design verification testing (DVT), and manufacturing automation, for example, the latest standards features are requiring test-and-measurement instrument designers to dramatically increase modularity and bandwidth. Here are discussions of the six top challenges of wireless signal generation and how the latest signal generators are stepping up.

1. We need more bandwidth. In the mid-2000s, the bandwidth expectation was pushing the boundary with UMTS at 5 MHz. Only a decade later, the demands for LTE and IEEE 802.11ac leapt forward with requirements to 100 and 160 MHz, respectively *(Figs. 1 and 2)*. As bandwidth climbed as a function of data demand on mobile devices, test-and-measurement companies began providing pre-release instruments until standard signal generators capable of those bandwidths were available—which was sometimes over a year. With 5G knocking on the door, there is again a significant demand for signal generators to exceed the bandwidths for current and later wireless standards.

According to Randy Becker, applications engineer for Keysight Technologies, "Key attributes for the next generation of wireless signal generators are wide bandwidths—up to a few gigahertz for future 5G applications—as well as the ability to simulate both multi-standard radios and a variety of interference signals." He added, "The highest-end signal generators will need to reach higher frequencies into the millimeter-wave bands, have multi-channel capabilities for MIMO/beamforming applications, and advanced channel emulation for determining receiver performance in repeatable 'real-world' conditions."

A challenge with cranking up the bandwidth of signal generators is maintaining a flat frequency and phase response across the bandwidth. Maintaining solid frequency and phase performance goes hand in hand with providing the ability to modulate

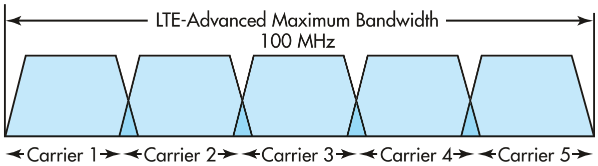

1. Thanks to carrier aggregation from the LTE-A standard, up to five 20-MHz carriers can be combined to generate an effective 100 MHz of bandwidth.

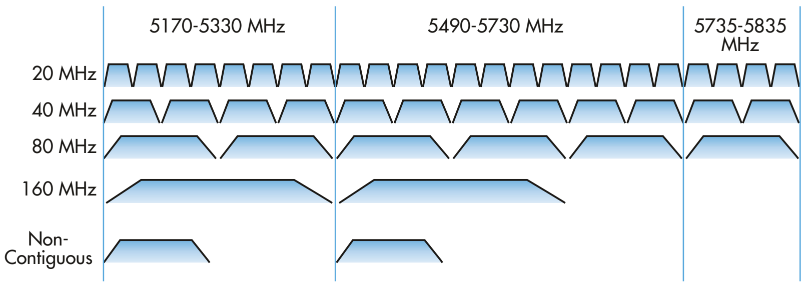

2. It's possible to implement 5-GHz WiFi with as much as 160-MHz effective bandwidth, which is either contiguous or noncontiguous. (Courtesy of National Instruments)

the latest wireless standards. Often, those standards have extremely narrow channel spacing and are susceptible to frequency and phase variations. For receiver testing, a signal generator also must maintain a very low noise floor and good voltage standing wave ratio (VSWR) in order to ensure accurate power of the applied signal. Thus, additional dimensions impact whether an instrument performs adequately over such a wide—and growing—bandwidth requirement.

2. Digital pre-distortion and envelope tracking require even more bandwidth. Another consideration is the need for signal generators to implement power-amplifier (PA) efficiency-enhancing techniques. To reduce spurious emissions and reach greater linear PA response, methods like digital pre-distortion (DPD) are used. They correct for signal distortion at the output of the PA. Envelope-tracking (ET) techniques are often used in conjunction with DPD, raising the PA's overall efficiency at the expense of increased complexity. Applying these techniques requires waveforms to be generated beyond the wireless standards' bandwidth in order to use the full bandwidth of the standard.

"Having 100 to 160 MHz of bandwidth from the signal generator to test a mobile device has become fairly standard, though testing PAs is actually still a challenge," said David Hall, marketing manager for National Instruments. "For example, many Wi-Fi PAs are now designed for use with DPD algorithms. As a result, in the IEEE 802.11ac case, the signal generator is required to supply a signal bandwidth that is higher than the 160-MHz channel bandwidth. In many cases, it is desirable for the signal generator to supply 2× to 3× the bandwidth of the channel—which is nearly 500 MHz in this case."

The large amount of bandwidth required to generate these signals is derived from the DPD and ET signals' need to include control of the modulated signal—control that will be achieved based upon distortion characteristics and the RF magnitude of the output signal. For ET and DPD, a lookup table (LUT) of finite correction factors is used. This approach induces clipping at the lower boundaries that are acceptable in the LUT.

With significantly enlarged bandwidths, however, very precise time resolution is required to successfully implement these techniques. Often, designers must reduce the practical bandwidth of their tests to accommodate the limits of modern signal generators. This limitation may prevent these techniques from being viable for the highest bandwidths of IEEE 802.11ac and 5G until the signal generators' performance can catch up.

3. Carrier aggregation, MIMO, and 5G require diversity and synchronization. Carrier aggregation (CA) requires that modulated signals be provided at various frequencies at the maximum bandwidth of an LTE channel. Using antenna diversity to increase data rate (such as with MIMO technology) requires modulated signals to be sent with a sophisticated layer of digital signal processing (DSP) over multiple antennas. Both of these techniques require multiple wide-bandwidth signal generators to transmit synchronized modulated signals. Understandably, the complexity and cost of synchronizing enough signal generators to realize a compound CA and MIMO system would scale with the number of carriers and antennas.

"Channel-to-channel synchronization and pure cost are some of the biggest challenges regarding MIMO testing," noted Hall. "In order to test receiver performance under true MIMO conditions, engineers must be able to provide a multichannel stimulus to the DUT. Typically, this stimulus comes from multiple signal generators and requires clock signals like the local-oscillator (LO) and reference clocks to be shared." Traditionally, this type of testing would require large numbers of costly rack-mount

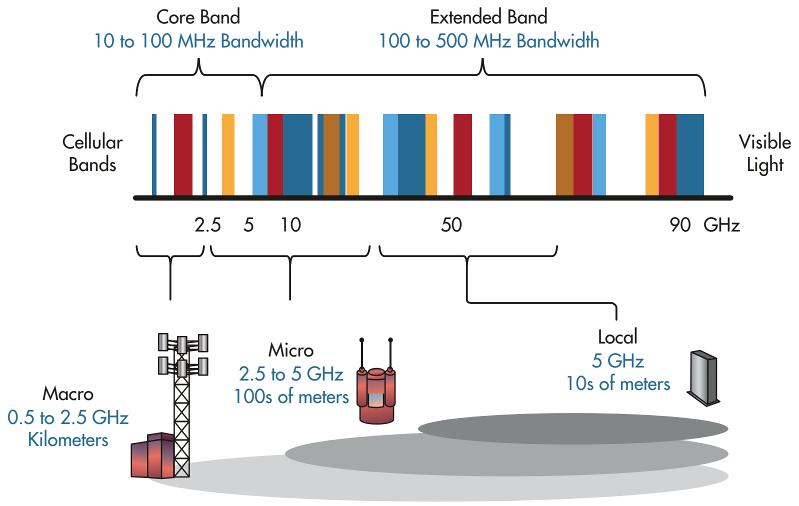

3. For short-range telecommunications, the latest 5G standard may operate deep into microwave frequencies with bandwidths ranging from hundreds of megahertz to 1 GHz.

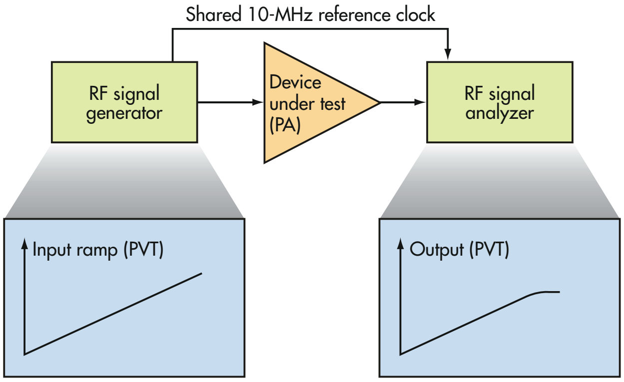

4. Any synchronization mismatch in the reference between a signal generator and a signal analyzer could induce significant errors in the test results for AM-AM/PM and memory effects.

equipment, which would not be feasible for higher-order and massive MIMO technologies as they scale.

Modular instruments packed with many multichannel signal generators can effectively tackle some of the latest wireless standard challenges. However, introducing 5G and other future applications—such as massive MIMO—may require hundreds of channels. The coherency challenges of synchronizing so many LOs and clock signals would be significant. However, signal generators designed on extremely integrated and modular platforms may be the only recourse, considering that 5G could reside in the upper microwave bands and use advanced beamforming techniques with active electronically steered arrays (AESAs) of antennas *(Fig. 3)*.

4. Wireless test requires generator and analyzer synchronization. In the testing of wireless devices, many instruments are used to measure the behavior of a passive or active component. Signal generators come into play when those components need to be tested using "real-world" signals. In contrast, signal/spectrum analyzers are used to measure component response *(Fig. 4)*. Naturally, these instruments require synchronization. For the latest modulation techniques, they also may need to coordinate their operation. For automated manufacturing test, this process needs to be performed rapidly.

"With a signal generator and signal/spectrum analyzer integrated into the same instrument, functionality opens up to test both the receiver and transmitter at the same time," said Becker. "Such an instrument enables new tests like ping-ponging and pipelining as well as system calibration—including the effects of the test fixture." With built-in automatic feedback, an integrated signal-generator-signal/spectrum analyzer is able to rapidly complete test routines and system calibrations while providing higher performance, thanks to the enhanced synchronization.

5. Theoretical and proprietary research requires flexibility. With wireless standards constantly evolving, a signal generator may quickly become obsolete as wireless standards incorporate new techniques and modes. In many research environments, multiple wireless standards may be of interest as well. Still, the cost of purchasing several instruments just to provide experimental justification for a wireless standard may not be in the budget. The customization of software-based signal-generator platforms may enable users to program their own waveform techniques. Yet self-creating and maintaining in-house

software for the latest standards can be time-consuming and resource-intensive. Many of the latest test instruments mitigate some of this challenge by building in the latest wireless standards, which can then be accessed using a simple soft-key.

"For signal generators not to be a limiting factor in wireless testing, they will need to become more flexible, as new and unforeseen needs will come along with future standards," noted Becker. "Field upgradability is also important alongside software with standards-compliant applications and the ability to custom-generate proprietary formats in the research phase."

While the performance specifications of modern signal generators remain critical, wireless testing has become so complex that raw performance is on par with the instrument's software features and configurability. To tackle the need for on-demand upgrades with the latest wireless standards, many test-and-measurement companies are including the ability to upgrade an instrument to the latest standards installments with a simple downloadable program or remote connection.

6. CPUs go out of style. Hardware obsolescence is one of the greatest challenges faced by equipment users in any technology field. Obviously, obsolescence makes maintaining precision test equipment difficult. It also means engineers must settle for using less optimal instruments for longer periods of time. In R&D and automated manufacturing test, this factor can increase costs and time for both developing and producing devices. With signal generators for wireless test in particular, the latest modulation techniques and waveforms could require more significant computation and DSP performance, which is often well beyond what present central processing units (CPUs) and field-programmable gate arrays (FPGAs) can handle. Modular and software-based instruments offer a partial solution to preventing an accumulation of costs and outdated equipment. Compared to traditional benchtop instruments, they often have components that can be more cheaply and rapidly replaced.

A significant drawback of many prior big-box instruments was that custom designs incorporated the CPU. This prevented upgrades and relegated an instrument to being obsolete in a few years. According to Hall, "Many engineers using PXI instruments in an automated wireless-test application can improve test time simply by upgrading the PXI controller. Because CPUs generally improve by 20% to 25% on an annual basis, maintaining the latest CPU is a great way to optimize measurement speed." mw

JEAN-JACQUES DELISLE | Technical Editor

Why More RF Engineers Are Choosing Fiber Connectors

Many applications, including indoor distributed-antenna and satcom systems, are adopting RF-over-Fiber technology, making it a useful technology for an RF engineer's toolbox. Here's why.

RF-OVER-FIBER TECHNOLOGY HAS been increasing in capability and dropping in cost over the past decade. Coupling these factors with the rising cost of coaxial-cable material has prompted many designers to choose RF-over-Fiber optic systems for distributed-antenna systems (DASs) and small-cell applications. Compared to traditional RF-transmission-line technologies, fiber optics offer additional benefits such as low loss, interference immunity, high reliability, and security.

RF-over-Fiber refers to the use of fiber-optic transmission cabling and RF-to-optical signal-conversion equipment that is used to transmit RF signals—generally over long distances. With many of the latest converters, the RF signal is sent directly to the electronics that power a laser diode. That diode is then used to transmit the optical signal along a single-mode fiber cable. The optical signal can be intensity-modulated. High-dynamic-range and low-noise applications typically employ a distributed-feedback (DFB) semiconductor laser. However, for lower-performance requirements, a Fabry-Perot (FP) laser is often implemented.

The optical fibers are made using a time-intensive and somewhat expensive process involving high-quality, specialized glass. This glass is formed into fibers with emphasis on an extremely consistent outer diameter and special jacketing. Specialized connectors and fiber-processing tools are needed to connect two fiber-optic lines together and reduce reflective losses. The single-mode fiber that serves RF applications will use an angle-physical-contact (FC/APC) connection.

For the optical-to-RF (O/RF) conversion, a high-speed PIN diode typically converts signals at a rate of 0.9 amperes per watt. Fortunately, the PIN diode has a relatively linear response curve, which limits the nonlinearities and distortion introduced into the signal chain by the conversion. Once it is converted into RF energy and amplified, the RF signal can be transmitted over short runs with traditional RF transmission lines to remote radio heads (RRUs) and then distributed antennas.

The key benefit of using fiber-optic cables for long-distance RF signal transmission is that fiber-optic transmission exhibits less than 0.5 dB of signal loss per kilometer of transmission. Coaxial cables tend to suffer loss ranging from tens to hundreds

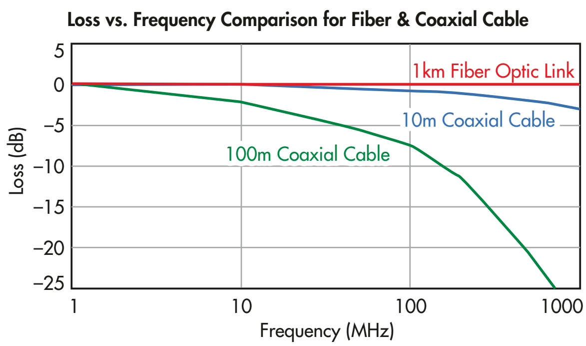

1. The transmission loss suffered by fiber-optic links is substantially less over distance when compared to a coaxial or waveguide transmission line. *(Courtesy of ViaLite)*

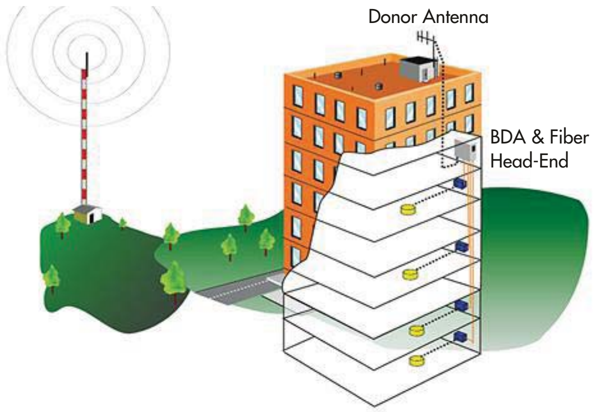

2. Using an RF-to-Fiber conversion can translate into much lower interference in the transmission line, as optical fibers are not conductive and not susceptible to RF interference. *(Courtesy of The Jack Daniel Company)*

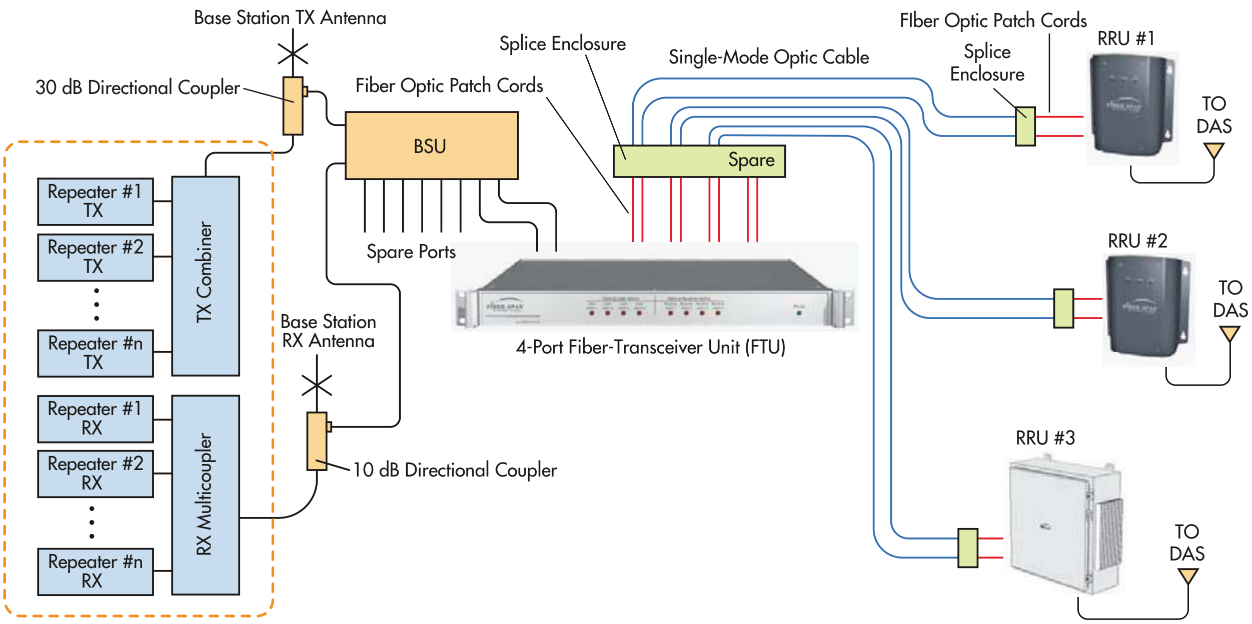

3. An RF-over-Fiber system requires an RF-to-optical and optical-to-RF conversion for transmission and reception from remote radio units. ***(Courtesy of Fiber-Span)***

of times worse than fiber optics. This loss depends on the frequency of the RF signals *(Fig. 1)*.

Although fiber-optic and RF cables have similar bending radius limits, fiber optics suffer additional loss from bends. Thus, they usually operate better under direct-run installations. Such straighter runs do not always pose a major challenge, as fiber-optic cabling is non-metallic and can be located near high-voltage and electrical cabling more safely.

The non-metallic and optical conversion in the RF-over-Fiber system also eliminates electromagnetic interference (EMI) and RF interference (RFI) from the transmission line *(Fig. 2)*. Resistive elements also produce noise naturally. As a result, fiber-optic systems tend to introduce less noise into the signal chain than coaxial cabling. Nevertheless, any interference encountered by the RF-to-optical or optical-to-RF conversion electronics will translate to noise and interference in the converted signal.

SAY GOODBYE TO MAINTENANCE WOES

While coaxial cables usually suffer from corrosion, moisture ingress, connector loosening, sparking from overvoltage, and dielectric breakdown, such factors are generally not concerns for fiber-optic lines. Particulates could build up within a fiber-optic connector, which would increase losses at the connector. Additionally, fiber-optic cables can be resilient in high-heat scenarios.

A distinct difference between fiber-optic and coaxial cables is that the conversion electronics "compress" the power envelope of the RF transmission *(Fig. 3)*. As a result, any electrical surges or noise outside of the transmission band of the RF-to-optical transmitter will not be carried through the optical conversion. Yet this bandpass-like function also reduces the maximum frequency of transmission through an optical line. Commonly available equipment ranges to 4 GHz.

As is the case with an RF system, there is a maximum power of transmission that an optical transmitter, the optical fiber, and the optical receiver can sustain and operate with linearity. The total power is a composite of all signal power across the whole bandwidth of the conversion operation. Often, bandpass filters are employed to enable passing of the bands of interest while limiting power in non-useful frequencies. This approach increases the channel-power headroom. The optical transmission system also is similar to an RF system in that it can induce interference if the same frequency of light is present on the fiber. To enable duplex operation, multiple fibers can be used for multiple uplink and downlink lanes.

Under conditions where limited fibers are available, duplexing can be done on a single fiber using different frequencies of transmission. This approach is called wavelength-division multiplexing (WDM). An optical fiber has a minimum and maximum frequency of operation, much as the different frequencies within a waveguide propagate with different transmission coefficients. Unlike an RF system, however, optical fiber lines are unidirectional and can have multiple frequencies transmitting in the same or different directions along the fiber.

Fiber optics have traditionally been cost-prohibitive in certain applications. But as the demand increases for multiple services and extremely wide-bandwidth operation, the return-on-investment considerations for RF-over-Fiber could certainly exceed those of coaxial cable. mw

Vector Signals at the touch of a button

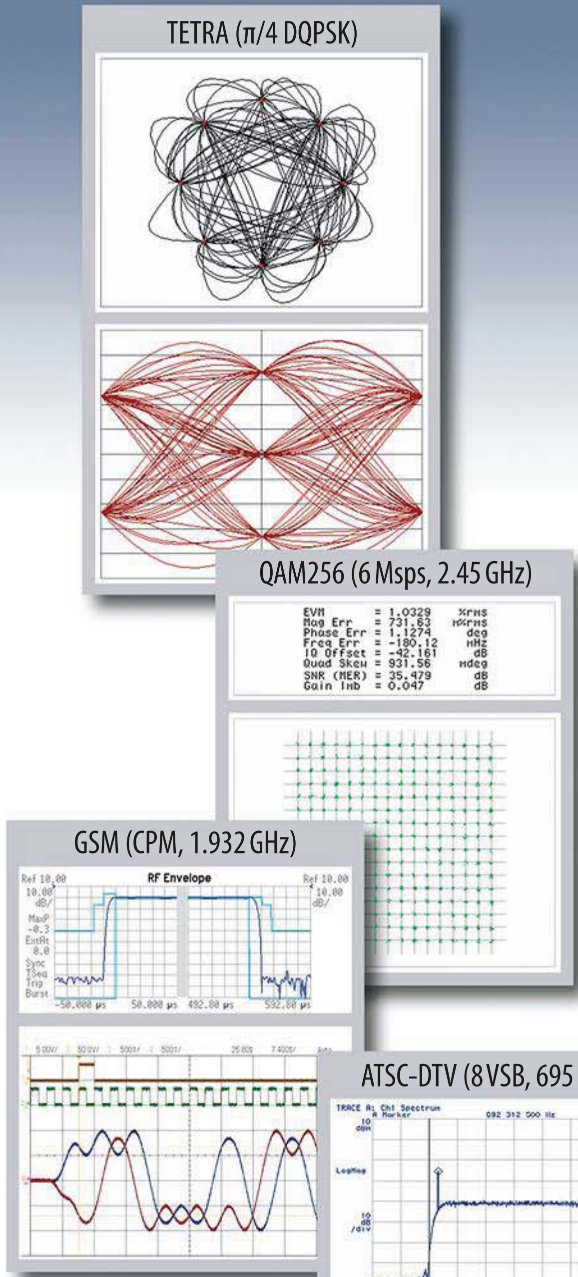

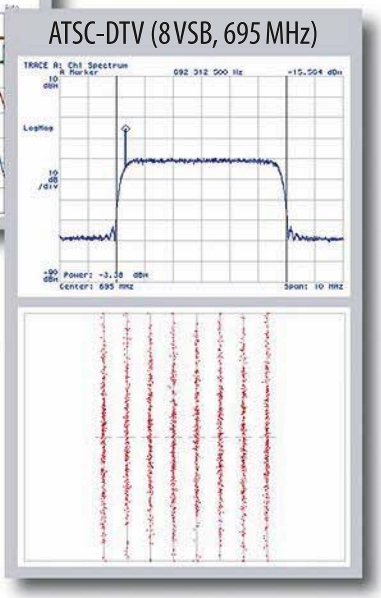

- 2 GHz, 4 GHz & 6 GHz models
- Dual baseband arb generators
- Vector & analog modulation
- I/Q modulation inputs (300 MHz RF BW)
- ASK, FSK, MSK, PSK, QAM, VSB & custom I/Q
- Presets for GSM, EDGE, W-CDMA, APCO-25, DECT, NADC, PDC, ATSC-DTV & TETRA
- GPIB, RS-232 & Ethernet interfaces

The SG390 Series ***Vector Signal Generators*** — taking communications testing to a new level.

The SG390 series has outstanding features and performance: complete vector and analog modulation, dual baseband arb generators, I/Q inputs with 300 MHz RF bandwidth, low phase noise, and an OCXO timebase are all included.

We've also made communications testing quick and easy — everything is available from the front panel of your instrument. Pulse shaping filters, TDMA gating signals, additive white noise, and event markers are all there. Use the built-in pattern or PRBS generators to create data, or upload your own symbol data. Map your symbols to any constellation and transmit at rates up to 6 Msps — it's that simple.

Pricing (U.S. list)

SG392 (2 GHz) ... $5,400
SG394 (4 GHz) ... $6,600
SG396 (6 GHz) ... $8,400

SRS Stanford Research Systems
Tel: (408)744-9040 • www.thinkSRS.com

What's the Difference between OpenVPX, OpenRFM, and MORA?

Using commercial strategies and technologies for military-grade RF/microwave systems promises to reduce costs while increasing flexibility.

AS A COST-SAVING strategy that adopts commercial processes, standards to increase the modularity and flexibility of electronic-warfare (EW) and signal-intelligence (SIGINT) equipment are being developed by military research organizations, device/component manufacturers, and standards groups. The motivation for this effort is to give warfighters the ability to compete in the rapidly evolving global arena. To keep pace with ever-changing commercial trends, standards like OpenVPX, OpenRFM, and MORA are seeking to provide swappable architectures that are openly available.

This approach requires a radical change in the thinking and philosophies around traditional EW equipment development. Common rack-mounting techniques and some widely used interfaces have become relatively standard in the warfighter. However, the development of these units has been led by only a few suppliers. OpenVPX, OpenRFM, and MORA seek to define a set of interface, control, software-layer, module dimensions, and powering protocols.

1. With the introduction of VITA 67.0, the coaxial interconnect through the backplane of the VPX card became standard. The result was decreased RF loss and noise to the card. *(Courtesy of CommAgility Ltd.)*

OPENVPX

The latest technologies for digital imaging, signal-intelligence (SIGINT) antennas, sensors, and radar continuously produce a massive amount of data; highly configurable real-time processing must be performed. OpenVPX is a widely adopted architecture framework within the system-level VPX standard. It specifically targets the support of a multi-module, integrated system environment, and multivendor interoperability using commercial-off-the-shelf (COTS) technologies. OpenVPX uses profiles, plans, and pipes as a basis for interoperability for plans, such as data, expansion, management, utility, and control. Profile hierarchies include slot, module, backplane, and development chassis profiles with pipes for serial communications.

OpenVPX has been embraced by companies like BittWare Signal Processing Systems, Mercury Computer Systems, and TEK Microsystems for the development of field-programmable gate arrays (FPGAs), digital-signal-processing (DSP) modules, and converter technology. These components are critical aspects of modern EW systems—specifically military radios. Yet FPGAs, CPUs, GPUs, and DSP electronics now rapidly become outdated due to the growth of the digital realm. As a result, the ability to rapidly design, upgrade, and deploy these devices is critical.

Although OpenVPX has been accepted as a major player in the embedded-computing portion of EW hardware, it is purely an embedded solution that interfaces with RF/microwave hardware. VITA 67 does address a common RF-coaxial-backplane connection. Yet there's much to be desired for an RF standard. As a basic concept and influencer on later RF/microwave EW open standards, OpenVPX has set the stage for the growth and development of common RF systems.

An example of an OpenVPX application is CommAgility's VPX-D16A4, which is a double-width AdvancedMC (AMC) card with RF mezzanines and a wireless-baseband-processing carrier card *(Fig. 1)*. The VPX-D16A4 provides military-grade and secure LTE and LTE-A communications capabilities for military communications and the wireless test market.

OPENRFM

Currently, OpenRFM is in the standards initiative phase. It was initially developed by Mercury Systems. The goal of OpenRFM is to follow what has been done with OpenVPX and other commercial standards for RF/microwave and digital subsystems for EW and SIGINT applications. The budding standard focuses on creating common approaches for EM and thermal interfaces, control-plane protocols, and software. OpenRFM uses OpenVPX or VXS/VME processing architectures. They are combined with the description for integrated-microwave-assembly (IMA) modules with an IP reuse structure *(Fig. 2)*.

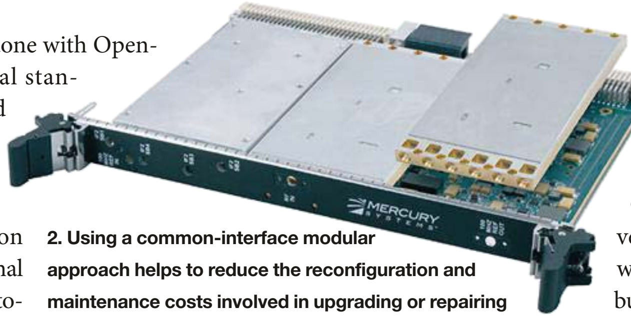

2. Using a common-interface modular approach helps to reduce the reconfiguration and maintenance costs involved in upgrading or repairing RF systems. *(Courtesy of Mercury Systems)*

"The common-core control architecture is based on a Xilinx system-on-a-chip (SoC) controller, which is at the heart of all of this. That is where the middleware and meta-command interpreter is," said Lorne Graves, chief technology officer for Mercury Systems. "With a 6U, OpenVPX allows us additional height so that power modules and other FPGAs can be added for the pre-processing of digitized data. As a result, you can basically combine RF, digital, and pre-processing all in one slot." For example, an IMA may comprise integrated switches/switch matrices, attenuators, oscillators, filters, and amplifiers along with other RF components.

According to Graves, "The current status of OpenRFM is still in development. But we have multiple modules already designed and products completed—a number of which are wideband carrier cards. There was an early introduction at AOC last October and the VITA annual conference this past January." OpenRFM also has been used in-house by Mercury Systems for several projects and products. Although its development is far from complete, the open invitation to participate in the growth of an RF standard with actual hardware and case-study examples could facilitate OpenRFM's adoption and evolution.

MORA

In a military-grown initiative, the U.S. Army Communications-Electronics Research, Development, and Engineering Center (CERDEC) has been developing the Modular Open RF Architecture (MORA). Although it is similar to OpenRFM, MORA encompasses a larger vehicle system. Its goal is to reduce the size, weight, and power (SWaP) of RF electronic systems by increasing hardware sharing and system flexibility, while at the same time reducing complexity and cost. Though OpenRFM can be applied to a variety of warfighter platforms, MORA aims to increase next-generation multifunction missions for military ground vehicles.

MORA uses the Vehicle Integration for C4ISR/EW Interoperability (VICTORY) data-bus-centric architecture for vehicle hardware platforms. Along with a common display, MORA strives to establish an open message interface that promotes the real-time coordination of support management operations.

MORA closely resembles OpenRFM with a ground-based vehicle spin, given its use of a software-defined radio (SDR), RF distribution device, Ethernet switch, VICTORY shared processing unit, and an integrated radio-head block. MORA also uses an IP-based interface on the VICTORY data bus. In addition, a MORA high-speed data bus could adopt 10 Gigabit Ethernet. A common RF cable bus, which could comprise coaxial cable or RF-over-Fiber optical transmission lines, connects the SDR, RF distribution device, and radio heads.

Like OpenRFM, MORA is still under development. Currently, it provides a backplane definition for each component in the standard. This includes a payload profile, RF switch profile, switch profile, and radio clock profile. It may use VITA 67.1 for RF coaxial interconnectivity, or VITA 47 for transporting RF signals digitally. Currently, PCI Express stands as a contender for the card-based radio and digital equipment.

Though OpenRFM, OpenVPX, and MORA share many of the same philosophies, their approaches and applications are somewhat divergent. OpenVPX is predominantly geared toward embedded systems and interconnectivity for EW applications with a few RF-connectivity add-ons. OpenRFM is a budding initiative that looks to bring the success of OpenVPX and commercial-computer system integration and standardization to the RF world. In doing so, it will make integrated modules and software abstraction protocols available for warfighters.

In contrast, MORA is geared toward creating common hardware and connectivity buses for military ground vehicles, which will translate into SWaP savings and increased ruggedness through redundancy. According to Adam Melber, Lead Electronics Engineer with of CERDEC I2WD's Intel Technology and Architecture branch,"Compared to a traditional radio solution, MORA provides the system integrator with increased flexibility to address technical challenges. Specifically MORA separates signal processing from signal conditioning to allow for hardware access where it is currently unavailable today.

"This decoupling, in turn, enables hardware reuse and pooling, rapid third-party technology insertion, reduced dependence on proprietary hardware and software, and the ability to improve compatibility and/or interoperability. MORA improves system efficiency and reduces overall power consumption by routing low-power signals between components and collocating amplifiers with antennas. Real-time control is accomplished using an addressable bus as opposed to point-to-point discrete signals to improve the scalability of a distributed system." mw

Amazingly Low Phase Noise

SAW VCO's

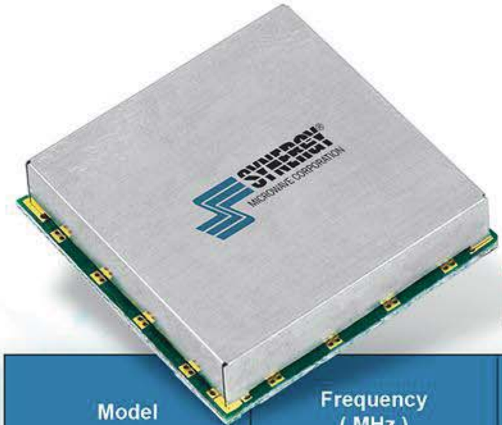

Features:

| Very Low Post Thermal Drift
| Small Size 0.5" x 0.5"

Note: * (0.75" x 0.75" models)

RoHS REL-PRO® Patented Technology

Model	Frequency (MHz)	Tuning Voltage (VDC)	DC Bias VDC @ I [Max.]	Phase Noise @ 10 kHz (dBc/Hz) [Typ.]
HFSO800-5	800	1 - 12	+5 @ 20	-146
HFSO800-5H	800	1 - 12	+5 @ 20	-150
HFSO800-5L	800	1 - 12	+5 @ 20	-142
HFSO1000-5	1000	1 - 12	+5 @ 35	-141
HFSO1000-5L	1000	1 - 12	+5 @ 35	-137
HFSO1600-5	1600	1 - 12	+5 @ 100	-137
HFSO1600-5L	1600	1 - 12	+5 @ 100	-133
HFSO2000-5 *	2000	1 - 12	+5 @ 100	-137
HFSO2000-5L *	2000	1 - 12	+5 @ 100	-133

Talk To Us About Your Custom Requirements.

SYNERGY®
MICROWAVE CORPORATION

Phone: (973) 881-8800 | Fax: (973) 881-8361
E-mail: sales@synergymwave.com
Web: WWW.SYNERGYMWAVE.COM
Mail: 201 McLean Boulevard, Paterson, NJ 07504

DR. AHMED BOUTEJDAR | Associate Professor
Chair of Microwave and Communication Engineering, Otto Von Guericke University of Magdeburg, Magdeburg, Germany; e-mail: boutejdar69@gmail.com, www.uni-magdeburg.de

AHMED A. IBRAHIM | Lecturer
Communications and Electronic Engineering Department, Minia University, El-Minia, Eqypt, e-mail: ahmedabdel_monem@mu.edu.eg, www.minia.edu.eg

DR. EDMUND P. BURTE | Professor, Chair of Semiconductors and Sensors
Otto Von Guericke University of Magdeburg, Magdeburg, Germany; e-mail: edmundburte@ovgu.de, www.ovgu.de

DGS RESONATORS Form Compact Filters

The use of DGS resonators can help to shrink bandpass and bandstop filters—at the same time achieving both high selectivity and sharp transitions from passbands to stopbands.

Rapid growth of modern communication systems has encouraged the development of a number of different compact filters with special specifications, such as multiband operation.[1] Defected ground structures (DGS) have been employed in a growing number of RF/microwave components, including power dividers/combiners and filters, to achieve high performance with small size.[2-9]

A DGS is constructed by etching a defected pattern on a printed-circuit board's (PCB) metallic ground plane, changing the effective capacitance and inductance of a microstrip line formed on that circuit and altering the current distribution on the ground plane. By consequence, a DGS exhibits slow-wave characteristics and rejects harmonics in microwave circuits, improving the performance of filters and other microwave circuits.

An inductive-capacitive (LC) equivalent circuit can be used to model a DGS resonator for calculations and circuit simulations.[10-14] Different DGS resonators used in microwave filters include low-pass, bandpass, and bandstop circuits consisting of certain resonators or transmission lines, with the DGS added to improve filter performance. For example, a bandstop filter (BSF) can be implemented using all shunt stubs or by means of series-connected high-low stepped impedance lines.

DGS resonators have been proposed for improving the spurious responses of microstrip filters.[15-18] When attempting to achieve good performance with high selectivity, microwave

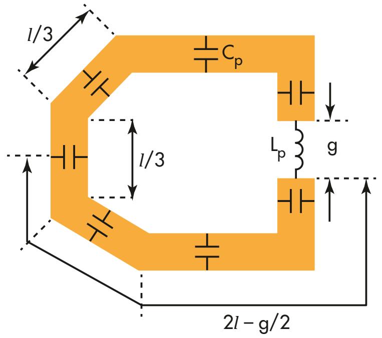

1. This represents a proposed DGS resonator and its equivalent-circuit model.

> "Different DGS resonators used in microwave filters include low-pass, bandpass, and bandstop circuits consisting of certain resonators or transmission lines, with the DGS added to improve filter performance."

filters with transmission zeros should be designed.[2] Having transmission zeros at finite frequencies provides sharp cutoff slopes at transitions from passbands to stopbands, which can be useful for many applications.

To demonstrate the present design approach, both compact microstrip bandstop and bandpass filters (BPFs) will be spotlighted—each based on the use of two DGS resonators. The filters are compact and also provide sharp transition responses. The design technique will be explored through the use of commercial circuit simulation software, including popular simulators from Applied Wave Research (www.awrcorp.com) and Computer Simulation Technology (CST; www.cst.com), with measurements of prototypes compared with the simulations to see how closely they match.

A DGS resonator etched in a metal ground plane is shown in *Fig. 1*. The open-loop DGS resonator features sharp angles to reduce passive parasitic capacitances and decrease the size of the DGS cell. The open-loop DGS resonator consists of two capacitive arms that are connected via a rectangular metal stub. The etched DGS achieves an equivalent capacitance while the metal area between the two arms achieves an equivalent inductance. The size of the open-loop DGS arm equals 4l – g from *Fig. 1*. The proposed DGS resonator corresponds to the equivalent-circuit LC model[3] demonstrated in *Fig. 1*.

Values for the resonator's inductor and capacitor, L_p and C_p, can be computed by means of Eqs. 1 and 2[7]:

$$C_p = 5f_c/\pi(f^2_0 f^2_c)\text{pF} \quad (1)$$

$$L_p = 250/C(\pi f_0)^2\text{nH} \quad (2)$$

where:
f_c = the cutoff frequency (in GHz), and
f_0 = the resonant frequency (in GHz) calculated from the transmission characteristics of the quasi-ring DGS slot.

When the quasi-ring DGS slot in the ground plane of *Fig. 1* is excited by a 50-Ω transmission line, it performs as a parallel LC resonant circuit[10] and also exhibits one-pole bandstop characteristics *(Fig. 2)*. To better understand how changes in the dimensions of the DGS cell affected the behavior of the bandstop filter, a parametric analysis was conducted.

For example, *Fig. 2* includes the effects of changes in stub width, g, in the open-loop-ring DGS slot on the resonant frequencies of the filter. By changing the width of g, the cutoff frequency and attenuation pole can be readily modified.

The length of the gap (arm) controls the effective capacitance of the microstrip line. As the metal stub width g increases, the cutoff frequency and the attenuation poles shift to higher frequencies. As *Fig. 2* shows, the resonant frequency jumps from 4.0 to 6.5 GHz as g increases from 3 to 7 mm. As g increases, the effective inductance decreases, so the resonant frequency increases. In this way, it can be seen that the stub width g controls the effective inductance, which in turn controls the resonant frequency.

Figure 3 contains a three-dimensional (3D) view of the proposed BSF. The filter consists of two overlapped DGS resonators etched into the bottom layer of the filter circuit, where distance,

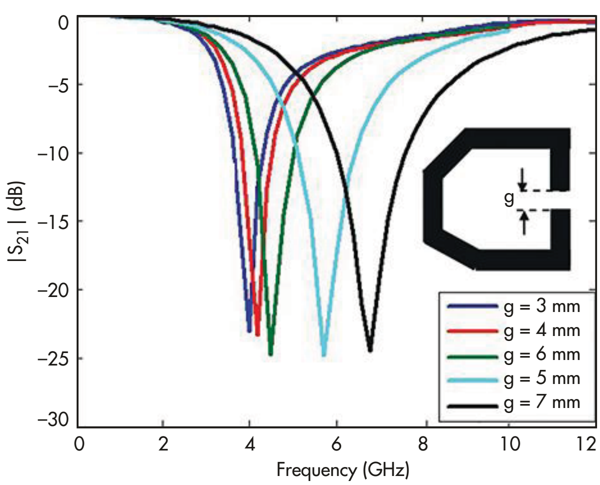

2. These simulations of S_{21} insertion loss show the impact of changing gap width g.

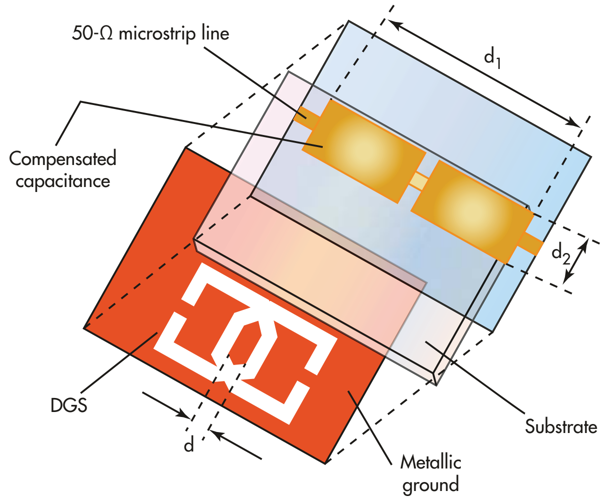

3. This is a three-dimensional (3D) view of the DGS bandstop filter (BSF).

d, equals 2.5 mm. In addition, two compensating microstrip capacitances on the top layer are connected by means of a 50-Ω microstrip line. Electrical coupling between the two DGS resonators is employed to improve filter performance.

The proposed bandstop filter was fabricated and measured with a model HP8722D vector network analyzer (VNA) from Agilent Technologies (now Keysight Technologies; www.keysight.com). The filter was printed on Rogers RO4003 PCB material from Rogers Corp. (www.rogerscorp.com) with a relative dielectric constant, ε_r, of 3.38 measured at 10 GHz through the z-axis (thickness) of the material.

The PCB material had a thickness, h, of 0.813 mm. *Figure 4* is a photograph of the fabricated BSF.

This use of DGS resonators for the BSF makes possible an extremely compact filter. A total area of $0.50\lambda_g \times 0.25\lambda_g$ is occupied by the filter circuitry, where the wavelength λ_g equals 38.5 mm. *Figure 5* offers a comparison of measured performance with simulations from the commercial simulation software. It is clear from the simulations that the filter's center frequency $f_0 = 4.1$ GHz with a cutoff frequency $f_c = 2.5$ GHz.

The simulated 3-dB stopband bandwidth equals 2.7 GHz. The simulation results showed that the designed filter has good transition characteristics and a symmetrical response *(Fig. 5)*. In addition, the measured stopband return loss and insertion loss are quite respectable: less than –20 dB and 0.7 dB, respectively.

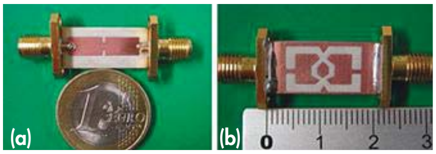

4. These photographs show the fabricated DGS BSF: (a) top and (b) bottom.

The results of *Fig. 5* show that the use of electric coupling between the two DGS resonators serves to enhance the performance of the BSF, arming it with a wide rejection band and sharp transition from the stopband to the passband. The design strategy produces reflection transmission zeros on both sides of the stopband center frequency to help increase the selectivity of the filter.

Less-than-positive results were achieved for the BPF; *Fig. 6* offers a 3D view. The structure has a small gap with separation distance, s, equal to 5 mm between the microstrip feeds to the admittance inverter, J. In this case, the transmission characteristics are inverted, causing the structure to act as a BPF. *Figure 7* offers results of a commercial electromagnetic (EM) simulation program used to analyze this structure. Simulated results reveal that the filter circuitry behaves much like a BPF, with center frequency f_0 at 5 GHz.

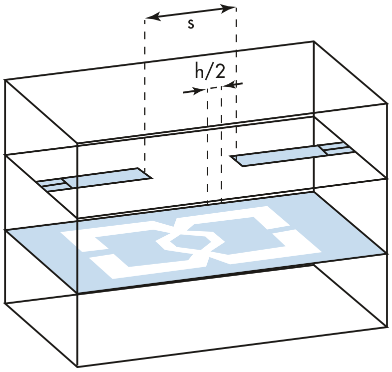

6. This is a 3D view of the DGS BPF formed from the use of a J-inverter with the BSF.

The return loss is predicted as being more than 20 dB across the passband from 4.5 to 5.7 GHz, while the simulated passband insertion loss is less than 1.9 dB from 4.5 to 5.5 GHz. Also, there's no spurious passband at $2f_0$. From the simulation results, two transmission zeros on both sides of the passband can be observed at 3.3 and 11.6 GHz. The BPF simulations show undue losses in the passband and a less-than-ideal upper-transition response. This poor performance can be attributed to poor coupling between the two adjacent DGS resonators.

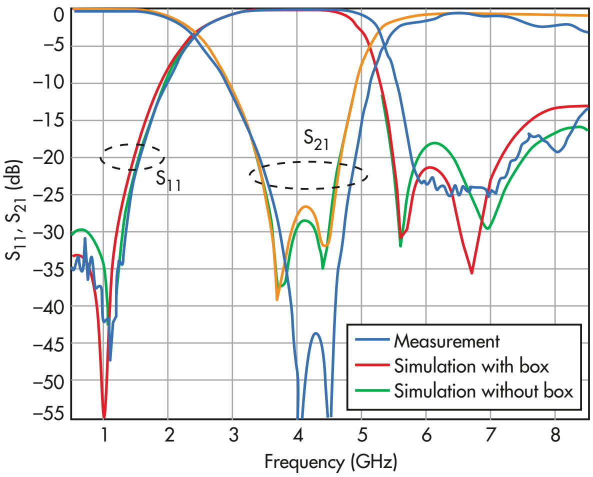

5. These traces are measured and simulated S-parameters.

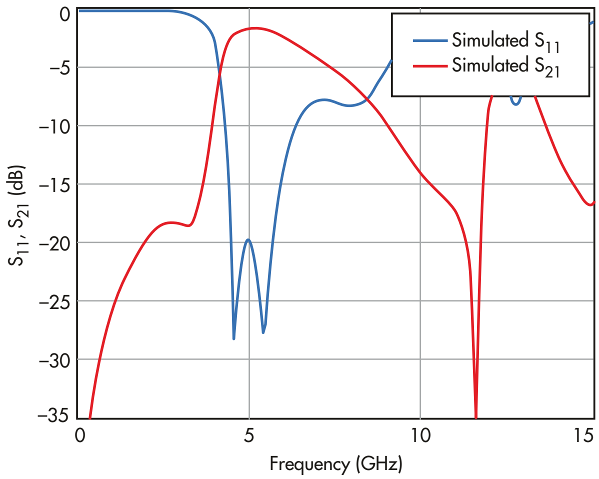

7. These traces show simulated S-parameters for the DGS BPF.

Turn Smart Power Sensors into Low-Cost RF Power Meters!

USB & Ethernet POWER SENSORS *from* $695 *ea. qty. (1-4)*

Mini-Circuits' RF power sensors turn almost any Windows® or Linux® based computer into a low-cost testing platform for all kinds of RF components and applications. To give you even more options, our new PWR-8GHS-RC model allows easy remote signal monitoring and data acquisition with USB and Ethernet control.

With 7 different models in stock offering measurement speeds as fast as 10 ms*, dynamic range as wide as -35 to +20 dBm†, and measurement capability for continuous wave and modulated signals, chances are, we have a power sensor to meet your needs and fit your budget!

Our user-friendly GUI provides a full range of measurement tools including measurement averaging, time-scheduled measurements, multi-sensor support, and measurement applications supporting RF testing of couplers, filters, amplifiers and more! View data and graphs on-screen or export to Excel® for reporting and data analysis.

All Mini-Circuits power sensors fit in your pocket and come supplied with all the accessories you need for immediate use right out of the box. Visit minicircuits.com and place your order today for delivery as soon as tomorrow!

RoHS compliant

Model	Power Measurement	Frequency MHz	Control Interface	Price $ ea. (Qty 1-4)
PWR-2.5GHS-75 (75Ω)	Peak	0.1 to 2500	USB	795.00
PWR-4GHS	Peak	0.009 to 4000	USB	795.00
PWR-6GHS	Peak	1 to 6000	USB	695.00
PWR-8GHS	Peak	1 to 8000	USB	869.00
NEW! PWR-8GHS-RC	Peak	1 to 8000	USB & Ethernet	969.00
PWR-8FS	Peak	1 to 8000	USB	969.00
PWR-4RMS	Average	50 to 4000	USB	1169.00

*Measurement speed as fast as 10 ms for model PWR-8-FS. All other models as fast as 30 ms.

†Dynamic range as wide as -35 to +20 dBm for model PWR-4RMS. All other models as wide as -30 to +20 dBm.
Excel is a registered trademark of Microsoft Corporation in the US and other countries.
Neither Mini-Circuits nor Mini-Circuits Power Sensors are affiliated with or endorsed by the owners of the above-referenced trademarks.

Mini-Circuits®

www.minicircuits.com P.O. Box 350166, Brooklyn, NY 11235-0003 (718) 934-4500 sales@minicircuits.com

532 rev A

As *Fig. 7* shows, the results for the proposed bandpass filter were not very satisfactory. The passband loss is relatively high, while the absence of transmission zeros can be blamed for the lack of passband flatness and transition sharpness. To improve upon these shortcomings, a structure with a different topology was designed. An optimized structure was investigated by examining the impact of the external coupling between the feeds and the DGS resonators. This was done by shifting, step by step ,the microstrip feeds from the center of the structure to the edge of the structure, as shown in *Figs. 8 and 9*.

When the feed was moved from the center of the DGS to the edge, the filter characteristics were greatly improved *(Fig. 10)*. Optimum results were achieved when the feed positions were located on the edge of the DGS. By moving the feed positions to the edge of the DGS resonator and using a prober to control the distance, k_2, between the two feeds, a BPF with high selectivity can be produced *(Fig. 11)*.

The simulations of this modified filter reveal a center frequency, f_0, of 4.9 GHz, with a 3-dB bandwidth of approximately 280 MHz from 4.70 to 5.01 GHz. This filter design also shows low passband insertion loss of around 0.1 dB and excellent response symmetry. The filter design has two transmission zeros at 4 and 6 GHz, located close to the edges of the passband. This provides good selectivity and high stopband rejection for the BPF.

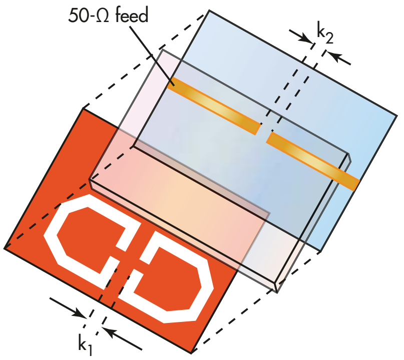

8. This is a 3D view of the DGS BF (with the feeds at the center).

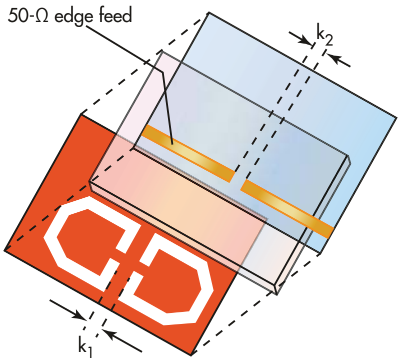

9. This is a 3D view of the DGS BF (with the feeds on the edges).

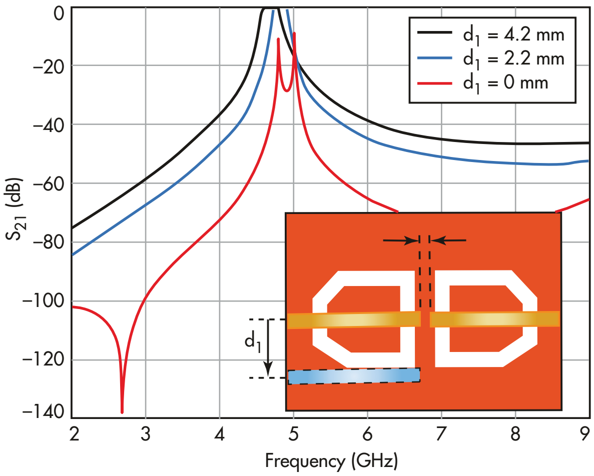

10. The S_{21} values are plotted for different values (in mm) of d_1.

To learn how to adjust the transmission zeros created in the lower and upper stopbands, and thus realize a desired passband bandwidth, as well as control sharp rejection characteristics, the effects of varying the width of gap k_2 on the transmission zeros were studied. *Figure 12* shows the dependence of J-inverter width k_2 on the positions of the transmission zeros. If all other parameters are kept constant and only k_2 is varied, it is relatively easy to control the position of the transmission zeros and the bandwidth and transition sharpness between passband and stopbands.

If k_2 increases, the positions of the upper and lower transmission zeros are shifted to higher and lower frequencies, respectively. Similarly, if k_2 decreases, the positions of the upper and lower transmission zeros are shifted to lower and higher frequencies, respectively.

To gain even greater insight into the filter design approach when using DGS resonators, a near-field distribution of the bandpass filter was computed *(Fig. 13)*. The filter's electric

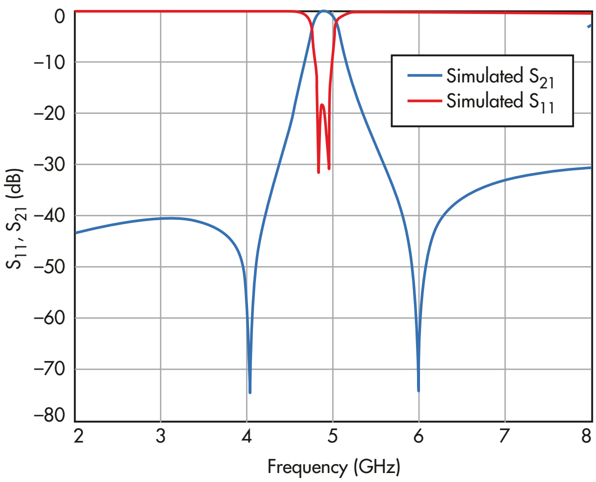

11. The traces show simulated S-parameters for the BPF.

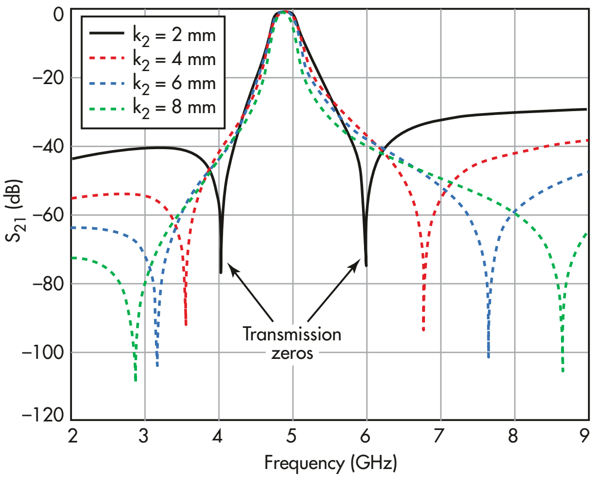

12. The plots show the S-parameters for different values of k_2 (in mm).

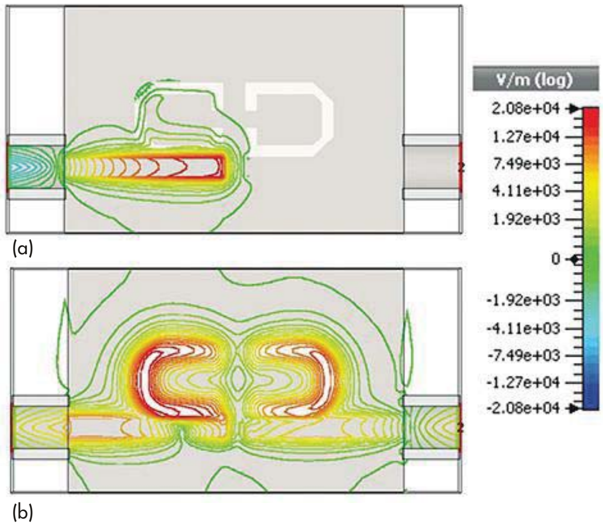

13. These are electric-field distribution results for the BPF: (a) in the stopband at 3.5 GHz and (b) in the passband at 4.8 GHz.

field was computed for two frequencies, in the passband and stopband regions. When at 3.5 GHz, the electric field exhibits high density around port 1 (the input feed port) with no energy flow around port 2, thus displaying strong stopband behavior *[Fig. 13(a)]*.

On the other hand, the electric field has high density at 4.8 GHz along the filter structure from ports 1 to 2 (across the DGS resonators) for good passband behavior *[Fig. 13(b)]*. The electric-field patterns indicate good coupling between the feeds and the DGS resonators.

In summary, the use of DGS resonators made it possible to design and fabricate compact filters in a microstrip. A simple transformation from a BSF to a BPF was achieved with the help of a J-inverter and some external coupling methods applied to the resonators.

FILTERING THROUGH FUNDAMENTAL SPECS

FILTERS HAVE LONG been a part of RF/microwave systems, as a means to isolate and separate signals in communications networks, radars, and other applications. Circuits such as bandpass filters (BPFs) and bandstop filters (BSFs) must often be specified for different applications, and selecting a "good fit" for a particular purpose is often more than simply searching for the smallest design possible. While the use of defected ground structures (DGSs) is one way to effectively shrink the size of a high-frequency BPF or BSF, a number of other specifications must be considered when sorting through RF/microwave filters from different suppliers.

BPFs and BSFs have considerably different functions; it therefore follows that their specifications will also be different. A BPF is typically judged by its passband characteristics, including passband insertion loss. Ideally, the passband insertion loss should be as low as possible and consistently low as possible across the full passband with no glitches. The BPF should provide as much rejection of unwanted signals as possible, both in its lower stopband and upper stopband outside of the low-loss passband. A BPF's passband insertion loss is also typically judged across an operating temperature range, and should remain as low as possible even when working at the highest temperatures within that range.

In contrast, an RF/microwave BSF is designed to remove signals from a certain band of frequencies within a system, while leaving signals outside of that stopband with little or no loss. Of course, every filter has limits on its total bandwidth, so this type of filter will be specified by the frequency range of its stopband as well as the frequency ranges of its upper and lower passbands. A BSF should provide a minimum amount of signal rejection in its stopband and minimal insertion loss in its passbands.

When attempting to shrink both types of filters, some laws of physics must still be obeyed, including the fact that handling power is generally a function of filter size and amount of loss. For example, a BPF that is designed for surface-mount packaging might simply be too small to handle continuous-wave (CW) power levels in excess of 50 W or more. If it suffers high insertion loss in its passband, the amount of power that it will handle will decrease as the amount of loss increases. Similarly, a bandstop filter will handle a certain amount of power based on its physical size, with smaller designs simply limited by the amount of heat they can dissipate.

The computer simulations performed on the filter circuits agree fairly well with measured results. They show that the use of DGS resonators offers great promise for the design of at least two types of compact microstrip filters. mw

REFERENCES

1. A. Boutejdar, A. Omar, and E. Burte, "LPF Builds On Quasi-Yagi DGS," Microwaves & RF, Vol. 52, No. 9, 2013.

2. Lung-Hwa Hsieh, "Tunable microstrip bandpass filters with two transmission zeros," IEEE Transactions on Microwave Theory & Techniques, Vol. 51 , No. 2, 2003, pp. 520-525.

3. A.A. Elrahman, A.Z. Eldein, A.A. Elmonem, and H. Fathi, "Small size defected ground structure (DGS) coupled resonator band pass filters with capacitor loaded slot using FDTD method," WSEAS Transactions on Communications, Vol. 10, No. 3, 2011, pp. 88-99.

4. A. Boutejdar, A. Omar, E.P. Burte, R. Mikuta, and A. Batmanov, "DGS and Multilayer Methods Make LPF," Microwaves & RF, Vol. 50, No. 3, 2011, pp. 61-72.

5. J.-S. Lim, Ch.-S. Kim, Y.-T. Lee, et al. "A new type of low pass filter with defected ground structure," Technical Program, European Microwave Week, Milan, Italy, September 24-26, 2002.

6. Adel B. Abdel-Rahman, Adel Z. El Dein, Hesham F.A. Hamed, and Ahmed A. Ibrahim, "Small Size Third order coupled resonator band-pass filter using capacitor loaded slots," IEEE Middle East Conference on Antennas and Propagation (MECAP), Cairo, Egypt, 2010.

7. A. Boutejdar, S. Amari, and A. Omar, "A novel compact J-Admittance inverter coupled microstrip bandpass filter using arrowhead shape as defected ground structure (DGS)," Microwave and Optical Technology Letters, Vol. 52, No. 1, January 2010, pp. 34-38.

8. Ahmed Boutejdar, "New Method to Transform Band-Pass to Low-Pass Filter Using Multilayer- and U-Slotted Ground Structure (SGS)-Technique," Microwave and Optical Technology Letters, Vol. 53, No. 10, October 2011, pp. 2427-2433.

9. A.K. Verma and A. Kumar, "Design of low-pass filters using some defected ground structures," AEU-International Journal of Electronics and Communications, Vol. 65, No. 10, 2011, pp. 864-872.

10. Mouloud Challal, A. Boutejdar, A. Azrar, and Danielle Vanhoenacker-Janvier, "Design of compact low-pass filter with large reject band using open circuit stubs and two-cascaded DGS quasi triangular resonators," Microwave and Optical Technology Letters, Vol. 55, 2013, pp. 122-127.

11. Dibakar Yadav, Tamasi Moyra, and Kaushik Debbarma, "Microstrip Hairpin Bandpass Filter with Improved Out of Band Performance", Emerging Trends in Computing and Communication Lecture Notes in Electrical Engineering, Vol. 298, 2014, pp. 27-32.

12. A. Abdel-Rahman, A. K. Verma, A. Boutejdar, and A.S. Omar, "Control of band-stop response of Hi-Lo microstrip low-pass filter using slot in ground plane," IEEE Transactions on Microwave Theory & Techniques, Vol. 52, March 2004, pp. 1008-1013.

13. A Boutejdar, "Design of broadstop band low pass filter using a novel quasi-Yagi-DGS-resonators and metal box-technique," Microwave and Optical Technology Letters, Vol. 56, No. 3, 2014, pp. 523-528.

14. A. Boutejdar and A. Omar, "Compensating For DGS Filter Loss," Microwaves & RF, Vol. 51, No. 2, 2012, pp. 68-76.

15. W.Q. Che, W.J. Feng, and K. Deng, "Microstrip dual-band bandstop filter of defected ground structure and stepped impedance resonators," International Journal of Electronics, Vol. 97, No. 11, 2010, pp. 1351-1359.

16. Jian-Kang Xiaoa and Yu-Feng Zhub, "Multiband bandstop filter using inner T-shaped defected microstrSip structure (DMS)," AEU International Journal of Electronics and Communications," Vol. 68, No. 2, February 2014, pp. 90-96.

17. Jia Shen, G. Hong, and M.J. Lancaster, Microstrip Filters for RF/Microwave Applications, second edition, (Wiley, New York, 2004).

18. A. Boutejdar, "New method to transform bandpass to lowpass filter using multilayer-and U-slotted ground structure-technique," Microwave and Optical Technology Letters, Vol. 53, No. 10, 2011, pp.

BOUALEM MANSOURI | Doctor
MEHADJI ABRI | Doctor
Telecommunications Laboratory, Faculty of Technology, University of Tlemcen, Algeria

MOHAMED AMINE RABAH | Doctor
HADJIRA ABRI | Doctor
STIC Laboratory, Faculty of Technology, University of Tlemcen, Algeria

JUNWA TAO | Professor
TAN-HOA VUONG | Doctor
LaPlace Laboratory, Ensheeiht, University of Toulouse, France

SIW Bandpass Filter Screens S-Band Signals

Substrate-integrated-waveguide (SIW) technology can be applied toward the design and fabrication of a low-cost, compact S-band bandpass filter.

Substrate-integrated-waveguide (SIW) technology can bring some of the performance benefits of waveguide transmission lines to compact microstrip printed-circuit-board (PCB) components, including filters. To demonstrate some of the promise of SIW technology, a bandpass filter was designed for use at S-band frequencies. By using resonant cavities based on SIW technology, excellent filtering results were achieved in the desired frequency bands. The filter achieved a passband of 2.75 to 3.40 GHz with low passband loss, with close agreement between measured and simulated results.

Expansion of telecom systems in recent years has required the development of high-performance equipment at reasonable prices. This need has impacted systems at all frequencies, including at RF and microwave frequencies. Some low-loss components, such as waveguide filters, have provided good performance—albeit with a tradeoff in size and weight, where some applications were in need of lighter, more compact components. SIW technology is one of the approaches that has provided high-performance component solutions at a fraction of the size and weight of traditional rectangular waveguide components.[1-4]

SIW technology combines some of the performance benefits of traditional rectangular waveguide with the compact size of planar transmission lines. The waveguide benefits include low loss, compact size, high quality factor (Q), and the potential for handling high power levels with low electromagnetic (EM) radiation. SIW approaches allow different components to be designed and constructed as integrated components with one manufacturing process, rather than build them separately and then combine them into a subassembly.

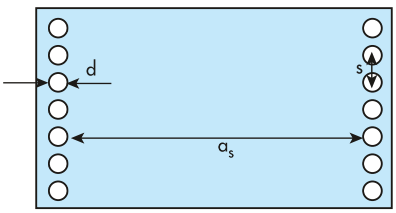

1. This diagram illustrates the SIW topology adoped for the bandpass filter.

Filters, phase shifters, antennas, and other components can be designed and constructed in SIW rather than in rectangular waveguide. This helps to reduce both the overall dimensions of a telecommunications system and the cost of manufacturing these components. Although SIW technology is still relatively new and not considered a mature technology, it has been applied to a number of different components and subsystems by different design teams and has shown consistent, stable performance over time and temperature.

In addition, with time, a growing number of SIW component models become available in commercial computer-aided-

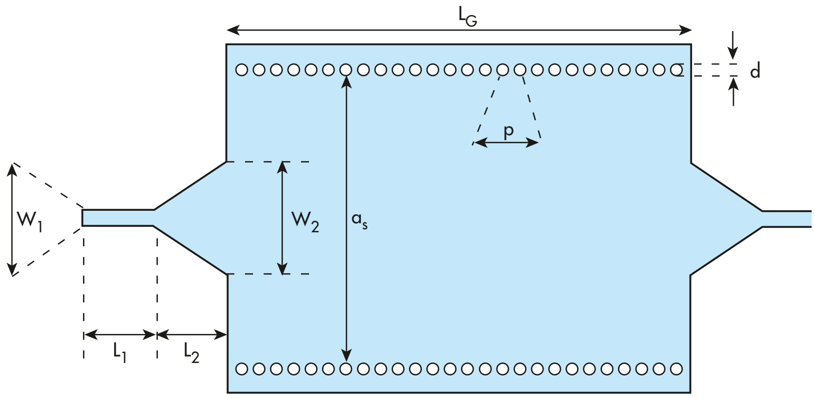

2. This is a top view of the SIW filter, with the following parameters: p = 3 mm; L_G = 80 mm; d = 2 mm; a_s = 51.4 mm; W_2 = 19.28 mm; W_1 = 2.99 mm, L_1 = 12.35 mm; and L_2 = 12.34 mm.

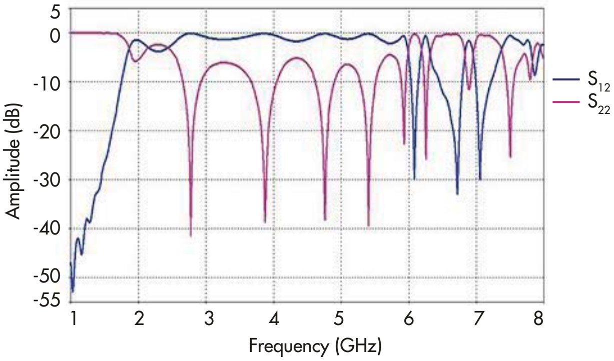

3. These are the return loss and transmission parameters for the filter with parameters of Fig. 2.

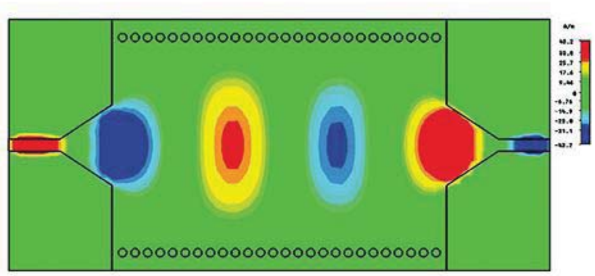

4. This image represents the electric-field propagation for the SIW conductors.

engineering (CAE) circuit simulation software. As examples, filters, couplers, and slot antennas have already been made with this technology with good results.[5-13] In addition, a number of different methods have been used for the characterization of these components to better understand the performance and behavior of SIW components.[14-19]

Filters, of course, are one type of component widely used in modern telecommunications systems, both for processing and providing selectivity among different signals. To explore the capabilities of SIW technology for fabricating filters for a variety of communications applications, a bandpass filter was designed for S-band frequency use based on SIW technology. A commercial circuit simulation software program, CST Microwave Studio from Computer Simulation Technology (www.cst.com),[20] was used to simulate the performance of the SIW bandpass filter design and help determine the validity of the design approach.

The cutoff frequency, f_c, for the transverse-electromagnetic (TE) mode of an SIW component is the same as that for a waveguide filled with a dielectric material having relative permittivity of ε_r, as computed by Eq. 1:

$$f_c = v/2\pi[(m\pi/a)^2 + (n\pi/b)^2]^{0.5} \quad (1)$$

where:

m and n = mode numbers,
b = waveguide dimensions, and

$$v = c/(\varepsilon_r)^{0.5} \quad (2)$$

and

v = the relative velocity through the dielectric-filled waveguide,
c = the speed of light, and
ε_r = the relative permittivity of the dielectric material.

For operation in the transverse-electromagnetic TE10 mode, Eq. 1 can be simplified to the form of Eq. 3:

$$f_c = v/2a \quad (3)$$

where dimension a equals the width of a rectangular waveguide filled with dielectric material of relative permittivity, ε_r, and can be found by means of Eq. 4[1,2]:

$$a = c/2f_c(\varepsilon)^{1,2} \quad (4)$$

where:

$$a_{SIW} = a + d^2/0.95p \quad (5)$$

and

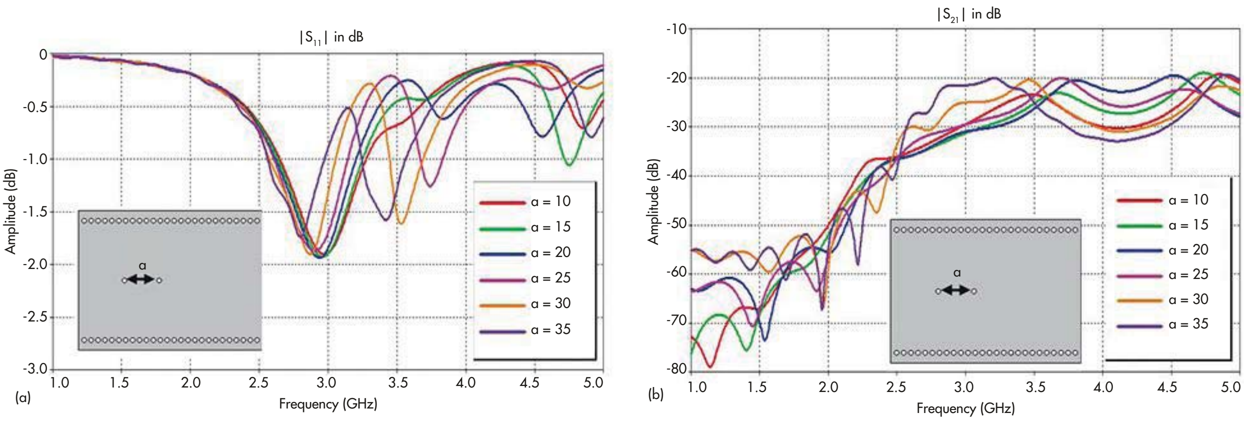

5. The plots show the (a) return loss and (b) transmission coefficient characteristics for an SIW filter with transmission coefficients, a, of 10, 15, 20, 25, 30, and 35 mm.

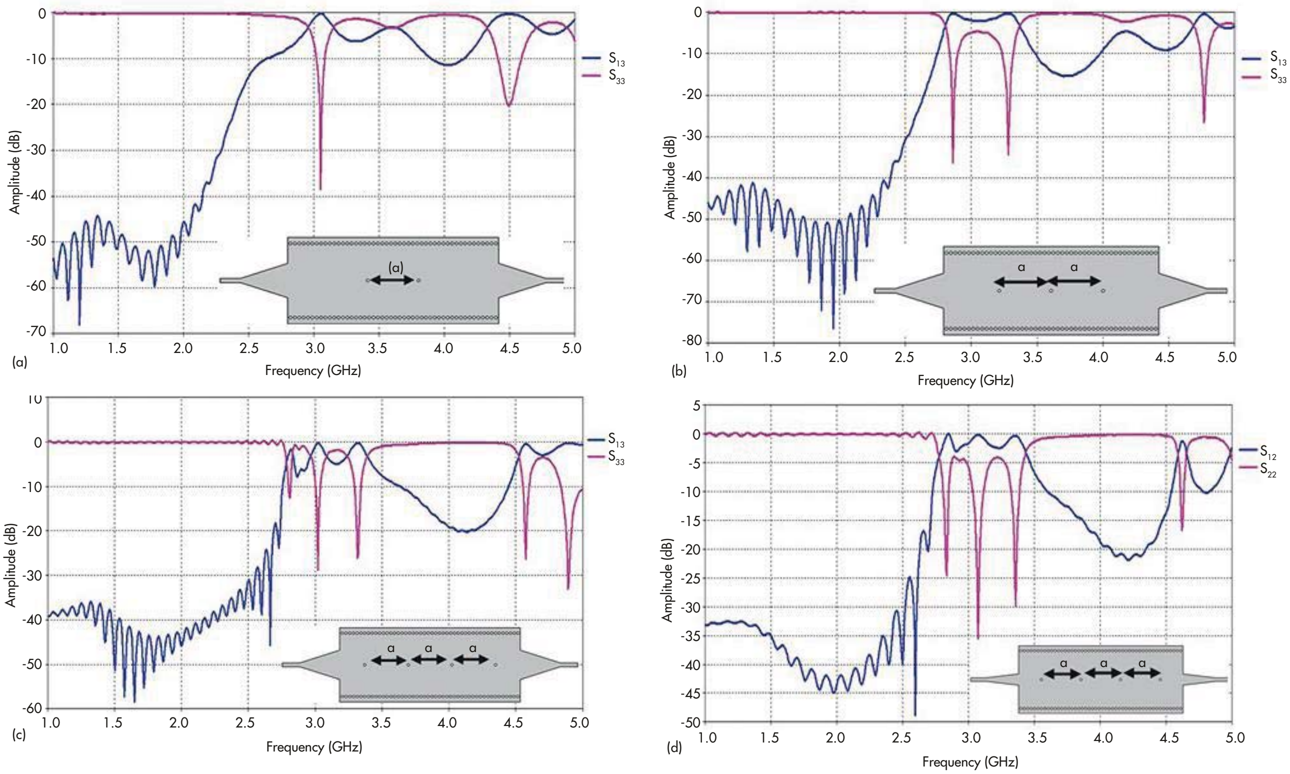

6. The plots show the return loss and transmission coefficient responses for the filter (a) with one cavity, (b) with two cavities, (c) with three cavities, and (d) with three cavities and taper modification, with a = 35 mm, W_2 = 10 mm, W_1 = 3.06 mm, L_2 = 29.14 mm, and L_1 = 12.84 mm.

d = the diameter of the viaholes, and
p = the distance between the viaholes.

When designing SIW circuits, a number of conditions are required, including those detailed by Eqs. 6 and 7:

$$d < \lambda_g/5 \quad (6)$$

$$p \leq 2d \quad (7)$$

To adapt a microstrip feedline to an SIW guide, it is necessary to calculate the impedance of the SIW guide according to Eq. 8:

$$Z_{pi} = Z_{TE}(\pi^2 h/8a_s) \quad (8)$$

where Z_{TE} represents the wave impedance for the TE10 mode, as given by Eq. 9[1,2]:

$$Z_{TE} = (\mu/\varepsilon)^{0.5} \quad (9)$$

For the design of an SIW filter operating at S-band frequencies (2 to 4 GHz), the design equations were used to calculate the SIW dimensions. For operation on the TE10 mode, the cutoff frequency, f_c, of 2 GHz was calculated from the effective width of the guide for a dielectric material with relative permittivity, ε_r, of 2.17 when measured through the z direction (thickness) of the material at 10 GHz and at a dissipation factor of 0.0013 at 10 GHz.

The nonwoven, fiberglass-reinforced polytetrafluoroethylene (PTFE) dielectric material is known commercially as Iso-Clad 917, and is available from Arlon Materials for Electronics (www.arlon-med.com).

After calculating the input impedance of the SIW filter, the next step involved the design of a taper transition for the filter. *Figure 2* shows a top view of the SIW waveguide with two tapers operating in the S-band range. *Figure 3* presents the performance of this SIW guide with SIW transitions in terms of

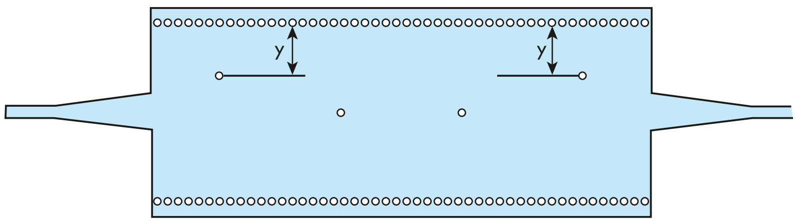

7. This simple diagram represents the S-band filter with its modified cavities.

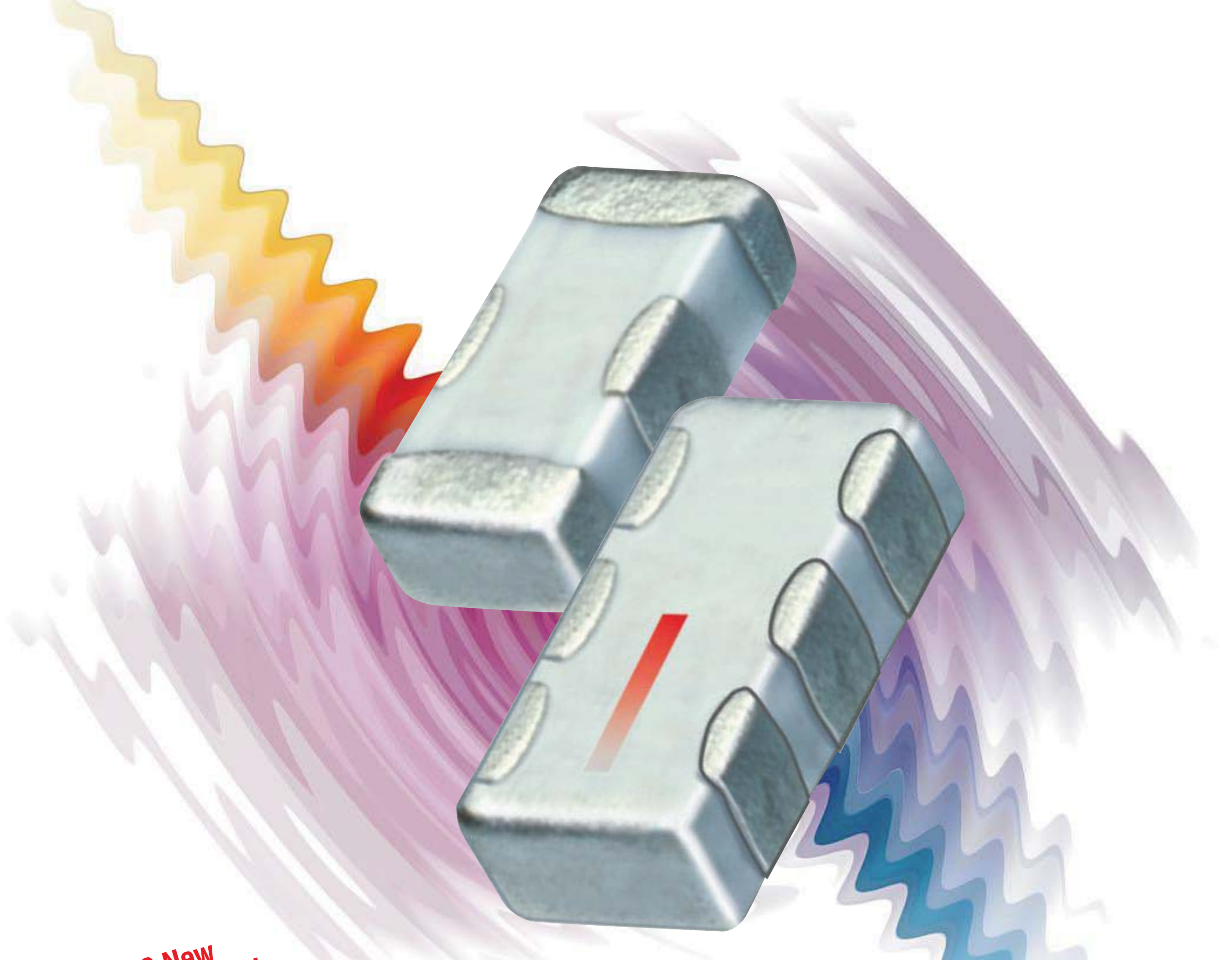

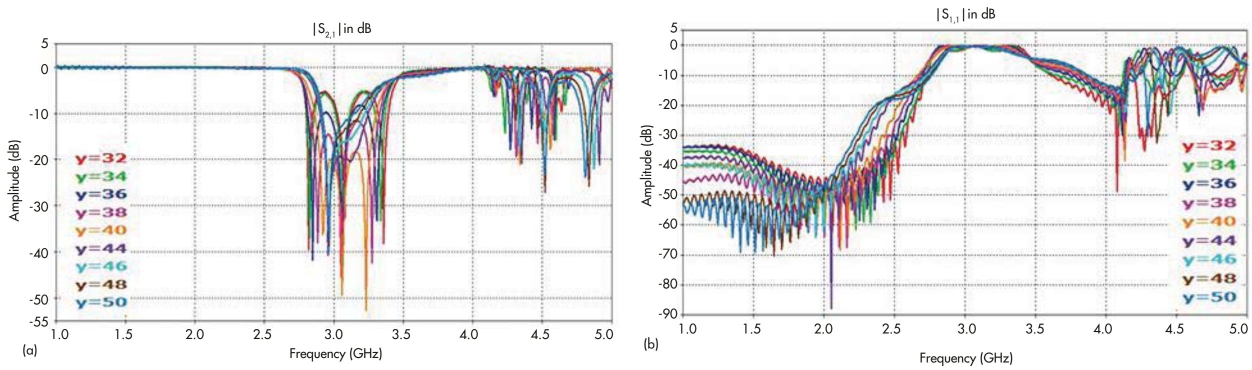

8. These plots offer a parametric study for different values of y: (a) return losses and (b) transmission coefficient.

transmission and reflection. Below the design cutoff frequency, f_C, of 2 GHz, minimum transmission and maximum reflection can be seen in *Fig. 3*.

Beyond 2 GHz, the transmission characteristics improve significantly by means of the taper transition. Several resonant peaks show levels to –41 dB. *Figure 4* presents the magnetic-field propagation within the SIW structure at 3 GHz.

For the design of the filter's resonant cavities, it was necessary to add several metal viaholes to the SIW structure. As part of the design process, two viaholes were inserted and the impact of varying distance a between the viaholes was analyzed. *Figure 5* offers return losses and transmission coefficients for different values of parameter a for the SIW filter.

According to *Fig. 5*, good bandpass-filter characteristics were achieved for a distance of 35 mm. As the distance between the viaholes increased, the filter passband and the cutoff frequency moved higher in frequency. To design a practical transition for the SIW filter input, a taper was optimized and integrated into the SIW filter.

Figure 6 shows the topology of the SIW filter and its transmission and reflection performance from 1 to 5 GHz. Unfortunately, the design exhibits poor rejection in the band from 1 to

5 GHz. To improve rejection, it is necessary to increase the number of cavities in the SIW filter design. *Figures 6(b), (c), and 6(d)* show the results of filter topologies with two and three cavities; the performance of the design with the SIW transition, in terms of transmission and reflection, is plotted in those same figures.

Good rejection was achieved when three cavities were used, although adapting the design to an increased number of cavities required some modifications. To improve the design for use with three cavities, it was thought that the dimensions of the tapers could be adjusted appropriately. *Figure 6(d)* shows an optimized filter topology after several changes.

The position of the viaholes in the cavities was another structural design parameter that was analyzed for its impact on the SIW filter's performance. The performance of the SIW structure was studied for different positions of the viaholes within the resonant cavities.

Figure 7 shows the filter with its modified cavities, and *Fig. 8* offers some of the results of this study. Responses are plotted for return loss and transmission coefficient for different positions of the viaholes. From this analysis, it was found that optimum matching conditions occurred at y = 10 mm.

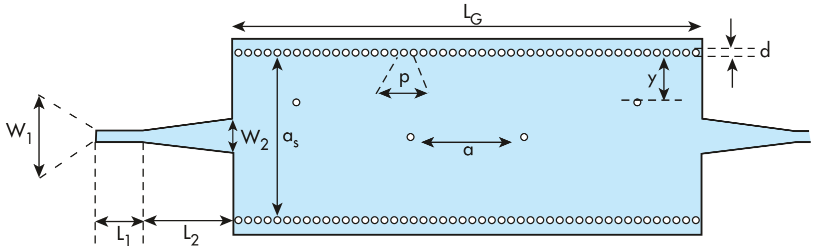

9. This is a top view of the final topology of the S-band BPF, with p = 3 mm, d = 2 mm, a_s = 51.4 mm, a = 35 mm, W_2 = 10 mm, W_1 = 3.06 mm, L_2 = 29.14, L_1 = 12.84 mm, and y = 10 mm.

Figure 9 shows the final topology of the filter and the responses for that construction, respectively. *Fig. 10* (online only) offers curves for the return-loss and transmission-coefficient performance projections from 1 to 5 GHz. A filter bandwidth from 2.75 to 3.40 GHz beyond the S-band passband was recorded, with good impedance matching and acceptable levels of rejection beyond the filter passband.

The filter was fully simulated with CST Microwave Studio. It offers great promise for communications applications at S-band and higher (with reduced dimensions). mw

Note: For Fig. 10 and references, see the online version of this article at www.mwrf.com.

DR. XIN XU | Lecturer
Chongqing College of Electronic Engineering, Campus Town, Shapingba District, Chongqing 40133, People's Republic of China; e-mail: eledear2015@163.com

Miniature Resonator Guides UWB Divider

A ring-multiple-mode-resonator (RMMR) structure enables a compact, two-way power divider to achieve consistent performance.

Ultrawideband (UWB) communications systems offer great promise for effective, short-range communications at relatively high data rates. To develop such systems, of course, various active and passive components are essential—e.g., amplifiers and filters, respectively. In support of these UWB communications applications, a compact UWB power divider was designed and fabricated with microstrip circuit technology using a ring-multiple-mode-resonator (RMMR) approach. To better understand the circuit design, the proposed resonator was studied by means of even- and odd-mode analyses.

By introducing the RMMR to a Wilkinson power-divider circuit layout, it was possible to design and fabricate a novel, compact microstrip UWB power divider. Simulated results and measured responses for the UWB power divider show close agreement, with low insertion loss and good return loss at all three ports and high isolation between the two output ports across the full UWB bandwidth of 3.1 to 10.6 GHz. The compact power divider measures just 20 × 30 mm.

Power dividers are essential passive microwave components widely used in both wired and wireless communications systems, as well as in satellite-communications (satcom) and radar systems. A two-way power divider provides an even division of input power into slightly less than one-half the power at the two output ports (after accounting for some losses due to circuitry, dielectric substrates, and connectors).

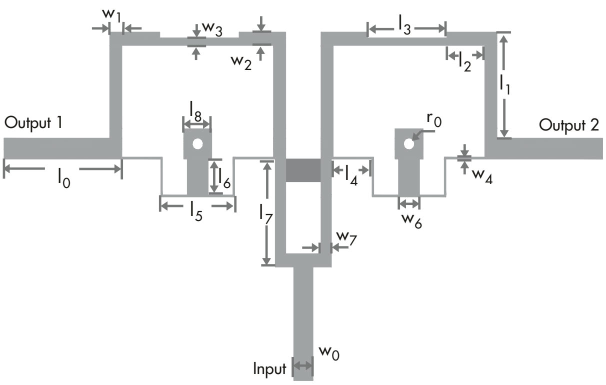

1. This layout represents the proposed UWB power divider.

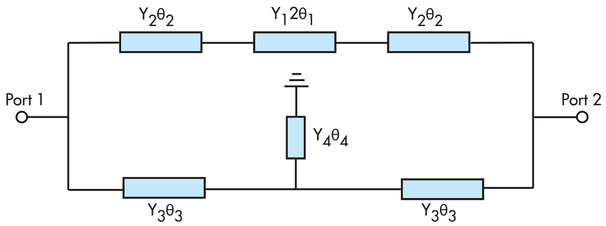

2. This is a schematic diagram of the proposed square RMMR.

Power dividers can be designed for more than two output ports, with the corresponding power division ratio determined by the number of output ports. Power dividers are also used in measurement systems; some performance characteristics, such as amplitude and phase consistency and flatness across the frequency range, can be critical.[1-8]

Conventional power dividers have been designed for octave and wider bandwidths once input and output ports have been properly matched to the system characteristic impedance (typically 50 Ω). That being said, UWB applications can place greater bandwidth demands on components such as power dividers. In 2002, the United States Federal Communications Commission (FCC; www.fcc.gov) proposed the frequency range from 3.1 to 10.6 GHz for UWB applications in the U.S.

A variety of commercial and industrial designs have been developed for research and practical use, and UWB devices and components with wide stopband characteristics have been the focus of many research efforts. Such circuits must be capable of providing good harmonic suppression and passband characteristics.

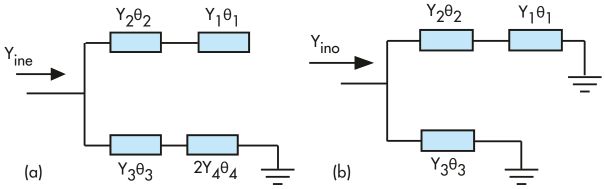

3. These equivalent-circuit models for the square RMMR were used to design the UWB power divider: (a) odd-mode circuit model and (b) even-mode circuit model.

A number of different power-divider configurations have been proposed for the extended bandwidth necessary to cover UWB applications. For example, cascading multisection matching networks at two output ports can provide broad bandwidth, but also increases the total size of the power-divider circuit and requires an increased number of resistors for higher isolation.

To serve the needs of emerging UWB systems, an in-phase power divider with bandpass response was developed[3] based on a multilayer microstrip-slotline coupling structure. The power divider employed a broadside coupling structure via a multilayer slot configuration and includes one narrow notch band.[4] Ring resonators were also used as part of the design to achieve miniaturization.[5-8]

A number of power-divider approaches were previously reviewed, so as to narrow down a design strategy suitable for achieving acceptable UWB performance. A four-way UWB coaxial-waveguide power divider was designed with a coaxial taper transition, oversized coaxial waveguide, and four coaxial probes.[5] In addition, an UWB power divider employing a ring-cavity multiple-way configuration was developed.[6]

A triband power divider was designed with the aid of network theory and even- and odd-mode analysis techniques, although the structure was complex. The design approach can be adapted to microstrip, which is relatively simple to implement and relatively low in cost.[7] Yet another power divider was created with a harmonic-suppressed ring resonator in a planar structure. However, it was relatively limited in bandwidth, with a frequency range from 1.41 to 2.68 GHz.

It was thought that a power divider based on a RMMR structure might provide the performance and bandwidth needed for UWB applications. The resonance behavior of the RMMR was first analyzed through application of electrical theory, then by studying the two pairs of resonance modes. Following this, the RMMR was incorporated into a basic Wilkinson power-divider circuit to achieve increased bandwidth, with computer simulations showing good results.

Finally, to validate the design approach, a microstrip power divider with RMMR was designed and fabricated. Measurement results reveal a wide bandwidth from 2.1 to 11.7 GHz with better than 10-dB return loss and quite good passband response, as evidenced by passband insertion loss of less than 3 dB.

Figure 1 shows the layout of the proposed UWB power divider. Isolation resistor R was placed at the end of transmission line L_1. The microstrip line $L_0 = \lambda_g/4$ (where λ_g is the guided wavelength at 6.85 GHz) is used to achieve good impedance match at port 1. Meander transmission lines were also used in this design to further reduce the size of the power divider. *Figure 2* shows the layout of the equivalent circuit for the square ring resonator.

The electromagnetic (EM) simulation software HFSS 13.0 from Ansoft Corp. (www.ansoft.com) was used to investigate the impact of using different dimensions on the performance of the UWB power divider. The power divider was fabricated on 0.508-mm-thick RO4350B printed-circuit-board (PCB) laminate from Rogers Corp. (www.rogerscorp.com). The circuit material exhibits a relative dielectric constant of 3.48 in the z-direction (thickness) of the material at 10 GHz, with loss tangent of 0.0027 at 10 GHz.

The following dimensions were used for the UWB power divider: $L_0 = 6$ mm; $L_1 = 5.7$ mm; $L_2 = 2$ mm; $L_3 = 6.7$ mm; $L_4 =$

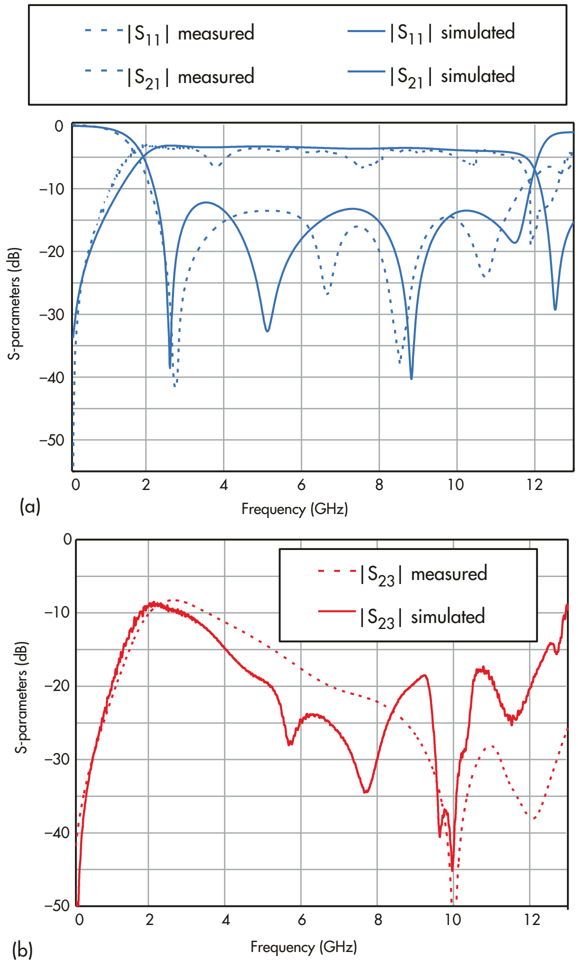

4. These plots provide views of the simulated and measured performance levels of the UWB power divider: (a) S_{11} and S_{21} magnitudes and (b) S_{23} magnitude.

> "With its strong performance and compact size, this power divider is a good candidate for UWB communications systems and in UWB radar imaging applications."

4.2 mm; L_5 = 1.5 mm; L_6 = 4.5 mm; L_7 = 10 mm; W_0 = 1.1 mm; W_1 = 2 mm; and W_2 = 0.1 mm. The total size of the power-divider circuit was 20 × 30 mm^2.

The even- and odd-mode analysis method can be applied to this proposed UWB power divider for studying the symmetry properties of the power divider. The simple schematic of the square RMMR is shown in *Fig. 2*, while the odd- and even-mode equivalent circuits are shown in *Figs. 3(a) and (b)*.

From port 1 to port 2, two transmission paths with characteristic admittances Y_2 and Y_3 were introduced, and a shorted stub with characteristic admittance Y_4 and electrical length λ_4 was connected by means of shunt in the center of the second transmission path. The characteristic impedance at port 1 is 50 Ω. When even/odd-mode signals are excited or introduced from ports 2 to 1, a virtual open/short appears along the center of the square ring resonator.

In the even mode, the stepped impedance stub is divided by one-half along the plane of symmetry. In the odd mode, the plane of symmetry can be considered as a ground plane, with no current flowing through the isolation resistor.

The even-/odd-mode input admittance Y_{ine}/Y_{ino} of *Fig. 3* can be computed via Eqs. 1 and 2:

$$Y_{ino} = -jY_3 \cot\theta_3 - \frac{Y_1 \cot\theta_3 - jY_2 \tan\theta_2}{Y_2 + Y_1 \cot\theta_1 \tan\theta_2} \quad (1)$$

$$Y_{ine} = jY_2 \frac{Y_1 \tan\theta_1 + Y_2 \tan\theta_2}{Y_2 \tan\theta_2 - Y_1 \tan\theta_1 \tan\theta_2} - jY_3 \frac{Y_4 \cot\theta_4 + 2Y_3 \tan\theta_3}{2Y_3 + Y_4 \cot\theta_4 \tan\theta_3} \quad (2)$$

Due to the symmetry of the square RMMR structure, resonant frequencies can be calculated when $Y_{ine}/Y_{ino} = 0$ from the one end of the even- and odd-mode circuit.[2] Thus, it cannot directly solve the expressions for the two pairs of resonant modes.

Moreover, another two odd-mode resonator frequencies, $f_{odd1}(\theta_1$ = 120 deg., $4f_0/3)$ and $f_{odd2}(\theta_1$ = 180 deg., $2f_0)$, can be realized. The bandwidth of the power divider increases as Z_1 increases and decreases as f_0, θ_2, and Z_2 increase. In this way, the bandwidth of the RMMR power divider can be conveniently controlled by changing the characteristic matrix values Y_1 and Y_4 and keeping Y_2 and Y_4 fixed. By properly tuning the dimensions of the RMMR, the desired bandwidth of the UWB power divider can be achieved.

Measurements on the fabricated power divider were performed with the aid of a model 8722ES microwave vector network analyzer (VNA) from Agilent Technologies (now Keysight Technologies; www.keysight.com). The measurements are compared to the simulated responses in *Fig. 4*. As shown, the fabricated UWB power divider features a wide passband from 2.1 to 11.7 GHz. The return loss is better than −10 dB across the passband, with insertion loss close to 3 dB across that same wide frequency range, which ensures good transmission performance across the passband of interest.

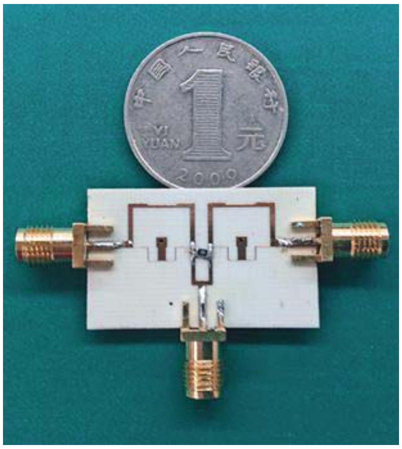

5. This photograph shows the fabricated UWB power divider with RMMR.

The isolation between the two output ports is better than 10 dB across the full UWB frequency range. Some deviations between simulations and measured results were expected, mainly due to reflections from connectors and the characteristics of the PCB material. The overall size of the fabricated divider was only 20 × 30 mm^2, which corresponds to a compact electrical size of $0.46\lambda_g \times 0.69\lambda_g$. With its strong performance and compact size, it becomes a good candidate for UWB communications systems as well as in UWB radar imaging applications. mw

REFERENCES

1. David M. Pozar, Microwave Engineering, 3rd ed., (Wiley, New York, 2005), pp. 412-415.
2. J.D. Zhao, J.P. Wang, and J.L. Lin, "Compact UWB bandpass filter with triple notched bands using parallel U-shaped defected microstrip structure," IET Electronic Letters, Vol. 50, No. 2, 2014, pp. 89-91.
3. W. Feng, W.-T. Li, X.-W. Shi, and Y.-Y. Wang, "Design of compact in-phase power divider with one narrow notch band for UWB application," Electronic Letters, Vol. 48, No. 3, 2012, pp.166-168.
4. K.-J. Song and Q. Xue, "Novel Ultra-wideband (UWB) multilayer slotline power divider with bandpass response," IEEE Microwave & Wireless Component Letters, Vol. 20, No. 1, 2010, pp. 13-15.
5. Q. Xue and K. Song, "Ultra-wideband coaxial-waveguide power divider with flat group delay response," Electronic Letters, Vol. 46, No. 17, 2010, pp.1236-1237.
6. K.-J. Song and Q. Xue, "Ultra-wideband ring-cavity multiple-way parallel power divider," IEEE Transactions on Microwave Theory & Techniques, Vol. 60, No. 10, 2013, pp. 4737-4745.
7. Q.-X. Chu, F. Lin, and Z. Gong, "Novel design method of tri-band power divider," IEEE Transactions on Microwave Theory & Techniques, Vol. 59, No. 9, 2011, pp. 2221-2226.
8. S.-S. Gao, S. Sun, and S.-H. Xiao, "A novel wideband bandpass power divider with harmonic-suppressed ring resonator," IEEE Microwave & Wireless Component Letters, Vol. 23, No. 3, 2013, pp. 119-121.

Design Feature

PAUL DILLIEN | Owner
High-Tech Marketing, 3 Woodside Dr.,
Hermitage, Berkshire, RG18 9QD, United Kingdom

Small Cells Challenge Measurement Capabilities

Advances in wireless communications systems push test-equipment suppliers to produce flexible, compute-intensive tools.

Wireless communications networks require test equipment that can keep pace with their ever-improving capabilities. By way of example: Fourth-generation (4G) wireless systems, such as Long Term Evolution (LTE), promise peak data download speeds of 100 Mb/s for high-mobility communications services. In support of the highest levels of performance possible, modern wireless networks are relying on a growing number of small cell sites to ensure that coverage is consistent throughout a service area. Of course, with the increased number of small cell sites comes an increased need to test and maintain their performance.

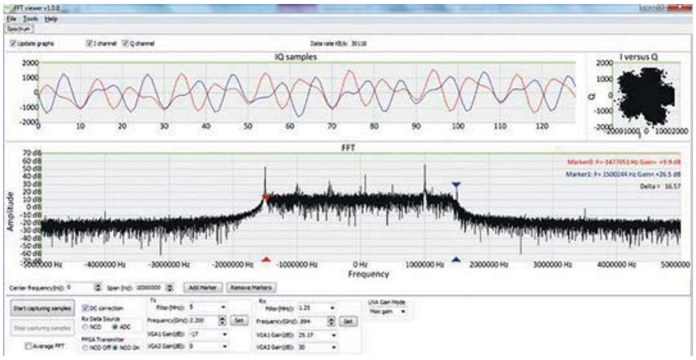

1. This screen presents an averaged FFT of cellular traffic showing typical complex modulation.

In their formative years, wireless communications systems involved cellular radio networks built from multiple base stations. Some base stations were formed from a group of macro nodes, each of which included a radio tower and antenna and their supporting transceivers. Macro base stations, or macrocells, were designed to cover wide service areas—perhaps as many as 2000 users over a range of 15 miles (20 to 30 km) or more. In such an arrangement, unfortunately, users near the boundaries of macro base stations tend to suffer reduced signal-to-noise (SNR) performance from their handsets due to decreasing signal strength from the macro base station.

Such lower-level signals translate into lower data-transfer rates in an LTE system, so the design of a modern wireless communications network also includes the option to supplement a macro base station with a number of smaller cells. These smaller cells are used to augment the coverage at the edges of a macro cell's range, achieving a range of 0.5 miles (1 km) or more. This "cell-within-a-cell" arrangement results in a more complex wireless communications network that presents a challenge to test-equipment manufacturers: They are being asked to deliver cost-effective solutions that can nonetheless tackle more complex testing requirements.

Smaller cells may be used for a number of reasons. The availability of smaller cells makes it possible to offload traffic from a macrocell in areas of heavy use, such as at airports, shopping centers, sports establishments, or anywhere else large numbers of users might gather. In such locations, there may be times when there is very little cellular traffic; smaller cells could depower or switch to a low-power state to save energy during these intervals *(Fig. 1)*.

Another use for smaller cells is to service small-office/home-office (SOHO) locations, where a smaller wireless communications cell provides enhanced performance for as few as 16 users. It can help offset the limitation that higher-frequency

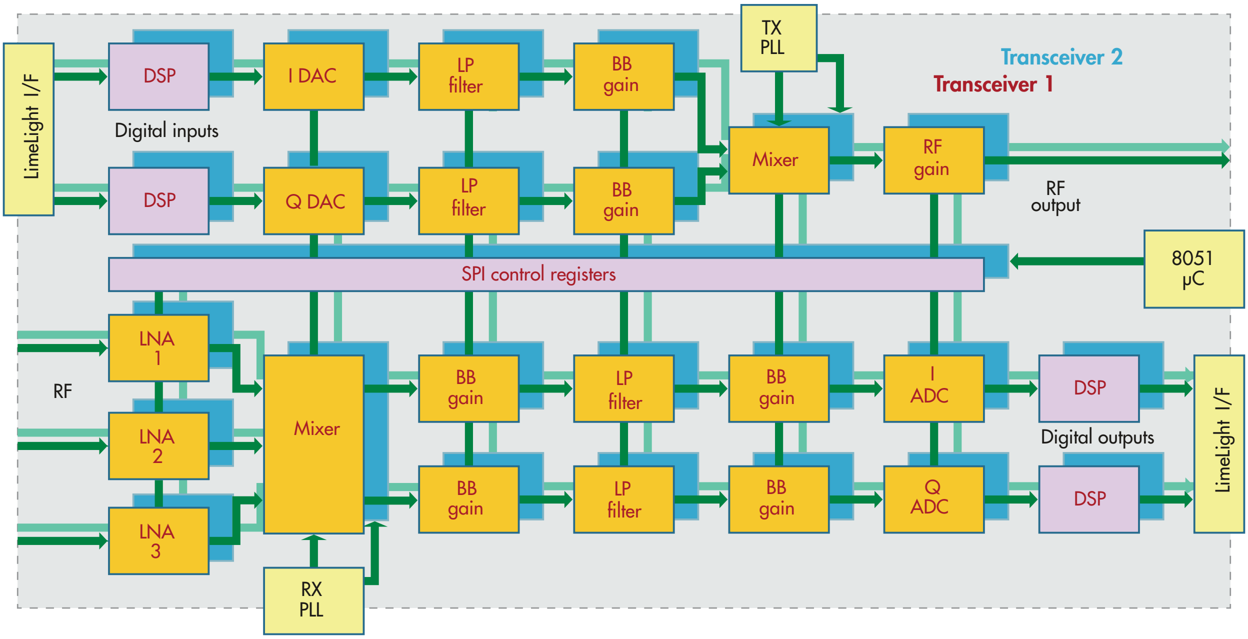

2. This block diagram represents the analog and digital components in the transceiver IC.

signals (typically to 2.6 GHz) used by LTE systems do not penetrate the materials of large buildings as effectively as the lower-frequency signals (700 to 900 MHz) of earlier cellular communications systems. The higher-frequency signals can also be subject to areas of poor reception, where macro signals are severely attenuated. To fill in these blank areas, known as dead zones, operators can provide small cells to reinstate service. Small cells are particularly attractive near cell boundaries, where they can restore high data throughput for users. The range of small cells spans what formerly were called metro/micro, pico, and femto cells, and also include Wi-Fi access points. These differ in capabilities, range, and the number of simultaneous users supported, but all need to function with the rest of the network to improve the overall performance of the system. The resulting complex network, containing both a macro cell and small supporting cells, is known as a heterogeneous mobile network (HetNet).

Earlier second- and third-generation (2G, 3G) wireless networks were carefully planned to ensure adequate coverage and avoid issues with interference between adjacent cells. Small cells in LTE systems must be slotted into what is known as a self-organizing network (SON), and are typically located wherever sufficient power and backhaul series are available. A SON prevents interference by measuring the signal activity in its operating environment, and subsequently determining which frequencies and power levels should be employed for minimum interference.

Those tasked with testing these smaller cells do not have the luxury of the high-precision laboratory equipment used for compliance testing. Because of the large number of small cells that will be deployed, flexible and portable test equipment that is less expensive than laboratory equipment is more suitable for in-field, on-site testing of small cells.

Consider the challenge presented by the wireless environment: The LTE specification includes more than 40 different RF bands spanning the frequency range from 700 to 2600 MHz. In addition, the LTE wireless communications standard encompasses both frequency-division-duplex (FDD) techniques (where different transmit and receive frequencies are used), and time-division-duplex (TDD) techniques (which assign alternating time slots to transmit and receive operations).

As the small cell may be SON-enabled, a suitable portable test solution must be capable of scanning across all possible channels. In such networks, power levels may range from 20 W/channel from a macro base station to just 1 mW/channel from a femtocell. This requires test equipment with a dynamic range of around 70 dB or more.

An added complication is that LTE wireless networks employ a number of different bandwidths—including 1.4, 3.0, 5.0, 10.0, 15.0, and 20.0 MHz—and can implement multiple different modulation schemes *(Fig. 2)*. Orthogonal-frequency-division-multiplex (OFDM) technology is employed as the signal bearer and the associated access schemes used are either based on orthogonal-frequency-division-multiplex (OFDMA) techniques or single-channel frequency-division-multiple-access (SC-FDMA).

OFDM uses transmissions that are composed of a large number of subcarriers spaced 15 kHz apart, each modulated at low data rates. The signals are orthogonal to each other so that there is no mutual interference, and each carrier contains part

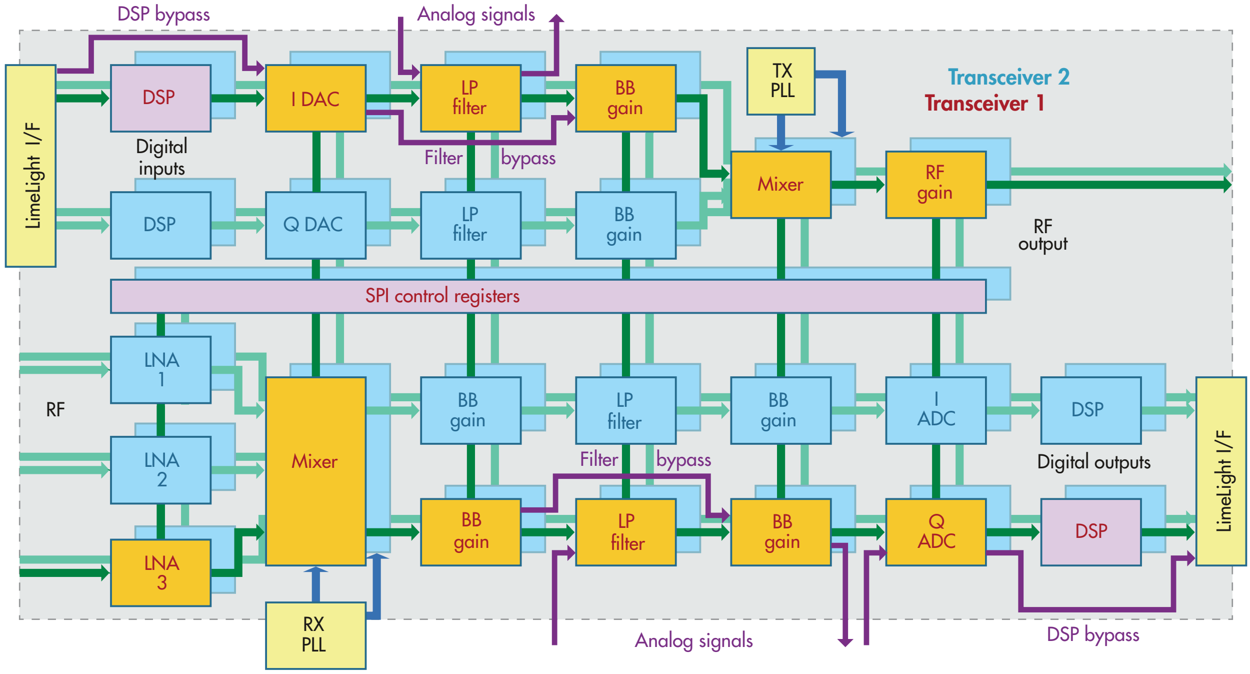

3. This block diagram highlights the signal breakouts and bypass options within the LMS7002M IC.

of the overall data pattern. The simplest modulation technique uses 2-b/symbol and quadrature-phase-shift-keying (QPSK) modulation, where the carrier can assume one of four different phases at a single amplitude level. QPSK supports low-data-rate transfers and is the default method employed under poor signal conditions.

Whenever possible, LTE modulation can be ramped to the use of 64-state quadrature-amplitude-modulation (64QAM) technology. In this scenario, the phase is shifted to one of multiple different angles and amplitudes to define different bit locations in the constellation, and the data carries 6 b/symbol. QAM provides a spectrally more efficient modulation scheme, but only under good SNR conditions. Wideband code-division-multiple-access (WCDMA) signals using a pair of 5-MHz-wide radio channels were introduced as part of 3G wireless communications technology. Such signals are based on code-division techniques that require complex baseband processing to encode and decode.

WCDMA transmissions are also included in the specifications for LTE wireless networks, and can be transmitted as part of the modulation scheme. LTE systems allow users to negotiate the modulation scheme depending on the SNR; as a result, transmitted RF/microwave signals in multiuser parts of these systems can grow quite complex (and quite challenging to measure with portable test equipment).

In support of growing demands for increased data throughput, wireless networks, including LTE systems, are adopting multiple-input, multiple-output (MIMO) antenna schemes. This is an approach that employs two or more antennas separated by some physical distance. MIMO techniques improve spectral efficiency and achieve a diversity gain that improves link reliability.

MIMO signals can provide robust performance, even under conditions of signal fading and interference or under multipath transmission conditions where the signals reflect off buildings, forming distorted signals at a cell site receiver. Multiple antennas, by careful arrangement of the signal phases sent to each element, can provide a composite signal with a beam-forming capability that can "illuminate" a user with a strong signal.

TEST SOLUTIONS

For developers of portable cellular test equipment, a dual transceiver semiconductor device available from Lime Microsystems (www.limemicro.com), model LMS7002M, provides a great deal of flexibility for these in-field wireless test challenges *(Fig. 3)*. This field-programmable radio-frequency (FPRF) chip can be programmed within a test instrument, with receive and transmit frequencies set anywhere from 100 kHz to 3.8 GHz. This wide range encompasses all LTE frequency bands.

The integrated circuit's (IC) receive path includes three low-noise amplifiers (LNAs), and bandwidth and gain are programmable on the fly and in the field for a great deal of measurement flexibility. The IC includes a received-signal-

strength-indication (RSSI) circuitry to aid in spectral analysis of an LTE system.

The LMS7002M transceiver IC can process incoming wireless signals and convert them to digital bit streams that represent the in-phase (I) and quadrature (Q) components of the modulated received signals. The transmit and receive frequencies, gain, and bandwidth are all programmed into the device via a serial-peripheral-interface (SPI) connection. The SPI data consists of a 16-b address and 16-b data word. Each element in the FPRF has a unique address, so that SPI data can adjust each of the programmable elements using random access, providing great flexibility for designers of portable LTE test equipment *(Fig. 4)*.

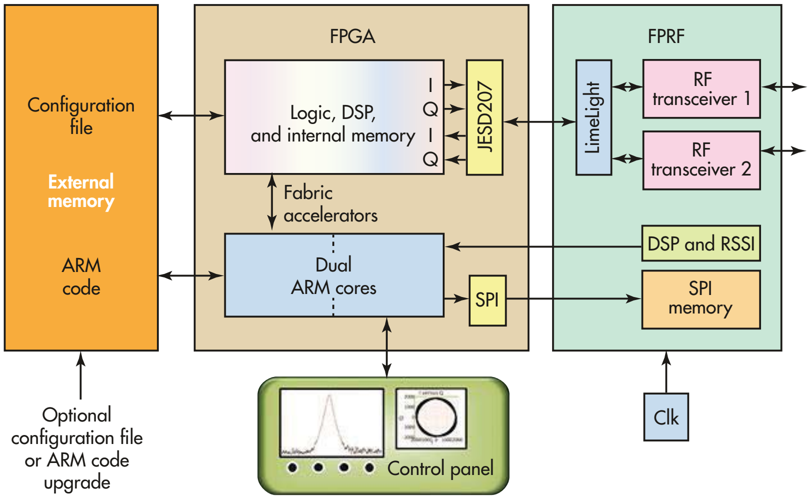

4. This diagram shows the combination of an FPRF and FPGA in a test-equipment application.

The transceiver IC detects and analyzes a received signal to determine frequency, modulation type, and other signal characteristics. The bandwidth of the FRPF can be adjusted to match an incoming signal, and the decoded I and Q signals can be evaluated for errors by the IC's companion baseband chip. The FPRF can also transmit across the range of frequencies and modulation schemes designed into the tester. These can be used in loopback mode to evaluate the quality of a wireless link. Transmit frequency, gain, and bandwidth parameters are programmed into on-chip SPI memory to facilitate testing.

The LMS7002M IC has been designed so that both analog and digital signals and key signal-processing elements within the chip can be accessed externally, or else internally bypassed. This provides a test-equipment manufacturer with options to substitute or enhance the filtering using alternative external components, or pass the decoded analog signal through alternative analog-to-digital converters (ADCs) if higher resolution (than available with the IC) is required. Any unused LMS7002M components can be depowered to reduce the device's power consumption within a portable test instrument.

The LMS7002M includes an on-chip microcontroller running industry-standard 8051 microcontroller code. This simplifies the calibration of the chip in a test instrument, which otherwise would involve complex interactions with the baseband logic. The microcontroller calibrates dc offset, transmit/receive low-pass filter bandwidth tuning, transmit local-oscillator (LO) leakage feedthrough, IQ gain, and phase mismatch in both transmit and receive signal chains, as well as handling on-chip resistor and capacitor calibration. To supplement the calibration functions, internal RF loopback paths can be enabled to test functionality as part of the IC's built-in self-test (BIST) capability.

The FPRF is controlled by an additional baseband chip. This is typically a field-programmable gate array (FPGA), such as a Cyclone V SE for cost-sensitive testers or an Arria V SX for high-performance test solutions—both FPGAs offered by Altera Corp. (www.altera.com). The function of the baseband chip is to encode or decode the I and Q data streams as well as program the FPRF via the SPI interface.

The 32-b ARM cores provide an integrated facility that can interface with the logic fabric or run external code. For example, the logic fabric, memory, and digital-signal-processing (DSP) elements can be configured to perform discrete Fourier transforms—either in the form of fast Fourier transforms (FFTs) or discrete Fourier transforms (DFTs) and forward error correction (FEC)—and generate the modulation patterns for MIMO techniques. These can be configured as required by the ARM microprocessor cores on the transceiver chip, which can initiate the required combination of functions.

The FPGAs are configured upon power up. The configuration file is typically held in an external nonvolatile memory (NMV), such as flash memory, which programs both the logic fabric and the ARM cores. The ARM executable file will typically also be stored in NMV. The NVM can also hold a copy of the SPI configuration data for the FPRF. This data provides a simple way for the processor to store and access the address and data for programming frequency, bandwidth, gain, and DSP elements on the FPRF. This capability gives a test-equipment manufacturer the opportunity to update the NVM with new firmware files in the field when adding new capabilities, supporting new standards, or correcting problems, such as programming mistakes ("bugs").

In terms of creating code, Altera fully supports the Open Computing Language (OpenCL) software. OpenCL allows programmers to quickly exploit the parallel architecture of an FPGA. It enables kernel code to be emulated and debugged, pinpoints performance bottlenecks, and profiles and recompiles programming to a hardware implementation.

Test-equipment manufacturers can, for example, use one core to form an interface with a test-instrument control panel, and the second core to control the FPGA fabric to the required modulation and the FPRF via the SPI interface. An instrument control panel can present the results as graphical displays of the FFT or as a spectral constellation; the core can compute statistics, such as bit error rate (BER), with the modulation being detected or the number of calls dropped. mw

Design Feature

THENG THENGQUEK | Business Development Manager
Keysight Technologies, Inc., 1400 Fountaingrove Pkwy., Santa Rosa, CA 95403-1738; (800) 829-4444, FAX: (800) 829-4433, www.keysight.com

Selecting Microwave Amps for Measurements

Choosing an amplifier for use with test instruments requires a unit with characteristics that optimally measure up to a particular application.

Amplifiers may not be the first piece to consider when setting up a test-and-measurement system. Nonetheless, amplifiers can play a major role in many different measurements, raising test signals to required levels and helping to boost the accuracy of results for RF and microwave analyses.

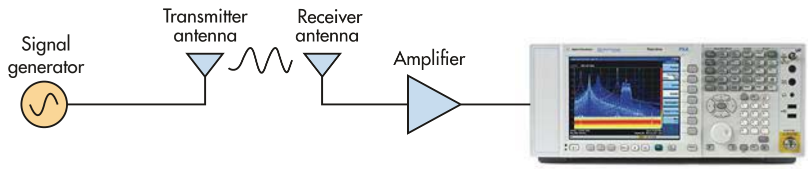

1. A low-noise amplifier can be used to improve test receiver signal-to-noise ratio.

Of course, amplifiers come in many shapes and sizes, from tiny surface-mount integrated-circuit (IC) amplifiers with low noise figures to larger high-power amplifiers that require heat sinks to maintain acceptable operating temperatures. The focus of this article will be on RF/microwave amplifiers well-suited for use in test-and-measurement applications.

Many different types of RF/microwave amplifiers are found in modern applications, falling within two main categories: narrowband and broadband amplifiers. Defining the two categories at times becomes somewhat subjective, since one user's broadband amplifier may be another user's narrowband amplifier. Narrowband frequency spans tend to refer to communications channels and can be rather narrow, for instance, 12.5 and 25.0 kHz.[1]

Solid-state amplifiers depend on impedance matching of active devices to achieve optimum gain over an operating bandwidth, so some amplifier parameters such as gain and gain flatness with frequency can also be affected by the relative bandwidth of an amplifier. For test-and-measurement applications, narrowband amplifiers are often used for lower-frequency setups, such as from 0.7 to 2.7 GHz. A broadband amplifier for test and measurement may be used to amplify a much wider span of frequencies (e.g., 100 kHz to 50 GHz).

In contrast to narrowband amplifiers, broadband amplifiers must overcome some complex design challenges, such as the need to achieve good impedance matching of the active devices over the broad frequency range. Part of selecting an amplifier for test applications is to keep the price-versus-performance tradeoffs in sight.

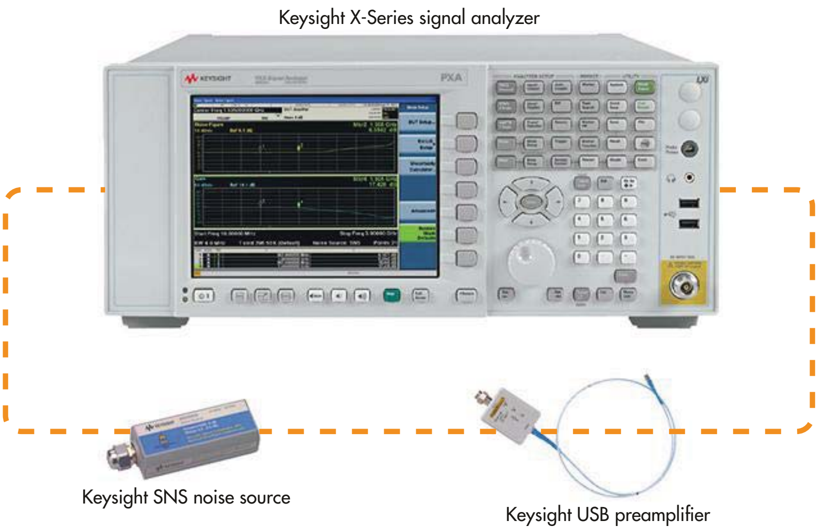

2. This is an example of a low-noise amplifier measurement calibration setup.

For example, the cost of a broadband amplifier may be 20 times that of a narrowband amplifier—operating at a fraction of that bandwidth—but the cost and inconvenience of replacing one broadband amplifier with multiple narrowband amplifiers may not add up. The use of a broadband amplifier can greatly simplify a test setup and lead to optimum performance compared to the required number of narrowband amplifiers to cover the same total bandwidth.

Microwave amplifiers are crucial in measurement systems when testing components (i.e., cellular handsets, antennas, transmitters, and receivers) in communication systems. Applications that need adequate RF/microwave signal power to overcome system losses, such as in electromagnetic-interference/electromagnetic-compatibility (EMI/EMC) test systems, require a high-performance, high-frequency amplifier.

Microwave amplifiers are often used with signal generators, spectrum analyzers, and vector network analyzers (VNAs) in high-frequency test systems. For measurement applications that may require higher signal power levels than available from test instruments such as signal generators, spectrum analyzers, and VNAs, one must decide whether the best approach is to select the high-power option for a given test instrument or use an external power amplifier.

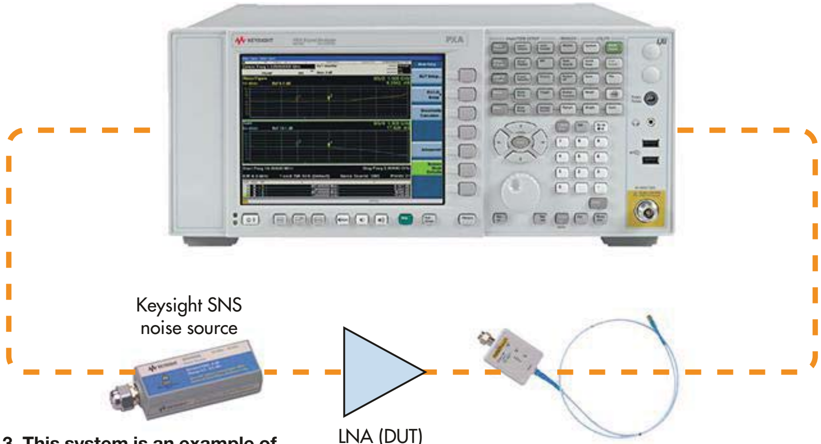

3. This system is an example of a test setup for characterizing low-noise amplifiers.

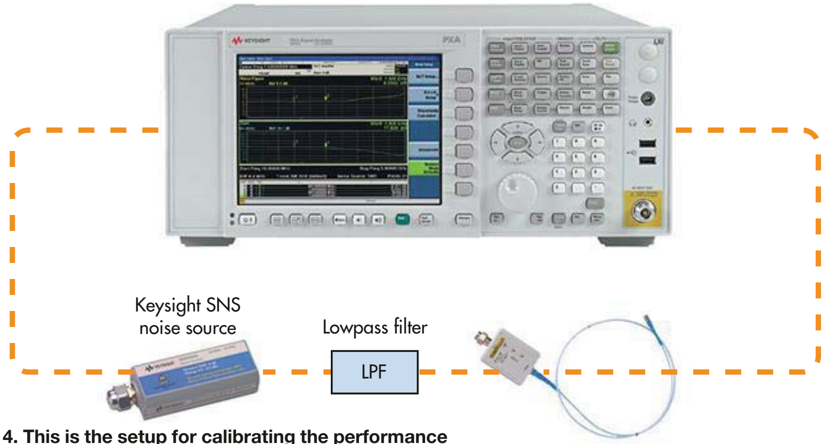

4. This is the setup for calibrating the performance of a mixer measurement system.

Adding a high-power option to a signal generator may seem like a simple solution, but it results in limited output power with tradeoffs that include increased harmonic levels and higher intermodulation distortion (IMD) compared to the standard model. Generally, a spectrum analyzer can make measurements on input signal levels to +30 dBm (1 W), with a preamplifier option helpful in lowering the noise floor when low-level input signals must be measured.

Signal generators may not provide that +30 dBm on their own, since they generally produce higher output-power levels at lower frequencies—typically around +20 dBm. A VNA will typically deliver output levels at around +5 dBm for further analysis.

Choosing an external microwave amplifier with low noise figure and high gain can significantly reduce overall test system noise figure and boost available power for a variety of measurements; this holds true both for broadband and narrowband measurements. Selecting the best amplifier is a matter of reviewing various amplifier performance parameters.

Among these parameters are frequency range; noise figure; output power; gain; input and output return loss or voltage standing wave ratio (VSWR); isolation between channels; phase noise; and matching the performance of an amplifier under consideration to the measurements to be performed. Considering these different parameters helps evaluate amplifiers for use with, for example, a signal generator and/or a spectrum analyzer.

Typical RF/microwave applications range in frequency from 100 MHz (for testing such components as semiconductors and ICs) to 60 GHz and higher [for line-of-sight communications and satellite-communications (satcom) components and systems]. Testing components for wireless communications systems may only call for an amplifier with high-end frequency of 3 or 5 GHz, although specifying an amplifier with broader frequency range increases the flexibility of the test system.

Ideally, the bandwidth of the amplifier matches the frequency range of the signal generator and/or spectrum analyzer in a given test system, although the frequency range for a particular set of measurements will also be application-specific. Also, a wider frequency range may be sacrificed for more optimum per-

formance in a narrower bandwidth, especially if price is also a key consideration.

For certain applications, such as evaluating receiver sensitivity, noise figure can be one of the more important specifications when selecting an amplifier for use with a test system. The noise figure is defined as the ratio of the signal-to-noise power ratio (SNR) at the input of the amplifier to the SNR at the output of the amplifier. The noise factor is thus the ratio of actual output noise to that which would remain if the amplifier itself did not introduce noise.

Amplifiers with low noise figures are generally preferred to those with higher noise figures, since a receiver's performance (in terms of sensitivity) is dominated by the noise figure of the receiver's preamplifier. For test systems required to measure noise figure, adding a preamplifier can reduce the total system noise figure:

$$F_{new} = G\{F_{pa} + (F_{sys} - 1)/ F_{pa}\}$$

By adding a preamplifier to noise-figure measurement systems, the total system noise figure can also be reduced.

where:

F = the noise figure of the preamplifier, and

G = the gain of the preamplifier, both in linear terms.

In terms of logarithmic value, the system noise figure (NF_{sys}) can be found from the equation:

$$NF_{sys} = 10\log(F_{sys}) \text{ (in dB)}$$

For test systems with a single preamplifier, where the gain of the preamplifier is greater than or equal to the noise figure of the spectrum analyzer, the system noise figure is approximately equal to the noise figure of the preamplifier.

Output power is another key specification to review. Output power can be described by a number of different specifications. For example, the saturated output power, or P_{sat}, refers to the maximum (or saturated) output power available from an amplifier when it is fully biased and fully driven at the input port. This is the output power of an amplifier when its input power (P_{in}) versus output power (P_{out}) or P_{in}/P_{out} curve slope goes to zero.

In contrast, an amplifier's P1dB output power refers to the amount of output power when the amplifier's gain is compressed by 1 dB. Since the amplifier has reached a state of 1-dB gain compression, it is assumed to have also reached a point of some degree of nonlinear behavior.

Broadband amplifiers are available with multiple-octave frequency coverage, high gain, and ample linear output power. When higher power levels are needed, the solution usually involves a number of narrowband amplifiers that are multiplexed or controlled by switching to cover the required frequency range. While such a solution can deliver very high test signal power levels, it also introduces discontinuities in the test signal power and gain curves with frequency at those switching points.

An amplifier's gain is usually tied to its output power. If no context for output power is given, its gain is usually assumed to be small-signal gain—i.e., the linear gain achieved for input signal levels that allow the amplifier to operate at considerably less than saturated levels. Conditions for small signals at an amplifier's input and output ports are usually easy to reproduce and verify, whereas gain and gain flatness with frequency can vary

(continued on p. 90)

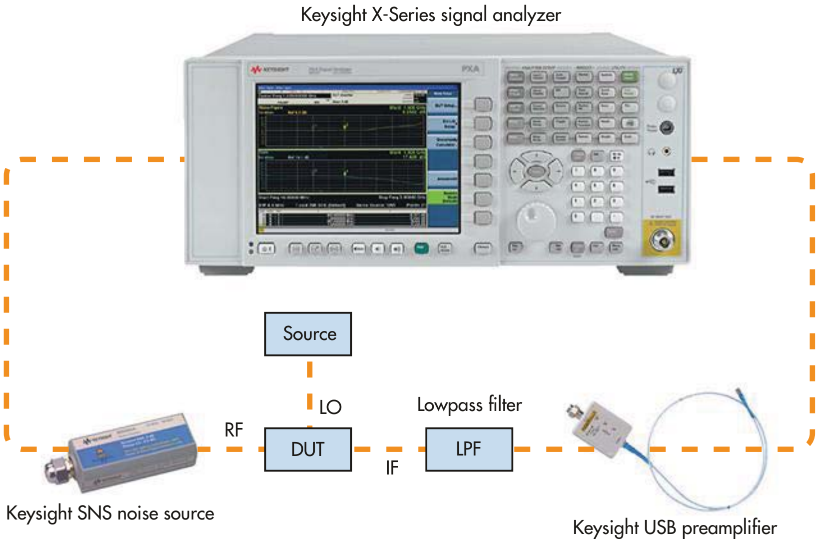

5. This is a basic mixer measurement setup based on a commercial signal analyzer and test sources for the RF and LO signals.

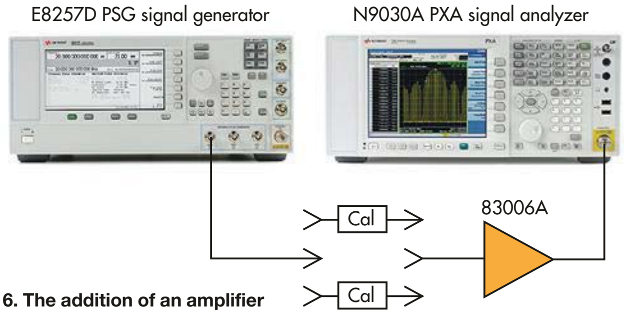

6. The addition of an amplifier helps improve test system signal sensitivity.

TIME-DOMAIN EM SIMULATORS OPTIMIZE AUTOMOTIVE RADAR

BY IDENTIFYING AND mitigating board-level parasitics and variations using finite-difference time-domain (FDTD) electromagnetic (EM) simulation techniques, engineers can boost automotive-radar performance while improving transportation safety. These EM simulations can benefit RF board, sensor, and fascia-level design by using graphics-processing-unit (GPU) enhancement technology. Such an approach promises to reduce days and weeks of simulations to a matter of hours. REMCOM provides insight into the use of time-domain techniques with automotive radar in the application note, "Benefits of Time-Domain Electromagnetic Simulation for Automotive Radar."

The document reviews the simulation of a multilayer printed-circuit board containing both radiating elements and feed structures. At 25 and 77 GHz, analysis is performed on the parasitic coupling between conductors, current distribution on groundplanes, and the effects of secondary sources [i.e., the local-oscillator (LO) line]. To meet OEM specifications, the complete sensor system needs to be analyzed for performance and degradation factors—including the case covered with a radome. The app note discusses the FDTD simulation of the RF board, radome, packaging, data connector, sensor case, and digital board.

Remcom
315 S. Allen St., Ste. 416
State College, PA 16801
www.remcom.com

The simulation uses a parameterized geometry of the radome structure to enable its optimization, as the radome significantly impacts the antenna-array sensor. In a lab situation, the note details that multiple radome structures would have to be fabricated and measured for performance. The simulation setup, in contrast, only takes a few minutes. Factors like paint color, brackets, and curves in the fascia are also included, as they may affect the antenna's behavior. To mitigate these concerns, the position of the antenna array relative to the fascia can be parameterized.

Understandably, including all of these features will increase the complexity of the simulation, and thus the calculations necessary to complete it. The note provides random-access-memory (RAM) usage and runtime results for simulations with just the RF board, the RF board/sensor, and the complete system. Because the RAM and run-time requirements would be prohibitive using central-processing-unit (CPU) technology exclusively, NVIDIA GPUs with the Kepler architecture are utilized to enhance simulation speed by up to 50 times.

LOW-COST BACKHAUL SOLUTIONS DEFINE MM-WAVE SMALL CELLS

SEEKING TO COMBINE approaches for implementing 4G networks, many telecom companies are hunting for the best of low-cost ownership, optimal range/capacity performance, and mitigation of line-of-sight (LOS) issues. The main technology contenders are point-to-multipoint (PtMP) and point-to-point (PtP) solutions from 2 to 80 GHz. Intracom Telecom covers the various wireless-backhaul technologies and their viability as a component in a multi-technology solution in the white paper, "Technology Synergies for Small-Cell Backhaul in 4G Networks."

Intracom Telecom
11360 Technology Circle
Duluth, GA 30097
www.intracom-telecom.com

The paper initially details an evolutionary path for the adoption and deployment of LTE macrocells. It then moves on to small cells equipped with LTE technologies, which are capable of future-upgrading to LTE-Advanced technologies. With the need to produce much denser small-cell grid networks in areas of economic interest, telecommunications organizations have the opportunity to open up "backhaul as a service" as a new profit stream. Unfortunately, there are challenges to incorporating the small-cell approach into the larger macrocell-dominated structure. The main issues include hand-off and integrated small cells as a seamless component of the core network with economically viable small-cell technologies.

The white paper reviews the following technologies: sub-6-GHz, 18 to 38 GHz, 26/28 GHz, 60-GHz unlicensed bands, and 70-/80-GHz light licensed bands. The main constraints for the upper-microwave and millimeter-wave spectrum technologies are generally LOS concerns. Short-hop issues also arise over 60 GHz. Spectrum availability and congestion are concerns for the 18-to-38-GHz and 26/28-GHz technologies. Yet these matters may not be significant compared to the issues faced by the limited-spectrum, interference-rife, and non-carrier-grade sub-6-GHz options—regardless of their cost and non-LOS advantages.

Because no single technology provides an optimal solution, the white paper suggests an efficient and synergistic solution using 26-/28-GHz PtMP and 60-GHz PtP systems. In order to implement this multi-technology solution, it will be necessary to overlay PtMP technologies with an underlay of PtP technologies in dense areas with high data demand. To transform the backhaul architecture, the paper concludes that the industry will need to embrace fiber-optic infrastructure for transport/aggregation, radio backhaul for one or two hops, and shorter radio link distance with greater link density.

CHARLES PARDO | Engineering Manager

Synergy Microwave Corp., 201 McLean Blvd., Paterson, NJ 07504; (973) 881-8800, FAX: (973) 881-8361, e-mail: sales@synergymwave.com, www.synergymwave.com

Novel ASIC Helps Sources Silence Noise

These synthesized signal sources are available in single- and dual-loop configurations for low-noise output signals to 15 GHz.

PHASE NOISE is a critical performance parameter in many applications—from communications to radar systems, and from commercial to military uses—and techniques that generate RF/microwave signals while minimizing phase noise are always of interest.

Synergy Microwave Corp. has long been associated with low-noise RF/microwave signal sources and novel techniques for signal generation. The firm has now developed a phase-locked synthesizer and fixed-frequency, phase-locked-oscillator (PLO) design that can be applied to the generation of low-noise fundamental-frequency signal sources from 100 MHz to 15 GHz—and extendable to 30 GHz , when using an external frequency doubler from Synergy. Even more remarkable, these quiet signal sources fit within compact industry-standard 2.25 × 2.25-in. module housings, or on a 1.0 × 1.25 in. surface-mount-technology (SMT) footprint.

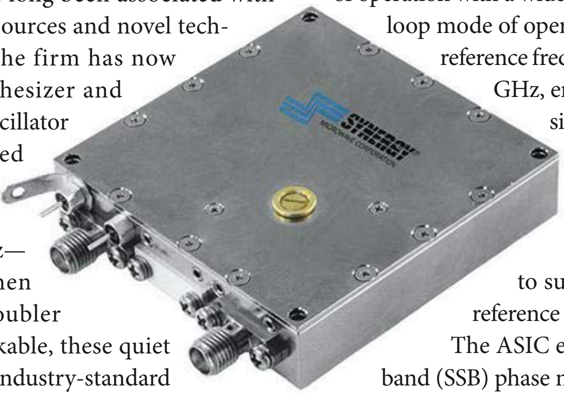

1. Photo of 2.25 × 2.25 in. SMT housing (PLL module with ASIC)

The low-noise PLO/synthesizer connectorized module version (*Fig. 1*) and surface-mount version build upon a unique state-of-the-art phase-locked-loop (PLL) application-specific integrated-circuit (ASIC) device—one that enables extremely high frequency range and versatile divider/phase-detector flexibility for phase-locking RF and microwave signal sources. These include dielectric-resonator oscillators (DROs) and various-topology voltage-controlled oscillators (VCOs). The proprietary ASIC makes it possible to phase lock these and other wide-band, high-frequency oscillators with bandwidths beyond octave tuning.

These synthesizers or fixed LO sources can lock to almost any reference source even through microwave frequencies, such as stable crystal oscillators and multiples thereof, and can function effectively in a number of different operating modes. The ASIC makes an excellent, low-noise starting point for such component functions as high-frequency dividers and phase detectors, as well as phase-locked fixed-frequency and tunable frequency sources.

The PLL design supports both single- and dual-loop modes of operation with a wide array of reference sources. In single-loop mode of operation, for example, it can work with reference frequencies from 1 MHz to as high as 2.2 GHz, enabling the addition of a synthesized single-loop frequency source to a wide range of systems. In dual-loop mode of operation, the PLL ASIC can lock a first-loop reference crystal/frequency-multiplier combination to supply an output, second-loop PLL a reference frequency signal up to 1 GHz.

The ASIC enables particularly low single-sideband (SSB) phase noise from both the single- and dual-loop source configurations with the industry-leading lowest-noise digital divider and phase detector. Measurements taken with a model FSUP signal source analyzer from Rohde & Schwarz (www.rohdeschwarz.com) for a 10-GHz dual-loop synthesizer at 10 GHz show the excellent loop noise performance and sharp drop in phase noise further from the carrier using a low-noise voltage-tuned DRO from Synergy (*Fig. 2*).

A frequency-synthesizer PLO module with this ASIC can be utilized to construct dual-loop phase-locked DROs to 14.5 GHz, as well as dual-loop frequency synthesizers in octave bands to 10 GHz. These latter sources tend to have frequency settling times that are less than 100 µs. Either of these dual-loop configurations will also be able to accommodate virtually any reference frequency. Furthermore, dual-loop capability provides the benefit of reference cleanup of unwanted spurious signal products and noise that may exist on a necessary reference time standard.

The initial primary loop's narrow bandwidth and excellent crystal or surface-acoustic-wave (SAW) oscillator noise performance—coupled with the lowest available digital phase detector noise floor—yields performance only previously seen using analog samplers or fundamental mixer/phase-detector techniques. Fixed and frequency agile models are both available with dual output or coupled sample output. Modules can also be configured to output a reference or internal first loop sample.

Both connectorized single- and dual-loop KDSLO versions communicate using a simple channel-select SPI connection. Custom program interfaces are also available to suit specific interface applications. It is only necessary to communicate with one channel-select register.

Working much the same as the modular connectorized versions, the PLL ASIC has also been integrated within smaller SMT frequency-synthesizer products, in a compact 1.0 × 1.25 in. footprint. The single-loop surface-mount version is designed for use with input frequencies to 2.2 GHz and supplying stable, low-noise octave-band output signals to about 10 GHz. This surface-mount footprint *(Fig. 3)* has been used to accommodate a custom VCO for radar and communications-band frequencies. For this particular custom design, moderately wide locked bandwidths are achieved by using one of Synergy's low-noise, wide-tuning-range microstrip VCO designs. For sources requiring reference frequencies below 100 MHz, internal low-noise reference multiplying techniques are employed to achieve the highest possible phase detector operating rate for best output noise performance that takes advantage of the PLL ASIC's unique capabilities.

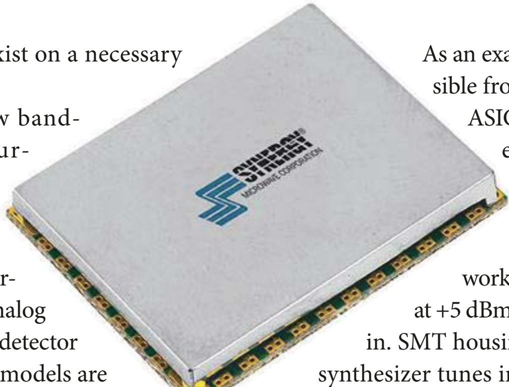

3. The synthesized sources can also be supplied within a 1.0 × 1.25 in. SMT footprint.

As an example of the source performance possible from synthesizers employing this novel ASIC in a single-loop configuration, model LSLO220270-500 is a phase-locked frequency synthesizer that delivers a 500-MHz output bandwidth from 2200 to 2700 MHz. It is designed to work with an 80-MHz frequency reference at +5 dBm and fits within the smaller 1.0 × 1.25-in. SMT housing. This RoHS-compliant frequency synthesizer tunes in 5-MHz steps and provides at least +8-dBm output power across its 500-MHz tuning range.

It achieves −23 dBc typical second-harmonic suppression with impressive SSB phase-noise performance *(Fig. 4)*. Spurious noise levels are typically −65 dBc or better. The phase noise is a low −118 dBc/Hz even as close as 1 kHz from the carrier, dropping to −123 dBc/Hz offset 10 kHz from the carrier, better than −135 dBc/Hz offset 1 MHz from the carrier, and −155 dBc/Hz or less for offset frequencies beyond 1 MHz from the carrier. The signal source can be programmed via serial peripheral interface (SPI) or parallel port, and features settling time within 100 µs to a new frequency when programmed with SPI fast-lock mode.

The 2.2-to-2.7 GHz source draws no more than 100 mA current from a +5-V dc supply and tunes by means of a +12-V dc source, drawing no more than 60 mA current. A +3.3-V dc digital supply draws maximum current of 550 mA. Operating temperature for the source ranges from −30 to +70°C.

The surface-mount SLSO and SLFO sources also communicate using the simple channel-select SPI command interface. The surface-mount version can accommodate a limited channel number parallel interface using up to seven parallel interface lines.

As with the company's other single-loop and dual-loop phase-locked SMT source designs and VCO products, the 2.2-to-

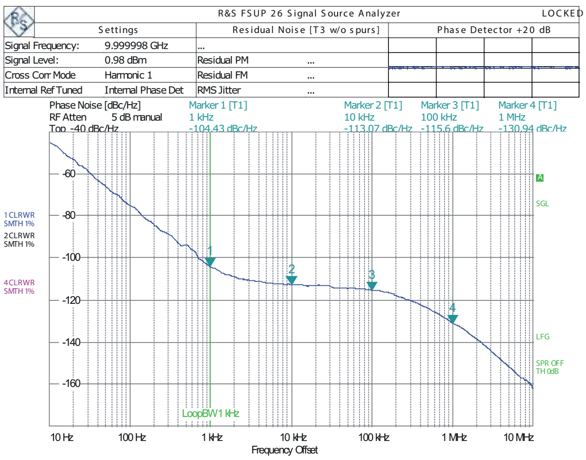

2. This phase-noise plot was made for a 10-GHz dual-loop synthesizer using a DRO.

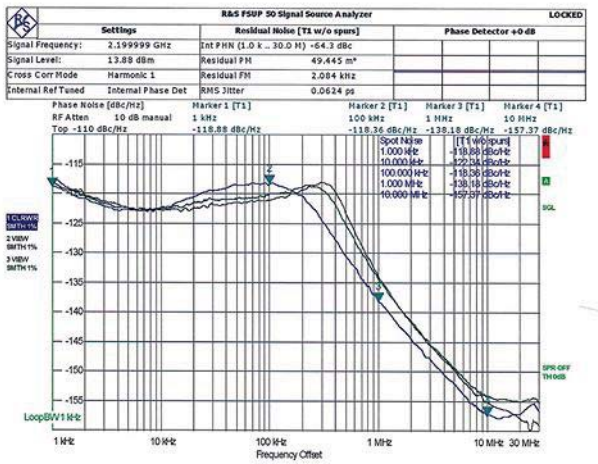

4. This plot shows the phase-noise performance of the model LSLO220270-500 synthesizer.

2.7-GHz frequency synthesizer employs the firm's patented REL-PRO technology for reliable surface-mount electrical connections. The approach avoids the use of contacts with castellations, which are larger-diameter plated-through holes (PTHs) formed through printed-circuit boards (PCBs) to make electrical contacts and signal transitions between two or more PCBs in an assembly.

Since REL-PRO contacts do not critically depend upon the punching, routing, and alignment measures employed in forming castellation contacts, higher yields with more reliable contacts are possible with them. Unlike PCBs formed through a castellation process, the REL-PRO process does not produce the exposed copper from punching or routing PTHs. Without exposed copper, there is less concern about the long-term reliability problems resulting from oxidation and corrosion.

The product lines of frequency synthesizers and phase-locked oscillators using this new ASIC are suitable for a wide range of applications through 15 GHz, including in microwave radios, satellite-communications (satcom) systems, radar systems, and test equipment. The sources are available for a standard operating-temperature range of −10 to +60°C, with an extended operating temperature range of −40 to +85°C also available. For single-and dual-loop frequency synthesizers, the standard connectorized module size is 2.5 × 2.5 × 0.5 in.

The frequency synthesizers provide standard output-power levels to +12 dBm, with optional output power to +16 dBm also available. The synthesized signal sources can be designed with dual RF/microwave frequency outputs or with a reference sample output in addition to the standard frequency output. mw

SYNERGY MICROWAVE CORP., 201 McLean Blvd., Paterson, NJ 07504; (973) 881-8800, FAX: (973) 881-8361, e-mail: sales@synergymwave.com, *www.synergymwave.com*

Selecting Amplifiers

(continued from p. 82)

significantly when an amplifier approaches compression.

For an amplifier with broad frequency range, the gain flatness with frequency is usually specified for subsections of the frequency range. An amplifier's gain and gain-flatness specifications typically include the implicit assumption that the reverse gain—from the output to the input—is negligible, and that the amplifier is unilateral.

Extremely good gain flatness is usually only achieved for narrow bandwidths when using classic reactive impedance-matching techniques, such as those used with internally matched active devices in amplifiers. Attempts to broaden the gain bandwidth of a high-power microwave amplifier require tradeoffs with resistive matching, or feedback techniques that sacrifice some output power. Amplifiers with spatially combined device topologies can overcome these gain/power performance limitations.

An amplifier's input and output return losses (in dB), or VSWR (in a numerical ratio value), are representative of how closely the amplifier can achieve impedance matches to connected components and test equipment at the characteristic impedance of a test system, typically 50 Ω at RF/microwave frequencies. These parameters provide insight into the wave interference caused by impedance mismatches. The peaks and troughs in a given EM field pattern will remain static as long as the sources of interference do not change with respect to each other.

At RF and microwave frequencies, the material properties as well as the physical dimensions of a network element, such as a circuit's transmission line, can play a significant role in determining the impedance match or mismatch caused by the distributed effect. Ideally, an amplifier for test-and-measurement applications should exhibit the lowest-possible VSWR to minimize impedance mismatches.

Amplifier isolation is a measure of the degree of attenuation of an unwanted signal at a port of interest. This parameter indicates an amplifier's capability to boost desired signals versus undesired signals. High isolation in an amplifier reduces the influence of signals from other channels, sustains the integrity of the measured signal, and reduces system measurement uncertainties.

Since test systems are typically maintained in temperature-controlled laboratories, some performance parameters—e.g., variations in gain and power with temperature—may not be overly critical when comparing amplifiers for test system use. But one additional amplifier parameter that can play a role in measurements (especially with spectrum analyzers) is amplifier phase noise. Phase noise tends to be higher at higher frequencies, and can impact the accuracy of receiver measurements with a spectrum analyzer.

Phase noise is also a function of different active device technologies, tending to be higher for amplifiers based on GaAs high-electron-mobility transistors (HEMTs) than for silicon bipolar transistors or GaAs field-effect transistors. So, a careful review of amplifier performance levels may reveal which units have the lowest phase noise for critical receiver measurements.

In short, selecting an amplifier for use with test-and-measurement systems is a matter of comparing many of the key performance parameters. But it is also a matter of considering the measurement capabilities of a test system, in terms of bandwidth and maximum test power (before, say, overloading a spectrum analyzer), and trying to select an amplifier that can deliver the required performance levels for the best price. mw

REFERENCE

1. Jean-Jacques DeLisle, "What's the Difference Between Broadband and Narrowband Communications?" Microwaves & RF, Vol. 53, No. 11, November 2014, pp. 50-52.

JEAN-JACQUES DELISLE | Technical Editor

AESAs Boost Multi-Role Capabilities for Warfighters, UAVs, and Wi-Fi

Advanced electronic-warfare technologies and techniques have taken hold of AESA solutions to create applications ranging from electronic attack to UAVs and data links.

BOTH IN THE United States and across the globe, active electronically scanned array (AESA) radar is being increasingly recognized and adopted for its key features. For example, AESA technology provides the simultaneous detection, identification, and tracking of multiple air and surface targets. Compared to mechanically scanned arrays, it features up to 10× increased operational availability. In addition, its higher resolution leads to increased standoff range. Now, modular techniques and low-cost retrofit modules are beginning to surface for AESA technology. As a result, they are considered more viable for legacy warfighters while offering more application scalability *(Fig. 1)*.

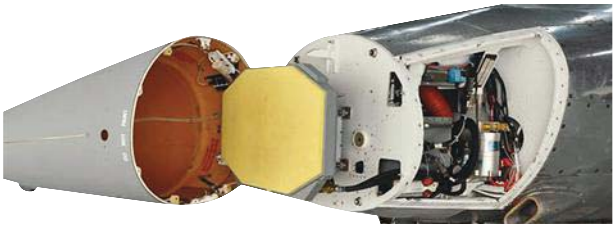

1. Several companies have developed retrofit AESAs to replace mechanically scanned arrays. In doing so, they have raised the relevance of legacy aircraft. *(Courtesy of Northrop Grumman)*

These cost-cutting and modular techniques also are prompting reviews of AESA technology for land, naval, and even commercial applications. For earlier generations of warfighters, passive phased-array radar brought a huge advance in electronic-warfare (EW) capability by allowing the radar to be steered with mechanical motors. To eliminate the need for such adjustments, AESAs rely on beamforming and beam-steering technologies. The ability of these arrays to handle multi-role capabilities also has been enhanced due to the emergence of solid-state technologies, such as gallium-nitride (GaN) and software-defined-radio (SDR) architectures.

Thanks to the advancement of wideband, solid-state electronics such as GaN power amplifiers (PAs), several fourth- and fifth-generation warfighters are now being equipped with AESAs. These retrofits are converting warfighters from a wide range of countries into multi-role-capable airframes—a major upgrade. In addition, these systems promise to provide increased mechanical reliability and lower maintenance costs, thereby decreasing the cost over time and downtime of warfighters. Generally, these devices are designed for a variety of aircraft and platforms as drop-in modules—a feature that brings repair and servicing closer to the field.

2. Using a modular approach to AESA construction can increase the scalability of a technology while easing integration into older platforms and technologies. *(Courtesy of API Technologies)*

LOW-COST AESA TECHNOLOGY

As AESAs further their reach into retrofit applications, companies like BAE, Northrop Grumman, Raytheon, and others are increasing the lifetime of aging warfighter platforms. Prompting these retrofits are two factors: the decrease in available funding for the num-

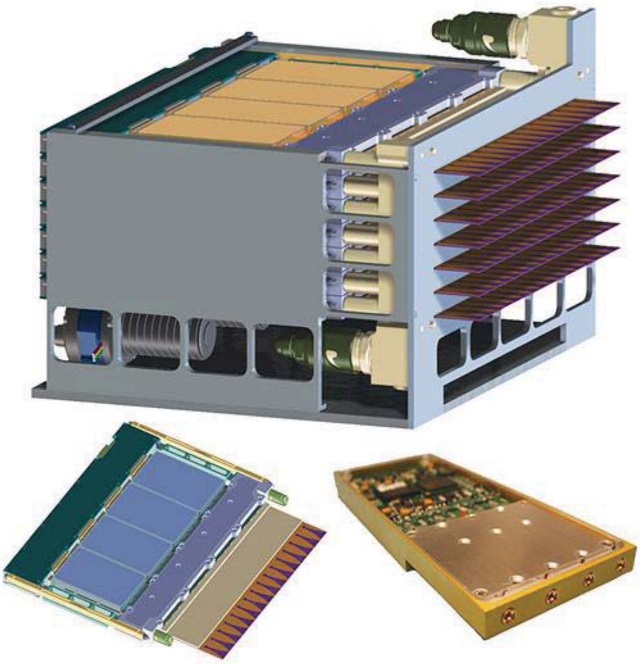

3. **Many new AESAs are capable of multi-role applications ranging from anti-surface and anti-submarine to surveillance and tactical air-support roles.** ***(Courtesy of Thales)***

4. **Active-steering antenna technology is beginning to be embraced for commercial technologies, such as enhancing Wi-Fi data rates, by eliminating dead zones and tracking high-demand devices.** ***(Courtesy of Ethertronics)***

ber of warfighters that are being demanded and the lower cost of AESA technology after the initial development and deployment. The investment in AESA also has been reduced as a result of advancing field-programmable gate arrays (FPGAs) and SDR techniques *(Fig. 2)*.

The latest AESA technologies also offer a dramatically reduced weight and size profile, which allows the radar to provide operational cost savings via payload reduction. These systems are small enough to be mounted on many unmanned-aerial-vehicle (UAV) platforms *(Fig. 3)*. As a result of such enhancements, UAV warfighters are being planned by the U.S. Navy. There also is the possibility of making viable autonomy drop-in kits for helicopters and land vehicles. More potential applications will undoubtedly emerge, given AESA's ability to operate as a traditional EW antenna while providing software control and programmability *(Fig. 4)*. In fact, these devices can operate as long-range data links as well as high-resolution radar-imaging devices. They also operate over many different radar bands.

MODULAR AESA PLATFORMS

In addition to ease of integration, scalable design has become one of the primary focus factors for recent AESA developments. As a result, a number of organizations are developing module-based AESA platforms constructed from a combination of multiple building blocks. This common-module approach increases the manufacturability of an AESA platform while lowering its cost and complexity barriers of entry. It also brings AESA technology closer to infiltrating satcom, data-link, weather, and air-traffic-control applications.

With the contract for phase one of the Arrays on Commercial Timescales (ACT) program, for example, the DARPA Microsystems Technology Office is attempting to merge enhanced AESA development with the commercial infrastructure. The project focuses on AESA platforms based on a digital common module. That module is reusable, highly integrated, and uses commercial CMOS IC technology. The current vision of the common module is a commercial system-on-a-chip (SoC) with integrated, high-speed digital-to-analog and analog-to-digital converters (DACs and ADCs). It is capable of direction sampling and RF signal creation well into the K-band (18 to 27 GHz). Nonlinear digital-signal-processing (DSP) algorithms may enable the dynamic range needed to implement such a system.

AESA technology will continue to advance. For example, recent European investment has led to the development of metamaterial enhancements to AESA radars. These enhancements reduce the cost and size of RF feeding networks, thereby minimizing the coupling between the radiating elements while mitigating the parasitic back/side-lobe radiation from edging effects. On the home front, Raytheon developed a pod-based AESA radar jammer for the Navy that is essentially a high-powered SDR with networking capability.

As EW continues to dominate the arms race, AESA technologies will benefit from innovations that could trickle back to telecommunications and satcom technologies. mw

JACK BROWNE | Technical Contributor

Low-Noise Phase-Locked Loop Extends to 5 GHz

This integer-N frequency synthesizer builds on silicon CMOS semiconductor technology to achieve low-noise signals to 5 GHz from a compact, radiation-hardened CQFP package.

FREQUENCY SYNTHESIZERS ARE widely used both in ground and in space, where they must remain tolerant to different types of radiation. A new solution from Peregrine Semiconductor, the model PE97240, is a radiation-hardened integer-N phase-locked loop (PLL) that is offered in a compact surface-mount package capable of generating low-noise signals through 5 GHz. In addition to achieving low phase noise, the device uses very low power, typically drawing only 75 mA current from a +2.7-V dc supply. It is designed for use at operating temperatures from –40 to +85°C.

Model PE97240 is an integer-N frequency synthesizer that features low noise performance to 5 GHz.

The model PE97240 PLL *(see the figure)* is fabricated on the company's proven UltraCMOS semiconductor technology, which features silicon-on-insulator (SOI) circuitry on a sapphire substrate. Much like the firm's model PE42020 single-pole, double-throw (SPDT) surface-mount switch introduced one month earlier (see *Microwaves & RF*, February 2015, p. 82), this device benefits from the linearity and low noise of this semiconductor process. The PE97240 PLL was designed for commercial space applications, featuring radiation tolerance to 100 krad total ionizing dose (TID) and excellent immunity to single-event-effect (SEE) phenomena. With such specifications, this device will be able to perform reliably for 10 years or more in the harsh radiation conditions of space.

The PLL includes a prescaler with selectable 5/6 or 10/11 dual-modulus operation. The compact 44-lead ceramic-quad-flat-pack (CQFP) package also includes a reference divider, counters, phase comparator, and control logic. The counter values can be programmed by means of a serial interface or under direct-wired control. The dual-modulus prescaler divides an input from a voltage-controlled oscillator (VCO), and the counters work with the control logic and phase-frequency detector to generate control signals to stabilize output signals over the respective ranges of each division ratio.

When used with the 5/6 dual modulus, the PE97240 provides an output frequency range of 800 MHz to 4 GHz, with maximum input power of +7 dBm. When used with the 10/11 dual modulus, the PLL operates at frequencies from 800 MHz to 5 GHz with maximum input power of +7 dBm. The device works with a phase-detector comparison frequency to 100 MHz.

This space-ready PLL boasts very good spectral purity, with low phase noise when using either dual modulus. For example, with the 5/6 dual modulus, the typical single-sideband (SSB) phase noise measured for a 3-GHz carrier is –100 dBc/Hz at 100-Hz offset from the carrier; –109 dBc/Hz at 1-kHz offset from the carrier; –116 dBc/Hz at 10-kHz offset from the carrier; and –118 dBc/Hz at 100-kHz offset from the carrier. When using the 10/11 dual modulus, the SSB phase noise is typically –98 dBc/Hz at 100-Hz offset from the carrier; –104 dBc/Hz at 1-kHz offset from the carrier; –111 dBc/Hz at 10-kHz offset from the carrier; and –117 dBc/Hz at 100-kHz offset from the carrier.

The model PE97240 PLL synthesizer's hermetic CQFP package is RoHS-compliant. To assist specifiers interested in incorporating the device in their system, Peregrine offers an evaluation board with a Universal Serial Bus (USB) interface that helps demonstrate the optimum phase-noise performance of the PLL.

This evaluation board is fabricated with high-frequency 4350B printed-circuit-board (PCB) material from Rogers Corp. (www.rogerscorp.com) with relative dielectric constant (ε_r) of 3.48 and two inner layers of FR-4 PCB material. The board is well grounded for reliable performance when investigating the performance of the PE97240 PLL under the types of conditions that may be experienced in space-based applications. mw

PEREGRINE SEMICONDUCTOR CORP., 9380 Carroll Park Dr., San Diego, CA 92121; (858) 731-9400, FAX: (858) 731-9499, *www.psemi.com*

JACK BROWNE | Technical Contributor

Power Analyzer Integrates Scope

This versatile measurement tool packs a power analyzer and high-speed digital oscilloscope into a single compact housing to measure ac and dc voltage, current, and power.

POWER ANALYSIS HAS grown more complex as designers of electronic devices continue to add functionality, while at the same time attempting to curb power consumption for these increased capabilities. Power measurements on these devices usually require a power analyzer and a high-speed oscilloscope. But tracking down both instruments can be challenging in any workplace—unless, of course, an engineer or technician is fortunate enough to have a model PA2201A Integra-Vision Power Analyzer from Keysight Technologies on hand.

This single compact instrument combines an accurate power analyzer with 16-b resolution and 0.05% measurement accuracy (for 50-/60-Hz measurements) and a high-speed digital oscilloscope with touchscreen control. Packing both instruments into a single portable housing itself saves power while helping to speed and simplify both steady-state and dynamic power measurements.

The PA2201A IntegraVision Power Analyzer is a two-channel, single-phase measurement tool perhaps most distinguished by its large front-panel liquid-crystal-display (LCD) touchscreen *(see the figure)*. This truly is a "hybrid" instrument, with all of the measurement capability of an ac/dc power analyzer and the high-resolution display capabilities of a digital oscilloscope.

Power can be measured by feeding highly isolated test input ports (with 1000-V isolation between all input test ports) or by using an isolated BNC input to connect external current probes to measure current levels greater than 50 A. Test input ports are protected by a clever sliding cover when not in use.

The combination instrument itself is powered by a 5-MSample/s digitizer to capture voltage, current, and power (with 16-b resolution) in real time. It can analyze voltage to 1000 V (across voltage bandwidths as wide as wide as 2 MHz) and current to 50 A (across a current bandwidth as wide as 100 kHz).

The model PA2201A IntegraVision Power Analyzer combines a power analyzer with a digital oscilloscope, showing results with high resolution on a 12.1-in. diagonal LCD touchscreen display.

The power analyzer can capture continuous and transient power events while the digital oscilloscope is able to make repetitive and single-shot measurements. Results are shown on a bright, 12.1-in. (305-mm) diagonal liquid-crystal-display (LCD) screen that also provides touchscreen control of measurements.

The PA2201A IntegraVision Power Analyzer allows frequency- and time-domain analysis of power, current, and voltage in order to fully understand the constant and/or changing power consumption of an electronic circuit or design. The power analyzer/scope captures as many as 4 million data points simultaneously for each sampled waveform.

The compact instrument measures just 16.8 × 11.4 × 10.0 in. with a carrying handle. Its rear panel includes Universal Serial Bus (USB) and local-area-network (LAN) ports for connections to external computers and networks. Admittedly, measurements of current, voltage, and power are not typically high on the list of RF/microwave engineers when designing high-frequency components, devices, or systems. But power consumption is a critical parameter for any electronic device, and the PA2201A analyzer provides the versatility to study power use as a device under test (DUT) shifts operating modes and states.

Measuring power now requires a great deal of flexibility, since such measurements involve measuring ac and dc fundamental and harmonic frequencies; transient changes in power supply and consumption; and changes in operating states.

Finally, the IntegraVision Power Analyzer is well suited for analyzing power-conversion efficiency in power-conversion systems. It can be used to measure common ac power parameters, such as frequency, phase, and harmonics. mw

KEYSIGHT TECHNOLOGIES INC., 1400 Fountaingrove Pkwy., Santa Rosa, CA 95403; (707) 577-2663, *www.keysight.com*

JACK BROWNE | Technical Contributor

Digitizers Capture 1 GHz At 5 GSamples/s

With 8-b resolution and one, two-, and four-channel configurations, these digitizers can operate at sampling rates as high as 5 GSamples/s at single-channel bandwidths to 1 GHz.

TEST INSTRUMENTS NO LONGER require large enclosures to deliver heavyweight performance. A case in point is the M4i series of card-level high-speed digitizers from Spectrum Systementwicklung Microelectronic GmbH. These high-speed data-acquisition instruments each fit on a single circuit card—yet provide 8-b resolution at sampling rates to 5 GSamples/s for a single measurement channel, at bandwidths as wide as 1 GHz.

As many as eight of the cards can be synchronized by means of their own internal clock sources for tackling larger measurement assignments. Connecting one of the cards to a personal computer (PC) can transform the combination into a powerful test-and-measurement instrument; the card can perform continuous streaming of data to the PC at rates to 3.4 GB/s to create a “digital picture” of the most complex signals and waveforms.

The M4i series high-speed 8-b digitizers are available in single-, dual-, and four-channel versions with up to 4 GB of on-board digital memory *(see table)*. They provide sampling rates to 5 GSamples/s on one channel, to 2.5 GSamples/s for two channels, and to 1.25 GSamples/s on four channels, with simultaneous sampling being performed on all channels. Higher-resolution 14-/16-b versions of the digitizers are also available, with 2 GB of on-board data memory.

These digitizer cards include so much processing power—by merit of their own dedicated field-programmable gate arrays (FPGAs)—that they place only minimum loads on a connected system’s central processing unit (CPU). The cards use the on-board memory as a first-in-first-out (FIFO) buffer to ensure maximum data throughput over an extended operating period, even when a PC is involved in other activities.

THE M4i SERIES DIGITIZER CARDS AT A GLANCE

Model	Sampling rates (GSamples/s)			Bandwidth (GHz)
	One channel	Two channels	Four channels	
M4i.223x-x8	5.00	2.50	1.25	1.0
M4i.222x-x8	2.50	2.50	—	1.0
M4i.221x-x8	1.25	1.25	1.25	0.5

These high-performance digitizer cards operate with four input level ranges, from ±200 mV to ±2.5 V. For controlling and operating the M4i series digitizers, the firm offers its SBench6 software. It supports all of the key functions of the digitizer cards and provides display, storage, and analysis functions. The program provides both oscilloscope and transient recording modes. It also features a segmented view ideal for burst-type signals.

The cards are compatible with a wide range of computer operating systems, including Windows XP, Vista, 7, and 8, along with Windows/Linux 32- and 64-b programs. They also include a wide range of programming examples for different programs, including Visual C++, Borland C++ Builder, IVI, and LabWindows/CVI.

The cards feature full 32- and 64-b Linux support. They are shipped with precompiled kernel modules for the most common distributions, including RedHat, Fedora, Suse, Ubuntu, and Debian. With each digitizer card, the firm provides all of the software necessary for linking the card’s operating software to other useful software tools, including LabVIEW from National Instruments (www.ni.com) and MATLAB from MathWorks.

Several options are available for the digitizer cards, including the use of an external reference clock. The cards are available with a gated sampling mode that allows data recording to be controlled by an external gate signal, using a programmable level to record only certain signal information.

For connection to a PC or other system, each card requires a physical X8 or X16 PCIe slot with a Generation 2 or 3 interface. A variety of different product interfaces are available, such as with PCIe for fast data-transfer speeds, with LXI for ease of remote control, and with PXI for ease of integration with other instrument modules. mw

SPECTRUM SYSTEMENTWICKLUNG MICROELECTRONIC GMBH, Ahrensfelder Weg 13-17, 22927 Grosshansdorf, Germany; +49 4102 6956 0, FAX: +49 4102 6956 0, e-mail: Info@spec.de, *www.spectrum-instrumentation.com*

JACK BROWNE | Technical Contributor

Transcorder Tackles 50 MHz to 6 GHz

Within its nearly 6-GHz-wide bandwidth, this compact signal recorder/playback system can capture as much as 80 MHz of bandwidth in two 40-MHz frequency spans.

MEASURING RF/MICROWAVE SIGNAL activity is not always easy because of the changing nature of those signals, especially when the activity may be irregular or inconsistent. Yet, it is often necessary to have some form of record of a particular signal, especially when characterizing or documenting the activity of different wireless systems.

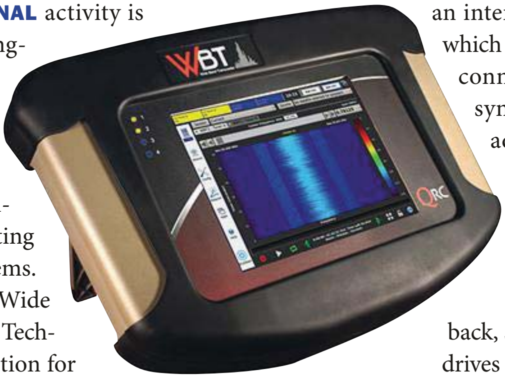

Model WBT-200 is a portable recorder/playback instrument capable of recording and playing back as much as 80 MHz of bandwidth from 50 MHz to 6 GHz.

Fortunately, the model WBT-200 Wide Band Transcorder (WBT) from QRC Technologies is a compact, portable solution for recording and playing back portions of RF/microwave bandwidth from 50 MHz to 6 GHz. With its two independent transceivers, it can be tuned to measure two separate 40-MHz sections of bandwidth across that nearly 6-GHz range and capture signals across a 74-dB instantaneous dynamic range. It is actually a system in a box, storing test results on solid-state drives for ease of data transport and analysis with external computers.

The WBT-200 (*see photo)* performs signal analysis and signal generation across its frequency range, all from a compact enclosure measuring just 18.7 × 12.4 × 3.1 in. and weighing less than 10 lb. It is relatively simple to operate, with a straightforward user interface and single button for activating RF/microwave signal recording and playback. The WBT-200's two transceivers each feature typical receiver sensitivity of –95 dBm on standard input ports and –110 dBm on special-use ports.

Each transceiver provides selectable bandwidths of 0.78125, 1.5625, 3.125, 6.25, 12.5, 25, and 40 MHz with as much as 30-dB input gain and 30-dB input attenuation to control the levels of input signals. The transceivers maintain high sensitivity due to low-noise tuning sources and reference clocks, with phase noise of better than -80 dBc/Hz offset 1 kHz from a 1-GHz carrier.

The WBT-200 incorporates an embedded Global Positioning System (GPS) disciplined oscillator (GPSDO) that produces an internal 10-MHz timing reference signal, which is also available at an output port (BNC connector) to be used as input signals for synchronizing other equipment, such as additional WBT-200 systems. The GPS signals exhibit stability of 1 PPS with ±50-ns accuracy and also serve to tag signal recordings with GPS geolocation details.

Each WBT-200 records to, and plays back, signals from standard 2.5-in. solid-state drives (SSDs) using the VITA 49 Radio Transport (VRT) standard open-memory format. Data from these drives can also be analyzed and visualized by means of the WBT's Signal Analysis Toolkit or other software.

Each WBT-200 has two SSD drive bays. For long recording sessions, one SSD can be replaced while the other SSD is active and recording. For applications where less than 80 MHz of instantaneous bandwidth is required, it is possible to operate with considerably less disk space.

The WBT-200 shows results on a 10.4-in diagonal liquid-crystal-display (LCD) screen with 1024- × 768-pixel resolution. The compact transcorder is designed for use with operating temperatures from 0 to +50°C. It includes a Gigabit Ethernet port for remote control of other WBTs or for transferring data.

The portable WBT-200 can be used for reference signal recording and playback, interference analysis, and general signal analysis. It is supported by numerous application software tools, and typically consumes 60 W power. It can run on dc voltage from 10 to 32 V dc, ac voltage of 120 or 240 V ac, an ac power adapter (that supplies 20 V dc), an internal UPS battery consisting of four $LiFePO_4$ rechargeable cells, and an automobile cigarette-lighter adapter. mw

QRC TECHNOLOGIES, 1211 Central Park Blvd., Fredericksburg, VA 22401; (540) 446-2270, *www.qrctech.com*

GaAs Low-Noise Amp Targets 17- to 27-GHz Apps

SOME MILITARY AND space applications require fairly broadband performance, but at higher frequencies. Luckily, the model CMD163 low-noise-amplifier (LNA) chip from Custom MMIC is well-suited for applications from 17 to 27 GHz. The amplifier, fabricated using gallium-arsenide (GaAs) semiconductor technology, employs an all-positive bias scheme for simplicity of installation and operation. The all-positive bias scheme eliminates the need for negative voltage supplies and costly sequencing circuitry in order to power the amplifier.

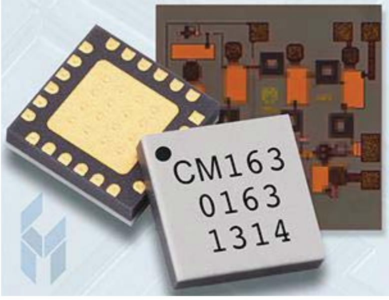

Model CMD163 is an LNA chip capable of 24-dB typical gain and 1.3-dB typical noise figure from 17 to 27 GHz.

The compact model CMD163 LNA chip achieves a noise figure of better than 1.3 dB with typical gain of 24 dB from 17 to 27 GHz. In addition, it reaches an output 1-dB compression point of +19 dBm across the full bandwidth. The typical input return loss is 10 dB, while typical output return loss is 20 dB across the full bandwidth. The robust amplifier is designed to handle maximum input power levels to +20 dBm. It is internally matched to 50 Ω and does not require external components other than bypass capacitors.

Furthermore, the LNA die is well suited for point-to-point and point-to-multipoint commercial communications systems, which typically require small size and high linearity. The bias requirements are 120 mA at a drain voltage (V_{dd}) of +4 V dc and a gate voltage (V_{gg}) of +3 V dc. The LNA is also available in packaged form as model CMD163C4.

CUSTOM MMIC, 1 Park Dr., Unit 12, Westford, MA 01886; (978) 467-4290, FAX: (978) 467-4294, www.custommmic.com

LNAs Emerge from New Supplier

A NEW LINE of low-noise amplifiers (LNAs) for applications through 6 GHz has been developed by a relatively new supplier that goes by the unlikely name of Guerrilla RF (www.guerrilla-rf.com). The firm, which started in the second half of 2014, introduced a pair of LNAs for mainly wireless communications applications through 3.8 GHz.

The GRF2051 and GRF2052 LNAs are usable through 3800 MHz and come supplied in 12-pin plastic QFN packages measuring 2.0 × 2.0 × 0.5 mm.

Model GRF2051 maintains low noise figure with reasonable gain from 1700 to 2700 MHz, while the higher-frequency model GRF2052 can be tuned for use from 2300 to 2700 MHz or from 3300 to 3800 MHz (via separate tuning). The amplifiers, which will find homes in small cellular-communications base stations and distributed antenna systems, come packaged in 12-pin plastic QFNs that measure 2.0 × 2.0 × 0.5 mm.

Model GRF2051 is a single-stage LNA that can serve as the first-stage amplifier in sensitive wireless receivers. It has been characterized within the firm's evaluation board, achieving 19-dB gain and 0.35-dB noise figure within the board at 1900 MHz. When measurements are de-embedded from the evaluation board, the noise figure is reported as a mere 0.25 dB at 1900 MHz. At that same test frequency, the LNA achieves +20-dBm output power at 1-dB compression and output third-order intercept point of +39 dBm. The input and output return losses are typically 12 dB.

This compact LNA operates over a supply (drain) voltage range of 0 to +9 V dc, drawing typical supply current of 55 mA at +5 V dc; the amplifier is rated for maximum power dissipation of 500 mW. It is designed for an operating temperature range of -40 to +105°C. The amplifier, which can handle fast-switching applications, is rated for 300-ns switching rise and fall time. The typical current draw is 55 mA at +5 V dc. Performance information is still preliminary for this model at higher-frequency applications; nevertheless, the GRF2052 LNA can be used from 2300 to 2700 MHz or 3300 to 3800 MHz with separate tuning.

Regarding the new amplifiers, Alan Ake, vice president of applications and technical marketing at Guerrilla RF, says: "We are excited to help our wireless infrastructure customers obtain maximum receiver sensitivity and improve receiver dynamic range with minimal external components, which ultimately yields a simple and low-cost application circuit that allows for optimal efficiency and reuse."

GUERRILLA RF INC., 1196 Pleasant Ridge Rd., Ste. 5, Greensboro, NC 27409; (336) 510-7840, e-mail: sales@guerrilla-rf.com, www.guerrilla-rf.com

This index is provided as an additional service by the publisher, who assumes no responsibility for errors or omissions.

Subscription Assistance and Information:
(ISSN 0745-2993)
Microwaves & RF is published monthly. Microwaves & RF is sent free to individuals actively engaged in high-frequency electronics engineering. In addition, paid subscriptions are available. Subscription rates for U.S. are $95 for 1 year ($120 in Canada, $150 for International). Published by Penton Media, Inc., 9800 Metcalfe Ave., Overland Park, KS 66212-2216. Periodicals Postage Paid at Kansas City and additional mailing offices. POSTMASTER: Send change of address to Microwaves & RF, Penton Media Inc., P.O. Box 2095, Skokie, IL 60076-7995. For paid subscription requests, please contact: Penton Media Inc., P.O. Box 2100, Skokie, IL 60076-7800. Canadian Post Publications Mail agreement No. 40612608. Canadian GST# R126431964. Canada return address: IMEX Global Solutions, P.O Box 25542,London, ON N6C6B2.

Back issues of MicroWaves and Microwaves & RF are available on microfilm and can be purchased from National Archive Publishing Company (NAPC). For more information, call NAPC at 734-302-6500 or 800-420-NAPC (6272) x 6578. Copying: Permission is granted to users registered with the Copyright Clearance Center, Inc. (CCC) to photocopy any article, with the exception of those for which separate copyright ownership is indicated on the first page of the article, provided that a base fee of $1.25 per copy of the article plus 60 cents per page is paid directly to the CCC, 222 Rosewood Dr., Danvers, MA 01923. (Code 0745–2993/02 $1.25 +.60) Copying done for other than personal or internal reference use without the expressed permission of Penton Media, Inc., is prohibited. Requests for special permission or bulk orders should be addressed in writing to the publisher.

SENIOR DESIGN ENGINEER: Required by RF Micro Devices (dba Qorvo) for a position in Greensboro, NC. Will be responsible for the design, test, and verification of RF Power Amplifier designs. Collaborate with customers and marketing engineers to architect/define/specify highly integrated solutions to wireless amplifier products for battery powered applications. On occasion, will work with small RF development teams to develop low cost solutions to high volume, commercial RFIC's using GaAs and Silicon IC Technologies. Perform conceptual and detailed IC design of critical RF elements associated RF Power Amplifiers. Critical RF elements include power amplifiers, bias circuits, etc. Requires a considerable amount of independent decision making and creativity in the design of circuits. Interacts will all areas of the company. Public interaction at conferences and in written articles/papers. Knowledge of PC and Workstation CAD/CAE tools used in the IC design process including Agilent ADS, Cadence, etc. Knowledge in RF Circuit design, silicon, and bipolar IC design. A MSEE or MS in Computer Information Systems (or foreign equivalent) and one year experience in RF circuit design is required. Relocation allowances are not offered for this position. Qualified candidates send resumes to **employment@qorvo.com** and refer to Job Code: **JLWEI**

Penton Revised Privacy Policy

At Penton, we constantly strive to improve our products, including by changing our use of the information we collect from you. We now share information with other subscribers to our services and/or third party vendors who are our partners so that they can provide you additional opportunities and benefits. Some partners may analyze our sites to identify future improvements or to offer additional products you may want.

Visit **http://www.penton.com/privacy-policy/** to read our updated Privacy Policy.

PXIe Signal Generators Extend to 12 GHz

THE QUANTUM Wave 4000 series of PXIe RF/microwave signal generators provide clean output signals to 12 GHz. These frequency-synthesized continuous-wave (CW) sources are supplied in single-slot 3U PXIe modules. They feature clean signals, with single-sideband (SSB) phase noise of typically –120 dBc/Hz offset 10 kHz from a 1-GHz carrier.

Amplitude can be varied from –10 to +10 dBm across a 20-dV calibrated range with resolution as fine as 0.1-dB steps. The output-power-level accuracy is typically ±0.3 dB. As an example of the product line, model 4061 is a single-channel synthesizer that operates from 75 MHz to 6 GHz, while model 4062 is a dual-channel synthesizer that covers the same frequency range. For those needing extended frequency coverage, dual-channel model 4122 packs two independent frequency synthesizers into a single-width 3U PXIe module: one spanning 75 MHz to 6 GHz and another that operates to 12 GHz.

CAMBRIDGE INSTRUMENTS, 330 Changebridge Rd., Pine Brook, NJ 07058; (617) 863-7948, *www.cambridgeinstruments.com*

Shielding Gaskets Stick to Their Marks

LOW-PROFILE BERYLLIUM-COPPER (BeCu) shielding gaskets in a variety of formats are now available with stick-on, hook-and-stick-on, and clip-on mounting configurations. These gasket materials provide EMI/RFI shielding effectiveness (SE) of better than 100 dB. They are supplied with free heights from 0.06 to 0.15 in. and can used to close packaging gaps from 0.030 to 0.120 in. The stick-on mounting format provides a reliable installation approach that can be used at ambient temperatures from –67 to +300°F. One side of the hook-and-stick-on gasket fits over the flange for additional mechanical security. Materials with an optional DiamondBack textured surface for high-frequency applications are available as an option.

TECH-ETCH INC., 45 Aldrin Rd., Plymouth, MA 02360; (508) 747-0300, *www.tech-etch.com*

Low-Noise VCO Tunes 5685 to 5780 MHz

MODEL CVCO55CXT-5685-5780 is a voltage-controlled oscillator (VCO) that tunes from 5685 to 5780 MHz by merit of a control voltage range of +0.3 to +4.7 V dc. The oscillator achieves typical phase noise of –102 dBc/Hz offset 10 kHz from the carrier with 0-dBm typical output power. Supplied in a 0.5 × 0.5 in., surface-mount package, the VCO controls second-harmonic levels to typically –30 dBc and exhibits pulling of 0.5 MHz and pushing of 1.5 MHz/V. The source is well-suited for wireless access, satellite-communications (satcom) systems, digital radios, and cellular base stations. Typical current consumption is 25 mA from a +5-V dc supply.

CRYSTEK CORP., 12730 Commonwealth Dr., Fort Myers, FL 33913; (800) 237-3061, (239) 561-3311, FAX: (239) 561-1025, e-mail: sales@crystek.com, *www.crystek.com*

Packaging and Substrate Solutions Gain Ground

A FIRM known for its ceramic packaging and substrate solutions has added a number of capabilities to its lineup, including copper-filled viaholes, copper-coated bore holes, and solder mask and assembly options. These capabilities enhance the design capabilities for packages and printed-circuit boards (PCBs) while also improving the reliability of designed based on the company's manufacturing processes. The packages and substrates use the company's plated copper on thick and thin film (PCTF) metallization for high reliability and effective thermal management.

REMTEC INC., 100 Morse St., Norwood, MA 02062; (781) 762-9191, FAX: (781) 762-9777, e-mail: sales@remtec.com, *www.remtec.com*

Broadband Phase Shifter Adjusts DC to 18 GHz

MODEL 9426A is a broadband phase shifter that provides consistent phase control from dc to 18 GHz. It offers a phase-adjustment range of at least 60 deg./GHz with 360-deg. control at 6 GHz. The insertion delay is as little as 0.88 ns and no worse than 1.10 ns across the frequency range. The maximum insertion loss ranges from 0.50 dB at 8 GHz, to 0.75 dB at 12 GHz, to 1.0 dB at 18 GHz. Maximum VSWR ranges from 1.30:1 at 8 GHz, to 1.50:1 at 12 GHz, to 1.60:1 at 18 GHz. The phase shifter, which comes in an aluminum housing with stainless-steel female SMA connectors, measures 5.50 × 3.625 in. It offers 100 W average power-handling capability and 5-kW peak power handling capability.

ARRA, INC., 15 Harold Court, Bay Shore, NY 11706-2296; (631) 231-8400, FAX: (631) 434-1116, e-mail: sales@arra.com, *www.arra.com*

Directional Coupler Connects 6.0 to 26.5 GHz

WELL-SUITED FOR electronic-warfare (EW), instrumentation and other applications requiring broad bandwidth, model 106026506 is a compact coaxial directional coupler that operates from 6.0 to 26.5 GHz. The stripline coupler offers 6-dB nominal coupling and maintains coupling flatness of ±0.5 dB across the frequency range. Insertion loss is less than 1.6 dB across the frequency range, while directivity exceeds 14 dB. The directional coupler, which is rated for average input power levels to 20 W and 3-kW peak power, exhibits its maximum VSWR of 1.45:1 at any port. It is designed for an operating temperature range of –54 to +85°C. The coupler measures 1.12 × 0.53 × 0.64 in. and is supplied with female SMA connectors, but male SMA connections are available as an option.

KRYTAR INC., 1288 Anvilwood Court, Sunnyvale, CA 94089; (408) 734-5999, (877) 734-5999, FAX: (408) 734-3017, e-mail: sales@krytar.com, *www.krytar.com*

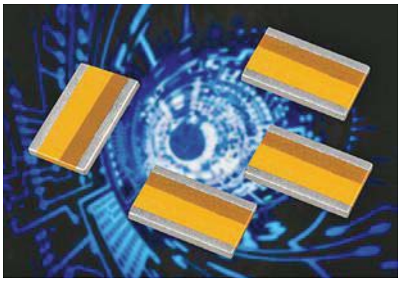

High CV Tantalum Cap Has Low Profile

FOR CIRCUITS designed to fit tight spaces, the 1206-06 D case TACmicrochip series tantalum capacitors measure 3.4 × 1.8 mm with a maximum height of only 0.6 mm, or about 0.15 mm shorter than existing 1206 V case TACmicrochip capacitors. These 47-µF capacitors, which are ideal for use in audio and higher-frequency amplifiers, can be embedded in 0.8-mm-thick printed-circuit boards (PCBs) and are well-suited for the latest-generation handheld electronic devices. The capacitors are supplied with 100% lead-free tin terminations and are rated for operating temperatures from –55 to +125°C.

AVX CORP., One AVX Blvd., Fountain Inn, SC 29644; (864) 967-2150, *www.avx.com*

Power Divider Spans 12 to 18 GHz

MODEL 2PA1500 is an example of a line of broadband two-way power dividers covering a total frequency range of 0.5 to 18.0 GHz. As an example, model 2PA1500 is a compact two-way coaxial power divider for applications from 12 to 18 GHz. It achieves insertion loss of 0.6 dB or less across that range, with input/output VSWR of 1.501 or less and at least 17-dB isolation. The power divider, which handles maximum input power to 10 W, holds amplitude imbalance to ±0.2 dB and phase imbalance to within ±5 deg. across the full frequency range. The power divider, which measures 1.0 × 1.0 × 0.5 in. less connectors, is supplied with female SMA connectors on all three ports. All of the firm's power dividers are constructed of materials selected for target PIM of –140 dBc or better. The company also offers custom power dividers, designed and manufactured to specific requirements, with no minimum order.

WERBEL MICROWAVE, LLC, 51 Chestnut St., Livingston, NJ 07039; (973) 900-2480, FAX: (973) 716-9430, e-mail: Sales@WerbelMicrowave.com, *www.WerbelMicrowave.com*